Automated Method Development for Measuring Trace Metals in the Open Ocean
by

Cassie Schwanger
B.A., Carthage College, 2004

A Thesis Submitted in Partial Fulfillment
of the Requirements for the Degree of

MASTER OF SCIENCE

in the Department of Earth and Ocean Sciences

© Cassie Schwanger, 2013
University of Victoria

All rights reserved. This thesis may not be reproduced in whole or in part, by photocopy or other means, without the permission of the author.

Supervisory Committee

Automated Method Development for Measuring Trace Metals in the Open Ocean

by

Cassie Schwanger
B.A., Carthage College, 2004

Supervisory Committee

Dr. Jay T. Cullen, Department of Earth and Ocean Science
Supervisor

Dr. Roberta C. Hamme, Department of Earth and Ocean Science
Departmental Member

Dr. Alexandre G. Brolo, Department of Chemistry
Outside Member

Abstract

Supervisory Committee
Dr. Jay T. Cullen, Department of Earth and Ocean Science
Supervisor
Dr. Roberta C. Hamme, Department of Earth and Ocean Science
Departmental Member
Dr. Alexandre G. Brolo, Department of Chemistry
Outside Member

New approaches to the analysis of trace metal concentrations in seawater have the potential to advance the field of oceanography and provide a more comprehensive understanding of the marine biogeochemical cycles of trace metals and the processes regulating these cycles. Traditional oceanographic methods of trace metal analysis were developed several decades ago using benchtop liquid-liquid extraction (Danielson et al., 1978; Kinrade and Van Loon, 1974; Miller and Bruland, 1994; Moffett and Zika, 1987). More modern techniques utilize flow based solid phase extraction to eliminate the high ionic strength matrix to determine dissolved concentrations with great accuracy and precision but do not allow for the determination of metal speciation in solution (Wells and Bruland, 1998). The method developed here measures oceanographically relevant concentrations of copper (Cu) in seawater via chemiluminescence (Marshall et al., 2003 and Coale et al., 1992) and micro-molar levels of silver (Ag) colorimetrically after automated liquid-liquid extraction. The Zone Fluidics (Marshall et al., 2003) analyzer for trace Cu determined SAFe D2 standard seawater (www.geotraces.org) to be 1.77 nM Cu comparable to the expected consensus value. The method was used to determine dissolved Cu depth profiles for major stations along the Line P Time-series transect (48°N 125°W - 50°N 145°W) in the Pacific Ocean during February 2011. This method consumes less than 200 µL of sample and reagents and is performed in less than 3 minutes making it suitable for ship or lab based analysis.

Table of Contents

List of Tables

List of Figures

Acknowledgments

Thank you to J. T. Cullen for honoring me with the opportunity to do this research, and a special thank you to C. Schallenberg and R. Ramirez, part of the Cullen Lab Group, for assistance around the lab with samples, reagents and clean bottles.

Thank you to my colleagues at Global FIA, D. Holdych, G. Marshall, S. Marshall, D. Olson and W. Wolcott for your dedication to seeing this project through to the end. Thank you for your help with software, chemicals, instrumentation, time and financial support.

Finally, a special thanks to my family and friends that supported and encouraged me along the way.

Dedication

This thesis is dedicated to my colleagues at Global FIA on Fox Island, WA. Thank you for your support and encouragement in my education and future.

Chapter 1. Introduction and Technique

The development of micro-fluid, incorporating low volume and automation, based methods represents an important and necessary advancement toward the goal of automating standard preconcentration and matrix removal procedures in marine chemistry. The aim of this study is to develop a robust, automated technique for trace element analysis of ocean water samples that lends itself to the determination of dissolved and in some cases the physicochemical speciation of metals. Manual techniques using solvent extraction for the determination of low concentrations of metals in environmental samples have proven to be sufficiently precise and accurate albeit labor intensive (Kinrade and Van Loon 1974; Bruland et al. 1979). Solvent extraction is a widely used separation technique that employs the relative solubility of compounds in immiscible fluids (Berg, 1963). A properly designed extraction procedure allows the analyte of interest to be isolated and concentrated from the sample matrix to limit the potential for interferences and improve precision, accuracy and limit of detection. While the manual technique has been used for centuries, even modern day usage is prone to certain critical shortcomings. Manual protocols are tedious and the consumption of reagents is often seen as a shortcoming through the generation of large volumes of hazardous waste. With improving technology and fluid manipulation techniques, classical analytical techniques like solvent extraction are becoming automated processes. An automated Zone Fluidics (ZF) system equipped with a micro-separation cell can efficiently perform solvent extraction on multiple samples without

compromising recovery. This device not only automates this technique but also reduces reagent use, experiment time, and limits the exposure of laboratory personnel to solvent vapors. This approach, applied to trace metal analysis in open ocean environments, will enhance the capability to realize low level detection in a laboratory or field setting. High quality measurements and observations are key to increasing our understanding of trace metal chemistry and biogeochemistry in natural waters.

The basin-scale distribution of many trace metals in seawater can provide valuable information on a variety of key oceanic processes which have a direct bearing on questions pertaining to global climate (Morel and Price, 2003; Henderson et al. 2007). Developing a comprehensive understanding of the marine biogeochemical cycles of trace metals and processes regulating these cycles, will thus bring many benefits to be shared across a wide spectrum of ocean disciplines and will greatly help in delineating the role and response of the ocean during future climatic fluctuations. For instance, some trace elements, such as cobalt (Co), copper (Cu), iron (Fe), and zinc (Zn), are essential micronutrients (Morel 2008; Morel et al. 2003; Sunda 1994; Sunda and Huntsman 1992; Morel and Price, 2003). Because the bioavailability of metals depends on chemical form as well as concentration, a better understanding of the factors controlling the distribution and speciation of these potentially biolimiting micronutrients will provide critical information for understanding their role in regulating the structure and productivity of marine ecosystems, the efficiency of these ecosystems at sequestering CO_2 and their sensitivity to climate change.

The first accurate and oceanographically consistent trace metal measurements in seawater were made only within the past 30-40 years (Boyle et al., 1977; Danielson et al., 1978; Bruland et al., 1979; Bruland et al., 1980). Despite the recognition of the importance of trace metals in biologically mediated transformations within the biogeochemical cycles of carbon (C), nitrogen (N) and sulfur (S), there still exist significant gaps in our knowledge of marine metal chemistry. Many of these gaps reflect the analytical challenges associated with determining metal concentrations and chemical speciation at total dissolved concentrations of 10^{-9}-10^{-12} molar in a high ionic strength medium.

The goal of this study is to begin to develop a technique that allows for trace metal determination that eventually provides detail on metal speciation on a smaller scale than the current literature techniques (Sunda 1984; Miller and Bruland, 1995, Wang et al., 2008) or for elements not lending themselves to determination by electrochemical techniques (van den Berg 1995; Rue and Bruland 1995). The proposed technique focuses on reducing sample and reagent volumes as well as method time with micro-scale liquid-liquid extraction with ZF described later in this chapter. The goal of this research is to progressively move from proof of concept methods for optimizing parameters at higher concentration samples to open ocean trace metal measurements and finally looking at field measurements from the Pacific Ocean. Method development begins in Chapter 2 where the understanding and optimization of flow-based, micro-scale liquid-liquid extraction is determined with a toluene-bromocresol purple extraction. In Chapter 3, a technique for colorimetric analysis of silver at the

micromolar level was adapted to the ZF platform followed by a micro-extraction technique based on the optimized conditions found in the previous study. From here, the research progresses into looking at relevant open ocean concentrations, nanomolar (nM), trace metals. Due to the high limit of detection for the silver colorimetric chemistry, the metal of focus changes to copper. This research, described in Chapter 4, starts with developing a chemilumenescence (CL) method for nM Cu detection. In Chapter 5, the ZF copper CL method is applied to open ocean samples collected in the subarctic Pacific Ocean. The concluding chapter brings into focus future research opportunities and outstanding problems left in the wake of this thesis project.

1.1 Flow Based Techniques

Flow based techniques have been used since the late 1950s through the introduction of segmented flow analysis (SFA) by Skeggs (1957). This technology spawned new designs for automated analyzers and led to increased development of flow-based techniques. The concept of flow injection analysis (FIA) was introduced in the mid-1970s (Stewart et al., 1976 and Ruzicka and Hansen, 1978). In FIA a sample plug is injected into a flowing carrier stream where the analyte is modified to become a detectable species and analysis occurs in a suitable detector flow cell. This technique uses a peristaltic pump to continuously flow solutions in one direction towards the detector. In FIA there are multiple streams that flow independently of one another from the pump and are merged downstream, mixed, reacted and sent to the detector. FIA differs from SFA in that no air bubbles are introduced into the stream.

Flow-based technology has developed from simple systems that deliver samples online to more complex sample manipulation. Following the introduction of FIA, sequential injection analysis (SIA) was developed in the 1990s by Ruzicka and Marshall. SIA introduces a multi-position valve and a holding coil that allows for greater control of the sample manipulation process. A bi-directional pump replaces the peristaltic pump reducing maintenance requirements and minimizing reagent use and waste generation with discontinuous operation. The reagents and sample are pumped into a holding coil and subsequently moved to the detector. This reduces reagent use and waste generation compared to a continuous flow based system like FIA.

Figure 1.1: Flow based techniques (a) FIA, (b) SIA, and (c) ZF

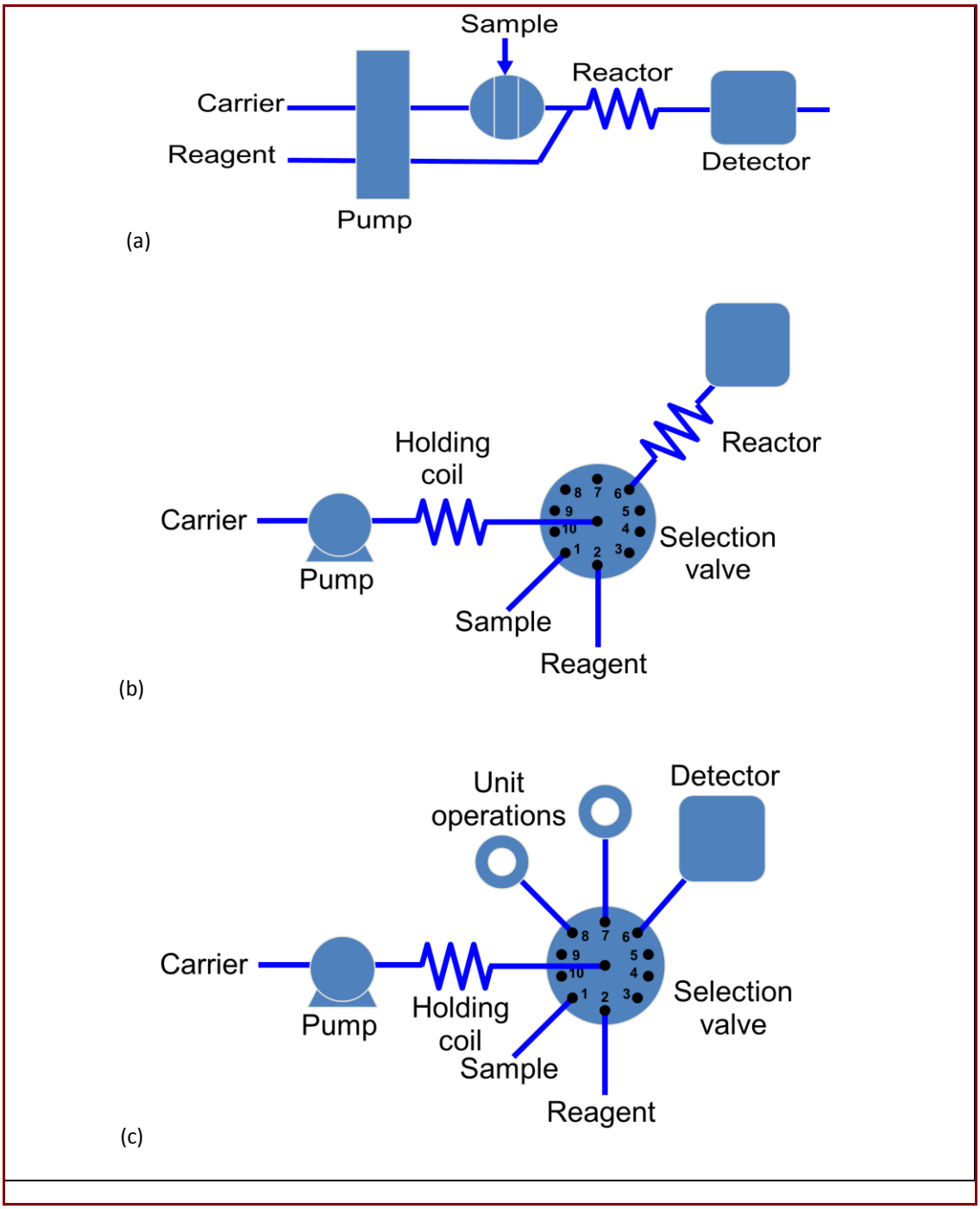

Building off of the concept of SIA, zone fluidics (ZF) was developed in the early 2000s.

This development enhanced the functionality of flow-based technology by introducing

automated sample handling devices, called unit operations, for further sample manipulation. With a platform similar to SIA, ZF positioned one or more sample manipulation unit operations into the fluidics manifold to facilitate the transformation of the sample into a detectable species. These unit operations include both sample preparation and measurement chemistry step. The unit operations are located off of a central multi-position valve and are adaptable for multiple chemistries while maintaining the advantage of controlled and precise flow rates.

In ZF a zone(s) of fluid is shuttled from one unit operation to the next within the manifold where a specified manipulation occurs (Marshall et al., 2003). The zone can be shuttled to multiple operations to render a detectable species. The term "unit operation" refers to the individual steps that function as a particular handling process and includes mixers, heaters, solid-phase extraction, solvent extraction, evaporation, de-bubbling, filtering, and dilution to name a few.

1.2 Zone Fluidics Apparatus

ZF is defined as the precisely controlled physical, chemical, and fluid-dynamic manipulation of zones of miscible and immiscible fluids and suspended solids in narrow bore conduits to accomplish sample conditioning and chemical analysis (Marshall et al., 2003). This flow-based technology merges sample handling and automated analytical processes into a compact instrument for multiple areas of analysis. ZF combines movement of fluid zones and micro-analytical processes to fully automate flow-based methods. The focus of this technique is sample manipulation that leads to a detectable product. The standard method development platform for ZF used for this project is the

mini-FloPro (Global FIA, Fox Island, WA). The basic system consists of a single pump, 1-2 selection valves and a detector. These components are described below.

Figure 1.2: Global FIA mini-FloPro for Zone Fluidics

1.2.1 Pump

A pump is used to propel solutions within the manifold. The milliGAT (Global FIA, Fox Island, WA) is the pump of choice in the mini-FloPro. The milliGAT is a bi-directional, high precision, low pulse metering pump which is critical for ZF. The internal design of the milliGAT is four pistons in a rotor. As the rotor turns a cam drives the pistons so that one piston is filling , one is dispensing, and the other two are moving between the dispense and fill ports. In this way, as one piston finishes dispensing its load another moves into position to continue the flow. Flow direction is determined by rotation direction and flow rate by the speed of rotation. Stepper motor control ensures high precision metering of small and large volumes.

Figure 1.3: milliGAT Pump

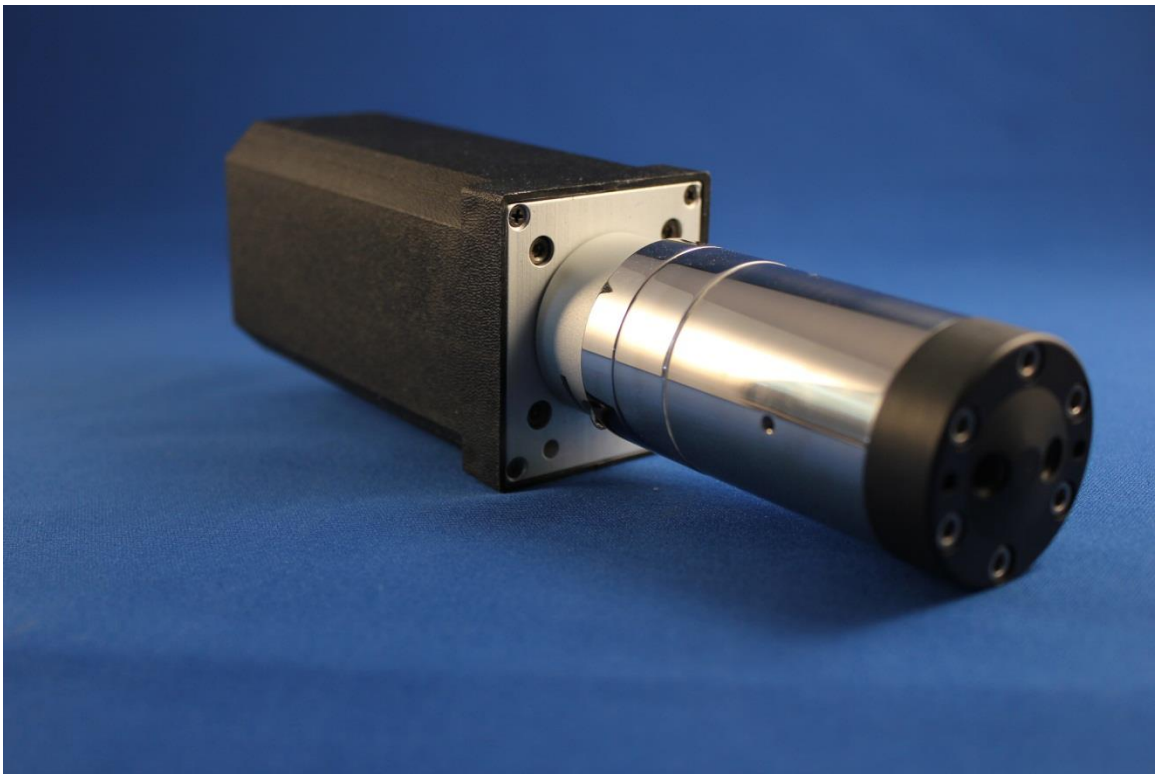

1.2.2 Valve

The mini-FloPro is built around a multi-position selection valve. The valve has a common center port that is coupled to the outer ports via a low dead volume channel. Port changes occur by rotating the channel on a rotor from one port to the next. The most commonly used valves are the Valco (Houston, TX) 10-port and 18-port selection valve although valves can range in port numbers from 3 to 18. Compression fittings are used to hold the conduits in place within the ports (see Section 1.2.3).

Figure 1.4: 18-Port selection valve from Valco (Houston, TX)

1.2.3 Conduits

The majority of the fluid channels are 0.030 in (0.76 mm) ID PFA tubing with corresponding fittings depending on the origin/destination of the tubing. These fittings include ¼-28 nuts and ferrules, 6-40 nuts with ferrule, and 10-32 nuts with corresponding ferrule. All ferrules were set with make-up tools specifically designed to allow the tube to protrude from the end of the ferrule or to be flush with the end of the tube depending on the use.

Figure 1.5: Conduits for flow-based systems

top left- tubing, top right- 10-32 plugs, bottom left - 1/4 28 nuts and ferrules, bottom right- 640 nut/ferrule

1.2.4 Reservoirs

All reagents were made and stored in polytetrafluoroethylene (PTFE) bottles. Before use, all bottles were washed with detergent, followed by multiple rinses with deionized, high purity water (>18.2 MΩ cm) hereafter referred to as MQ. Then the bottles were stored in 6M HCl (Environmental Grade) for 4 weeks. The bottles were stored with 1M HCl then rinsed multiple times with MQ prior to use.

1.2.5 Detectors

The Ocean Optics, (Dunedin, FL) USB 4000 spectrometer was used for colorimetric analysis. The flow cell for this detector was the Global FIA (Fox Island, WA) Bubble Tolerant Flow Cell (BTFC) with optical cables and white LED light source. The geometry of the BTFC is designed to pass bubbles without trapping air in the flow cell. The internal volume of the flow cell was approximately 40 µL and the path length was approximately 12 mm.

Figure 1.6: Global FIA bubble tolerant flow cell and Ocean Optics USB 4000 Spectrometer

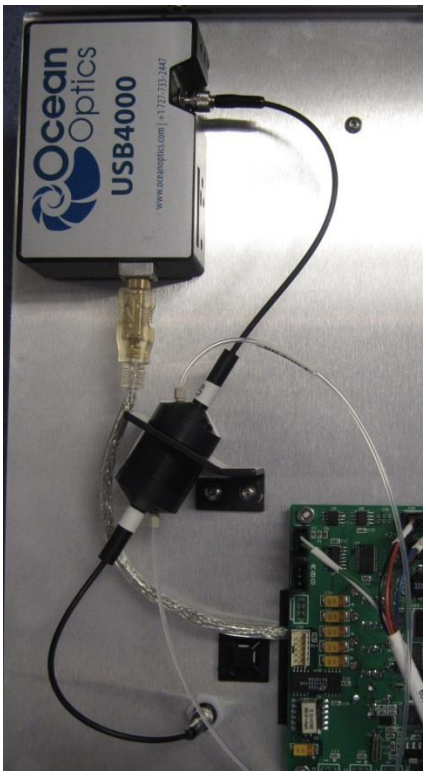

For CL detection of Cu, a P25232 Photon Counter (Senstech, Ruislip Middlesex) was housed in the Global FIA (Fox Island, WA) Firefly flow cell holder. The holder consisted of a tube with a flat interface where a quartz or sapphire window was held in place by a cap with 6 screws. The flow path was determined by an insert machined at Global FIA that was sandwiched between the cap and the window. In the described method three different inserts were used: a serpentine, a spiral and a dual inlet serpentine geometry.

1.2.6 Heater

In order to heat solutions in the ZF manifold, an aluminum block heater with 0.030" ID (0.76mm) tubing wrapped around the internal block was used. A temperature controller (Omron, Japan) and thermocouple minimized temperature fluctuations to within ±0.5ºC of the set point.

Figure 1.7: Aluminum block heater used for silver analysis

1.2.7 Extraction Unit Operations

There are numerous different techniques used to isolate an analyte of interest from the sample matrix for further manipulation and detection. Liquid-liquid extraction is one of the most common approaches to isolating an analyte in an aqueous solution. The technique utilizes the difference in activity of an analyte in an aqueous and an organic phase. The distribution coefficient at equilibrium of the given analyte determines the ratio of analyte that will move from one phase to the other (Berg, 1963). The equilibrium can be influenced by multiple factors including pH, ion concentration,

salting solutions and the addition of strong complexing agents (Berg, 1963). Liquid-liquid extraction can be repeated multiple times to achieve higher extraction recovery and/or to realize higher preconcentration factors.

The common, bench-based approach to solvent extraction often involves milliliter volumes of aqueous and organic phases (Kinrade and Van Loon 1974; Bruland et al. 1979; Miller and Bruland 1994, 1995). The two phases are vigorously shaken to maximize the surface area of the phase boundary across which the analyte is transported. The phases are then allowed to settle for several minutes to allow the phases to separate. A separatory funnel is used to isolate the two layers. This process is often repeated multiple times. For trace metal analysis, the organic phase is back extracted in the same manner with acid. The ratio of sample to organic and organic to acid along with the distribution coefficient determines the amount of preconcentration obtained. The distribution coefficient is the expression of dispersion of the solute across the two phases. In some methods the organic phase is evaporated to dryness and the sample is reconstituted in nitric acid (e.g. Bruland et al. 1979; Miller and Bruland 1995).

There are several methods for liquid-liquid extraction in ZF. The two methods described in this study utilize a tube based extraction and separation in a vial with a conical bottom or in a Silex separation cell (Global FIA, Fox Island, WA). Extraction takes place within the mixing coil tubing as alternating zones of the two phases are aspirated (Figure 1.8). The segmented phases flow through the tubing where laminar flow creates static interaction between the organic phase and the walls of the tubing. A thin film of organic forms on the walls of the tubing allowing the aqueous plug to interact with a

larger surface area and creating an environment for mass transfer of the analyte between the two phases. Research for enhancing extraction and the effect of parameters such as mixing, flow rate, and volume of each phase contribute to the efficiency achieved.

Figure 1.8: Liquid-liquid extraction of ligand bound silver (Ag) from seawater in tubing

Separation of the phases in ZF occurs by dispensing the segmented zones into a vial with a conical bottom or Silex separation cell. The Silex separation cell is fitted with a bottom inlet and a dip tube from the bottom that allows either layer to be removed independent of each other (Figure 1.9). In the conical bottom vial, the zones are aspirated from the bottom by a single dip tube that extends from the top of the vial to the bottom. The segmented zones are dispensed into the bottom of the vial/cell. As the two phases enter the vial/cell, the denser phase immediately settles out on the bottom forming two distinct layers. The layers are typically removed from the bottom. Either layer can be isolated at this point for the next step in the chemistry or dispensed to waste by selectively drawing from the vial/cell. There is a distinct interface between the two zones as they are pulled from bottom of the vial/cell allowing either phase to be collected. In the Silex separation cell, a tube comes up from the bottom to the interface of the two phases allowing the top phase to be removed first when necessary. Between

extractions, the vial/cell is flushed out with carrier and wash solution to prep for the next separation.

A third technique not discussed in this research is the use of an extraction shaker that allows larger volumes of phases to be used for higher preconcentration mimicking a bench top extraction.

Figure 1.9: Silex separation cell

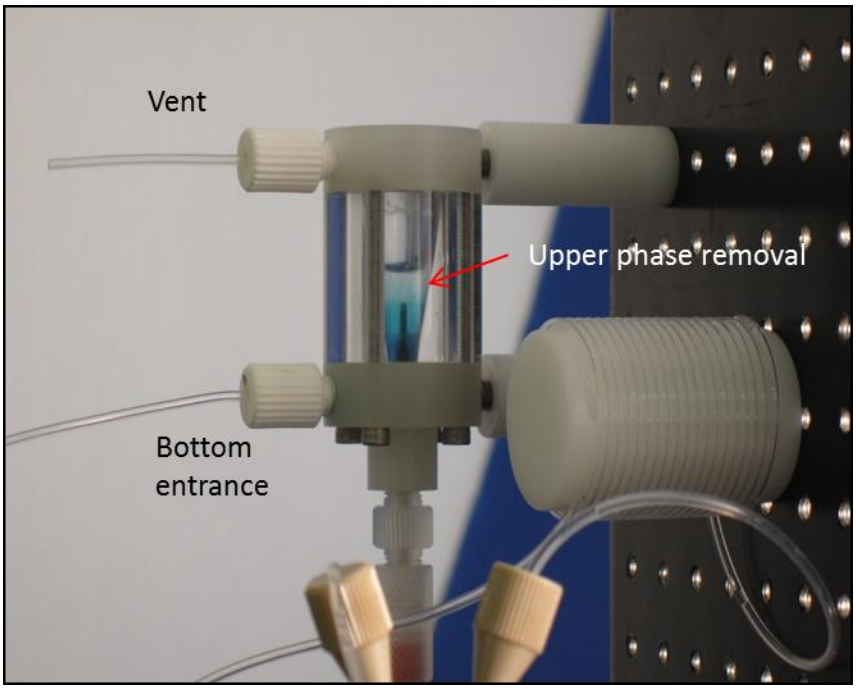

1.2.8 Software

Data acquisition and device control were performed with FloZF software (Global FIA, Fox Island). The LabVIEW-based software controlled all of the devices in the mini-FloPro and was developed at Global FIA (Fox Island, WA). This unique software packages controls sample handling by building multi-step sequences. Each specific

device has a specific set of built in commands that allows for device function and control. Through the individual device steps, sequences are built using multiple steps in a tree-like format. A library of sequences can be saved for repeat use. The software also handles data acquisition; data is collected into individual detector response profiles which can be manipulated using commands in the sequence to determine peak height, peak area, peak average, calculate concentration and add to calibration tables (Figure 1.10**Error! Reference source not found.**). Each profile is displayed in the software with pertinent analytical information specified by the user. Raw data files are also saved to allow data to be manipulated and displayed outside of the FloZF environment.

Figure 1.10: FloZF software measure page with collected data and calibration curve

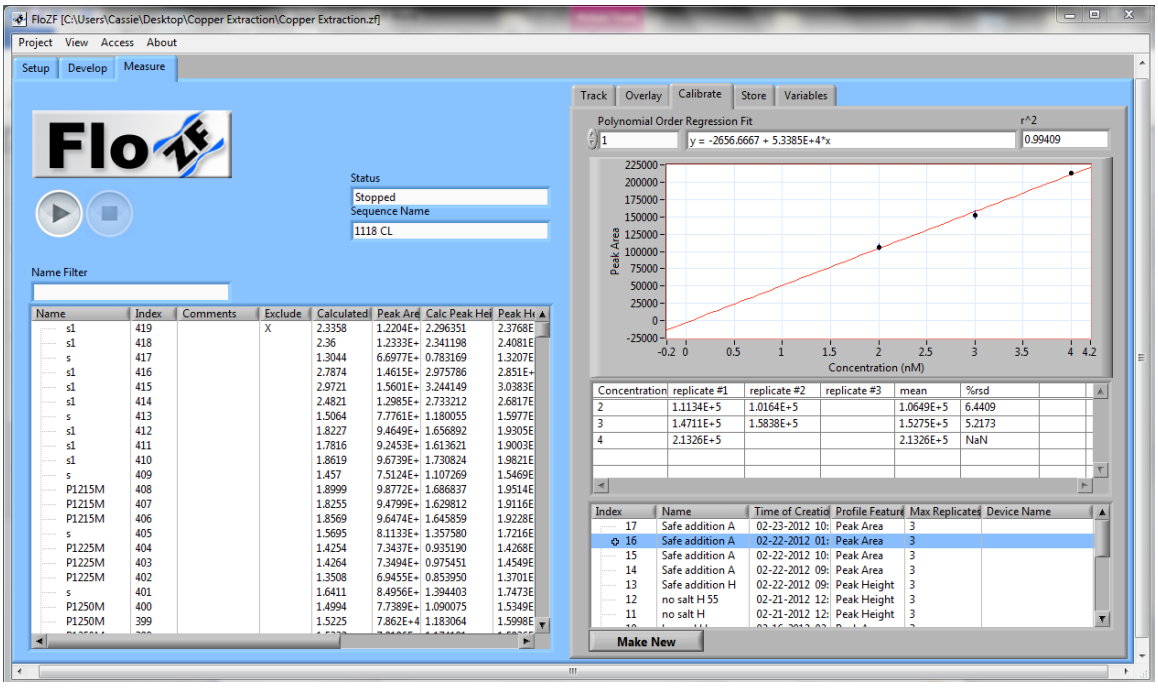

Chapter 2. Optimization of Liquid-Liquid Extraction with ZF

2.1 Purpose

Solvent extraction is yet another classical analytical technique that lends itself to automation using Zone Fluidics. In this research the main unit operation performed is the liquid-liquid phase separation following organic extraction. A miniaturized phase separator, discussed in Section 1.2.7, allows the two phases to settle and either phase to be isolated for analysis or further manipulation. These experiments were designed to understand and optimize the solvent extraction technique using the mini-FloPro. The intent of this study was to test various parameters and the effect on extraction efficiency. Tests were carried out with an extraction of bromocresol purple (BP) from the organic phase into a buffer solution.

2.2 Method

2.2.1 Apparatus

The platform for analysis is derived from the basic layout of the Global FIA mini-FloPro with the addition of unique unit operations for the development of a liquid-liquid extraction analyzer. In this study, the system is designed with the Silex micro-separation cell and a bubble tolerant flow cell connected to a spectrometer (for more detail see Section 1.2).

Figure 2.1: Zone fluidics manifold for liquid-liquid extraction and colorimetric analysis

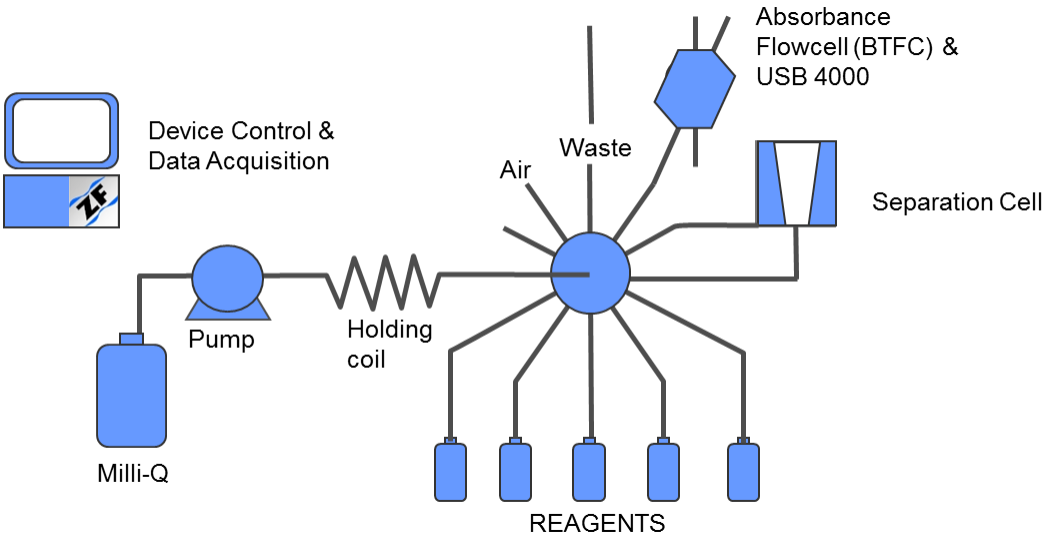

2.2.2 Reagents

A solution of 0.02 M Borax buffer, 0.763g of sodium borate decahydrate (S9640, Sigma) into 100 mL of deionized water, served as the aqueous phase and a 1 x 10^{-3} % V/V BP (B7930.50, Integra) in toluene (T290-1, Fischer) served as the organic phase. The carrier was a solution containing 2 drops of Zonyl FSN 100 fluorosurfactant (421413, Sigma) diluted to 100 mL with distilled water. A 90% isopropyl alcohol (IPA) solution was used as a washing agent.

2.2.3 Sequence

Alternating zones of buffer and toluene were aspirated into the holding coil and dispensed into the separation cell. The aqueous bottom layer is removed from the side port of the separation cell and passed through the bubble tolerant flow cell where the absorbance was measured at 585 nm. The data was collected by the FloZF software and peak height was determined.

2.3 Results

To optimize extraction efficiency and increase sensitivity of the method several parameters were isolated independently to maximize absorbance while maintaining precision. Extraction efficiency is a measurement of maximum peak height at an absorbing wavelength of 585 nm. The following sections outline the extraction optimization process in detail.

2.3.1 Mixing Pattern

Figure 2.2: Serpentine reactor used for mixing. The flowpath is through a cross-stitch pattern.

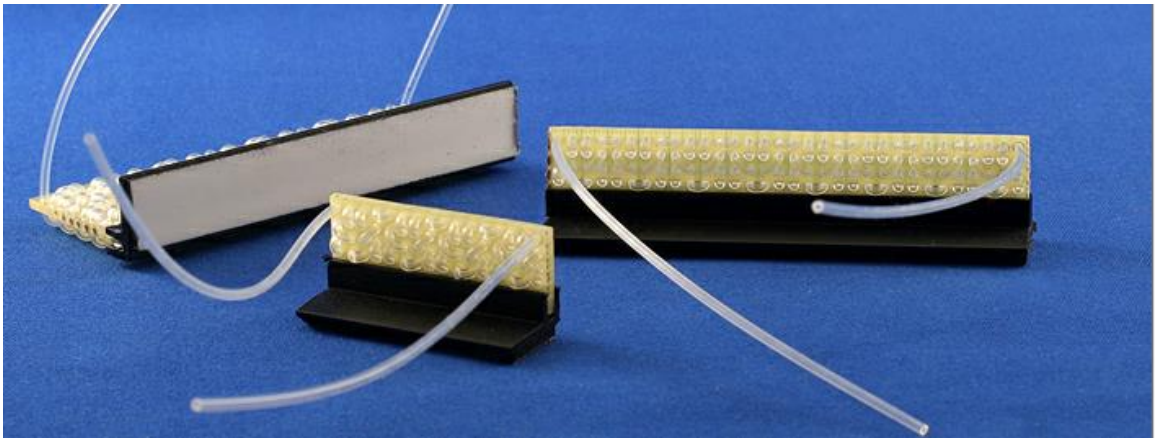

A test was performed to determine the impact of the extraction with a serpentine mixer and a cylindrical mixing coil. In both scenarios, 0.030" PFA tubing was used as a conduit. The mixing coil was wrapped around a 1" diameter cylindrical block and the serpentine is a knitted reactor shown in Figure 2.2. This test was designed to compare the extraction efficiency between a mixing coil and serpentine by monitoring absorbance at 585 nm. The data indicates that the mixing pattern does not significantly affect extraction efficiency or precision (**Error! Reference source not found.**). The

absorbance is comparable and the precision (%RSD) does not show a significant deviation (Table 2.1) when comparing the holding coil and serpentine. As a result, either the serpentine or the cylindrical mixing coil can be used. The mixing coil was used in all further experiments.

Table 2.1: Serpentine and Mixing Coil Comparison for Extraction Efficiency

	Serpentine		Mixing Coil	
	Peak Height		*Peak Height*	
% BP	*585 nm*	*%RSD*	*585 nm*	*%RSD*
0.001	0.220	6.7%	0.231	3.2%
0.002	0.371	3.9%	0.371	6.9%
0.003	0.518	5.1%	0.504	4.7%

Mixing flow rate = 25 µL sec^{-1}, n = 19

2.3.2 Mixing Volume

After aspirating the zone stacks into the holding coil, the zone is aspirated for mixing prior to dispensing into the micro-separation cell. The extraction takes place as the organic phase coats the tubing and the two zones come into contact. A test was performed to determine the effect of increasing the mixing volume on extraction efficiency. The initial sequence aspirated the sample zone and an additional 100 µL into the holding coil prior to dispensing the zone stack into the micro-separation cell. In this experiment, oscillating the zone stack in 100 µL increments multiple times to determine if the extraction efficiency would increase was tested. One oscillation is represented by aspirated the zone an additional 100 µL into the holding coil and then dispensed the zone back 100 µL. The test parameters for the experiment used a 3:1 organic to aqueous ratio at a flow rate of 25 µL sec^{-1}. An increase in absorbance would suggest

that the initial mixing step did not provide sufficient mixing for complete extraction of the model BP to take place. The data, in Table 2.2, shows that the absorbance does not show a significant change as the number of mixing oscillations increase; therefore, one oscillation provides enough mixing to achieve a near quantitative extraction.

Table 2.2: Absorbance of Extraction based on 100 µL Mixing Oscillations of the Zone Stack

# of 100 µL Oscillations	Peak Height 585 nm
0	0.521
1	0.527
2	0.485
4	0.508
8	0.512
10	0.528

Mixing flow rate = 25µL sec^{-1}

2.3.3 Mixing Flow rate

The mixing flow rate during the oscillation step described above was also monitored to determine the impact on extraction efficiency. A 3:1, organic to aqueous, preconcentration extraction was performed at a range of mixing flow rates between 10µL sec^{-1} to 55µL sec^{-1}. The movement of the two phases in the tubing is critical to create a fluid environment where extraction can occur.

Table 2.3: Absorbance of Variation in Mixing Flow rate, 0.003% BP

Flow rate (µL sec^{-1})	Peak Height 585 nm	%RSD
10	0.544	3.5%
25	0.541	4.7%
55	0.524	3.9%

n=5

At this concentration/preconcentration, the average absorbance of the varying mixing rates does not seem to have a substantial effect on the overall peak height and the reproducibility varies but is independent of pump speed (Table 2.3).

2.3.4 Zone Volume – 1:1 Extraction Ratio

An evaluation of zone size was performed using a 1:1 extraction ratio of the aqueous and organic phases. The method for extraction involves aspirating alternating zones of aqueous and organic solutions. To enhance extraction, multiple aqueous/organic zones are aspirated into the holding coil creating a segmented zone stack and increasing the surface area of interaction between the two phases. The volume of the alternating zones was analyzed in this experiment while the ratio of aqueous to organic was held constant. In each experiment, the zone volume of aqueous was equivalent to that of the organic. The total volume of the zone stack was 200 µL. The zone stack was sandwiched by air bubbles on both ends in order to maintain a constant volume of 200 µL.

Table 2.4: Variation in Zone Size on Extraction Efficiency, 0.001%BP

Aqueous:Organic Zone Size	Peak Height 585 nm	%RSD
10 µL	0.231	3.2%
25 µL	0.205	3.6%
50 µL	0.154	4.4%

Mixing flow rate = 25µL sec^{-1}, n = 5

By monitoring the absorbance of the aqueous fraction, the amount of BP extracted can be determined. The results in Table 2.4 show that decreasing the zone size from 50 µL to 10 µL increases the extraction efficiency and precision.

2.3.5 Comparison – Manual vs. Automated

After optimizing multiple parameters of the automated technique, a comparison was performed between the automated technique and the standard manual extraction method. The manual method was performed with a total sample volume of less than 1 mL, the two phases were manually shaken for 2 minutes and then allowed to settle out. The aqueous zone was removed and placed onto an open port on the mini-FloPro. This sample was put through the detector with the same detection method as the automated sequence.

Table 2.5: Comparison of Automated and Manual Extraction

	Manual 1:1	Automated 1:1	Manual 3:1	Automated 3:1
Peak Height, 585 nm	0.14	0.21	0.35	0.56
%RSD	16.4%	4.7%	2.1%	2.1%

n = 3

Based on the data in Table 2.5 it is evident that the automated technique developed here is more efficient for extracting our model analyte. The automated extraction efficiency is likely increased because the contact between the aqueous and organic phases is maximized in the narrow bore tubing. It is also important to note that the reproducibility of the 1:1 extraction is much improved for the automated method.

2.3.6 Extraction Efficiency

To determine the extraction efficiency of the ZF method extracting BP from Toluene into Borax buffer, 0.0015 g BP was dissolved in 100 mL of 0.02 M Borax buffer and passed through the detector. This is the same concentration of BP that is dissolved into Toluene used in the automated solvent extraction technique described above. The peak height of this solution represents the absorbance value of a 100% extraction of BP from Toluene for a 1:1 extraction. The efficiency was determined to be 91%, Table 2.6.

Table 2.6: Extraction Efficiency

	Abs units g^{-1} BP
No Extraction	134
Automated Extraction	122

2.3.7 Preconcentration

Preconcentration is an important step in increasing sensitivity for low level detection. Solvent extraction is a powerful preconcentration technique because the solute can be isolated in less volume than the original sample matrix. By varying the ratio of aqueous to organic phase in the zone stack of the automated extraction technique a preconcentration can be achieved. In this experiment, multiple ratios of toluene:borax buffer were tested. The absorbance at 585 nm of a 1:1 extraction served as baseline for a concentration factor of 1. In Figure 2.3 the data peaks of the preconcentration test show that the highest concentration factor achieved was ~5.3 although the toluene:borax buffer was 10:1. This indicates that the extraction efficiency at a ratio of 10:1 is only 53% on the automated system under these conditions suggesting that the interaction between the aqueous and organic phases was not

optimized. The preconcentration factor may have been improved had the preceding parameters been re-tested at preconcentration sample ratios; however, for this experiment these tests were not performed. A manual extraction was not performed for comparison.

Figure 2.3: Liquid-Liquid Extraction Preconcentration with ZF

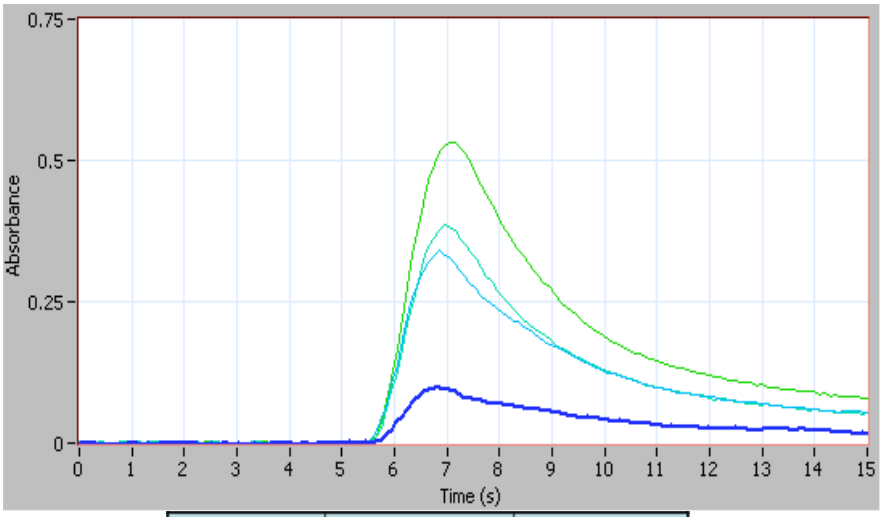

Toluene:Borax Ratio	Absorbance	Concentration Factor
1:1	0.10	1
3:1	0.34	3.4
5:1	0.39	3.9
10:1	0.53	5.3

2.4 Conclusions

The data collected in this chapter provides information on the effect of various experimental conditions on liquid-liquid extraction of the model BP compound in the ZF manifold. The ZF method provides effective liquid-liquid extraction, efficiency greater than 90%, and improved precision over a similarly scaled manual extraction approach. This information provides a library of parameters that will be implemented in the subsequent application of ZF for trace metal extraction and analysis.

Chapter 3. Micro-molar Silver (Ag) Extraction and Analysis

3.1 Purpose

The focus of this study was to develop a zone fluidics method for extracting Ag from seawater. The first step required a colorimetric analysis methodology (Ensafi and Zarei, 1997) to be adapted for the zone fluidics manifold and to determine the accuracy, precision and limit of detection.

3.2 Theoretical Background of Silver

3.2.1 Marine Geochemistry: Abundance and Distribution of Silver

The total dissolved (<0.2 μm based on filtration) concentration of Ag in seawater falls in the range of 1 to 35 pM (Kramer et al. 2011; Martin et al. 1983; Ndung'u et al. 2001; Ranville and Flegal 2005), and its chemical speciation in oxygenated seawater is dominated by the chloro-complexes $AgCl_2^-$ and $AgCl_3^{2-}$ (Miller and Bruland, 1995). The distribution of Ag follows those of the major algal nutrients, particularly silicic acid, typified by very low concentrations in ocean surface waters which increase significantly with depth through the main ocean thermocline (Ranville and Flegal 2005; Kramer et al. 2011). In the sunlit surface, Ag is assimilated by photosynthetic plankton which eventually sink from the upper ocean and decompose in the ocean interior transferring particulate Ag to the dissolved phase (Reinfelder and Chang 1999). Similar to other nutrient elements there is a strong interbasin concentration gradient for Ag along the path of deepwater circulation with deep Pacific waters having ~10-fold higher concentrations than north Atlantic deep waters (Kramer et al. 2011; Bruland and Lohan, 2004). Despite its nutrient-type distribution, there is no known biological function for

Ag. There are several hypotheses to explain the incorporation of Ag into organic matter including its mistaken active assimilation through non-specific cell surface transport proteins of the phytoplankton, the passive adsorption of Ag to cell surfaces or incorporation of Ag into biogenic opal (Phinney and Bruland, 1997).

Overall, the biogeochemical cycle of Ag is not well understood but there is evidence that surface ocean concentrations have been significantly altered by anthropogenic mobilization of the metal through industrial activities (Ranville and Flegal, 2005; Ranville et al. 2010). Silver's toxicity is largely due to its ability to inhibit intracellular enzyme activity leading to cell death. Historically, the major source of Ag to the marine environment was non-ferrous metal production and fossil fuel burning (Smith and Flegal, 1993). In the past few decades there has been an increased use of Ag nanoparticles (AgNPs) in electronics and optics because of their unique electrical and magnetic properties, and in household appliances and textiles given their antibacterial/antifugal properties. These industrial applications have likely led to an increase in Ag entering the aquatic environment. The fate of this Ag and AgNPs in the ocean and their potential impact on aquatic organisms are only poorly understood at present (Handy et al. 2008a; Handy et al. 2008b; Klaine et al. 2008).

3.2.2 Silver Speciation

In marine environments, there are four classes of Ag^+ complexes with markedly different behavior: ionic, inorganic ligand binding, hydrophilic organic ligand binding, and neutral lipophilic ligand binding. Silver ions (Ag^+) in marine environments are in an equilibrium state between inorganic and organic Ag-ligand complexes. Unlike other

trace metals, inorganic Ag complexes, mainly with chloride, dominate the equilibrium dissolved composition (Miller and Bruland, 1995). The charged inorganic and hydrophilic organic complexes are the least toxic due to their inability to diffuse across the cell membrane or through protein channels; however, the free Ag^{+} ion state allows some metal to easily pass through membrane protein channels. Neutral lipophilic complexes are able to enter cells through the lipid bilayer membrane by passive diffusion. The toxicity of Ag decreases with increasing salinity due to the interaction between Ag and chloride ions creating charged inorganic Ag complexes that cannot pass through the cell membrane or protein channels (Ratte 1999 and Reinfelder and Chang, 1999). The majority of dissolved Ag in marine environments is present as $AgCl_x^{1-x}$ complexes. Determination of the chemical speciation, as performed by Miller and Bruland (1995), demonstrated that sulfide (S^{2-}) and thiol ligands (-HS) have the strongest affinity for Ag^{+} ions; however, sulfide and thiols are not stable in oxygenated waters and therefore rare but will play a larger role in controlling the speciation of Ag in anoxic waters. The mechanism of Ag uptake by phytoplankton is only poorly understood. Reinfelder and Chang (1999), determined that the bioavailability of Ag to aquatic organisms increases in the $AgCl^{0}$ state but there is still little known about the kinetics and extent of accumulation in these organisms which is critical to understanding Ag toxicity. More study of the chemical speciation and its relation to bioavailability and uptake by the marine biota is required to understand the biogeochemical cycling of Ag in the marine environment.

3.3 Competitive Ligand Exchange for Metal Speciation

In order to classify naturally occurring ligands and metal speciation a titration curve is generated to determine the saturation point of the ligand. The generic model of total metal, in this scenario general metal (*M*), is displayed in Equation 1 where L_i is naturally occurring inorganic ligands and L_o is naturally occurring organic ligands and *x* is the charge of the metal ion.

Equation 1: Speciation of Metals

$$M_T = M^x + ML_i + ML_o$$

The approach used to determine speciation with liquid-liquid extraction involves competitive equilibration with a ligand followed by an *M* titration to determine the natural ligand concentration(s) and conditional stability constant (temperature, salinity and pressure dependent) describing the equilibrium state of the metal-ligand complex (Miller and Bruland, 1994, 1995). *M* (*x*) speciation is determined by forming a complex with an introduced ligand in the presence of naturally occurring organic chelators. The *M* (*x*) complex is extracted into the organic phase and back extracted into acid for analysis. This concentration is used to calculate the metal complex equilibrium for metal speciation (Moffett and Zika, 1987). By increasing the *M* titration concentration the M_T and *M** titration curve is generated to determine the saturation point of the natural ligand.

Equation 2: Equilibrium of Perturbed Metal Speciation: M_T = total metal, M^x =metal ion, ML_i =inorganic metal complexes, MX_o = organic metal complexes , A = introduced ligand species, M*= quantity of metal extracted (Miller and Bruland, 1994)

$$[M_T] = [M^x] + [ML_i] + [MX_o] + [MA^{x-1}] + [MA_x] + [M^*]$$

M_T is determined by strong ligand binding at low pH allowing all the *M* to dissociate and extract into the organic phase due to the ionic strength of the sample. The back extraction into strong acid breaks the ligand- *M* complex for extraction into the aqueous phase. *M** is determined by the competing ligand equilibrium extraction where the MA_x complex is extracted into the organic phase (Miller and Bruland, 1994). The remaining concentrations of species in Equation 2 can be calculated from equations found in Appendix A

Metal (M) Speciation Equation given predetermined distribution coefficients and formation constants. The curve generated from the titration is linearized to determine competitive ligand concentrations (Figure 3.1). If no competitive organic ligands are present, the curve is linear.

Figure 3.1: Competitive ligand titration curve for Cu from Miller and Bruland (1994) showing the hypothetical curve for Cu titration in the presence of an organic ligand.

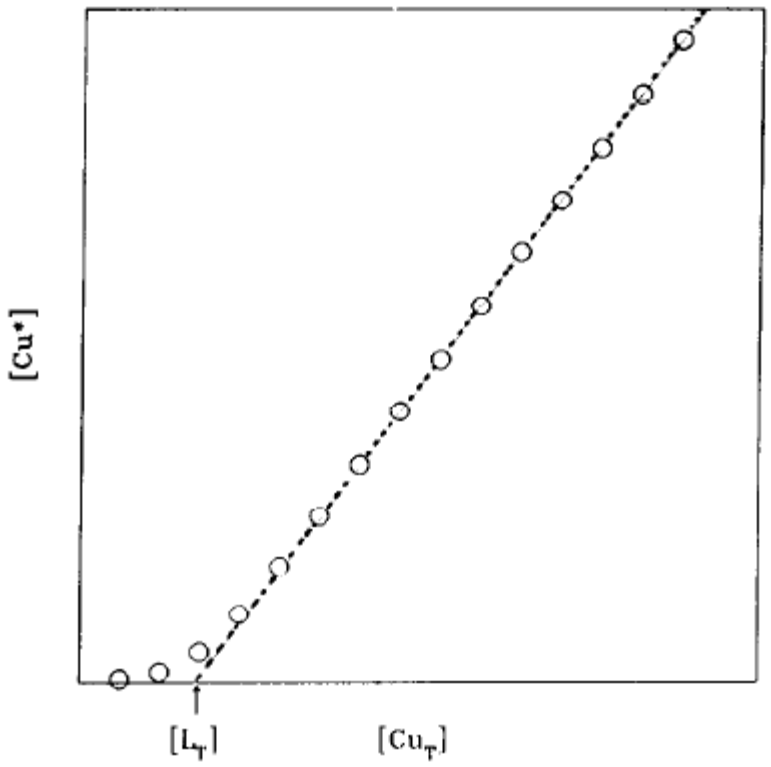

3.4 Method

A method for Ag quantification proposed by Ensafi and Zarei (1997) suggests that Ag detection via spectroscopy can be performed without preconcentration using a catalytic dye solution. Silver (I) and sodium persulfate ($Na_2S_2O_8$) react to form Ag (II) catalyzing the redox reaction of gallocyanine (GC) dye. The GC dye goes from purple to colorless as measured at an absorbance wavelength of 540 nm. The mechanism of the Ag (I) catalyzed reaction is unique. The kinetic disposition of this multistep reaction shows that the rate limiting step is the first order reaction involving the catalyzed oxidation of Ag (I) by persulfate (Anderson and Kochi, 1970). In the first step of the reaction Ag (I) is oxidized by persulfate to produce SO_4^{2-} ions and Ag (II) species. The overall mechanism behind this reaction is not completely understood; however, the

acidity of the reaction allows the Ag (II) high oxidation state to be stable long enough to oxidize the GC dye. At pH <4, the GC dye is ionized at the dimethylamino group (red color) resulting in a positive charge (Michaelis and Eagle, 1930).

The chemistry was adjusted to accommodate an acidified sample collected post liquid-liquid extraction based on the technique described by Kinrade and Van Loon (1974). For extraction, the sample was buffered and a 1% ligand solution was added. Alternating zones of chloroform and the buffered sample mixture were aspirated and extraction took place in the holding coil. The phases separated in the micro-extraction cell. The sample zone was discarded and chloroform was collected for a back extraction with 0.1M HNO_3. The back extraction was performed using the alternating microzone approach similar to the initial extraction.

3.4.1 Apparatus

In addition to the components outlined in the previous chapter and in more detail in Chapter 1, the Ag analyzer has a heated reactor that consists of heated aluminum block with 0.030" inner diameter tubing. The heater was held at 40±0.05 ºC with an Omron temperature controller.

Figure 3.2: Zone fluidics manifold for silver (Ag) extraction and colorimetric analysis

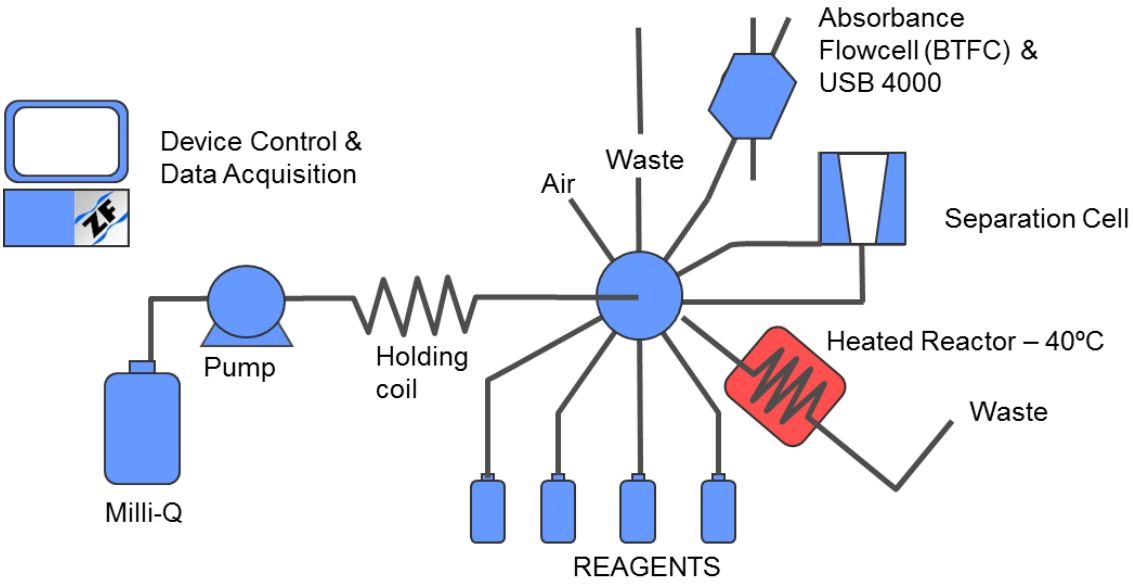

3.4.2 Reagents

Extraction reagents included a 0.1 M sodium acetate buffer (pH 5), 0.22 g acetic acid (127-09-3, Sigma) plus 0.87 g sodium acetate (6131-90-4, Fisher) dissolved in 100 mL deionized water, a 1% solution of diethyldithiocarbamic acid, diethylammonium salt (DDDC) (1518-58-7, Sigma), and chloroform (67-66-3, Integra). The back extraction was performed with 0.1 M HNO_3 (07697-37-2, Integra).

For colorimetric analysis, a stock solution of 0.018 M 1,10-phenanthroline (66-71-1, Alfa Aesar), with 1.62 g of 1,10-phenanthroline in 50 mL of ethanol, and a stock of 4×10^{-4} M GC (1562-85-2, Alfa Aesar), where 63 mg of GC was diluted to 50 mL of deionized water plus 5 µL of 1 M NaOH (1310-73-2, Integra) were made. The dye solution was made by diluting 10 mL of stock 1,10-phenanthroline solution and 10 mL of GC solution to 100 mL. An acidic (pH 1.8) sodium persulfate solution was made by dissolving 23.8 g of sodium persulfate (7775-27-1, Alfa Aesar) in 0.032 M H_2SO_4 (7664-93-9, The Science Company), that was made by slowly adding 200 µL of concentrated

sulfuric acid to 100 mL of deionized water and diluting the final solution to 125 mL with high purity water. Stock Ag solution was made by diluting 0.184 g $AgNO_3$ (7761-88-8, Alfa Aesar) to 120 mL of MilliQ water. The Ag standard concentrations used in this experiment were higher than ambient seawater concentrations for method development purposes.

3.4.3 Sequence

For extraction, alternating zones of sample, ligand and chloroform were aspirated. The zone stack was mixed back into the holding coil allowing extraction to take place. Separation occurred by dispensing the zone into the separation cell. The chloroform formed the bottom layer and was pulled from the bottom of the cell and mixed with alternating zones of 0.1 M HNO_3. The separation cell was emptied prior to dispensing the back extraction zone stack back into the cell. This time, the top layer was removed for colorimetric analysis.

The color chemistry for Ag was performed by mixing the reagents with the sample and heating at 40ºC in a bubble-bound zone for 3 minutes. The zone was pulled out of the heater and dispensed with bubbles into the detector and stopped. The peak average at 540 nm was determined by the FloZF software and the flow cell was flushed with carrier.

3.5 Results

3.5.1 Colorimetric Data

Initial colorimetric data was collected at varying concentrations of HNO_3 to determine if acid strength would impact the analytical performance. At concentrations

of Ag from 5-20 µM, colorimetric analysis was observed in 1 M HNO_3 (Figure 3.3). The %RSD for the curve was less than 10% for all standards. At Ag concentrations below 5 µM the acid concentration was decreased to 0.1 M to improve linearity. The regression correlation coefficient r^2 for 0 – 6 µM in 1 M HNO_3 was 0.986 which improved to 0.999 in 0.1 M HNO_3. The variability at lower concentrations of Ag could be attributed to pH affecting the progression of the reaction or variable system blank contribution at higher HNO_3 concentrations. At 20 µM Ag without HNO_3 present the color was completely reduced to zero compared to an absorbance of 0.43 at 540nm in 1 M HNO_3.

Figure 3.3: Silver colorimetric method in 1 M nitric acid for 5 to 20 µM Ag

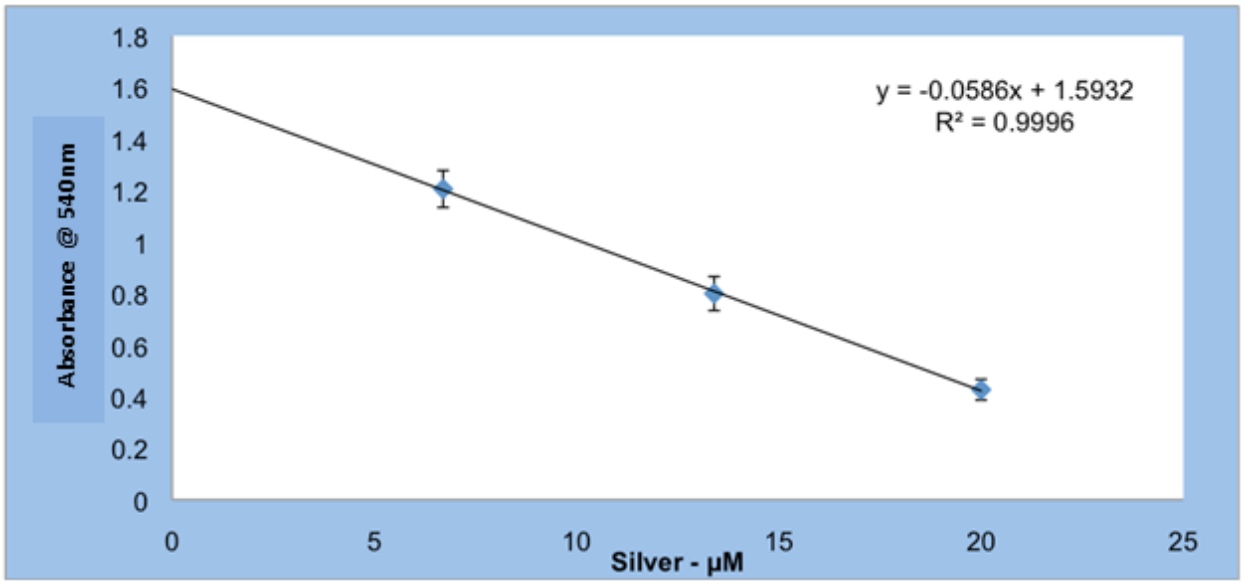

After determining ideal conditions for the colorimetric chemistry, the micro-scale liquid-liquid extraction was coupled to determine Ag concentrations in a seawater matrix.

3.5.2 Extraction Data

Initially a bench top extraction was performed using a 5 mL Mixxor extractor (Z420689, Sigma) based on the technique described by Kinrade and Van Loon (1974).

The chloroform was evaporated to dryness and reconstituted in 0.1 M HNO_3. The bench top extraction comparison tests were performed with a 100 µM Ag standard as a proof of concept. The peak difference for 100 µM Ag and a blank was 0.27 abs units. A comparison was performed online replacing the evaporation step with a back extraction into 0.1 M nitric acid. The difference in absorbance between the blank and the ZF extraction for 100 µM Ag was 0.63 abs units resulting in higher extraction efficiency with ZF than the bench top Mixxor extraction (Figure 3.4).

Figure 3.4: Comparison of bench top Mixxor extraction (–), ZF micro-scale extraction (–) and blank (–) for Ag (100µM). Data collected with FloZF software.

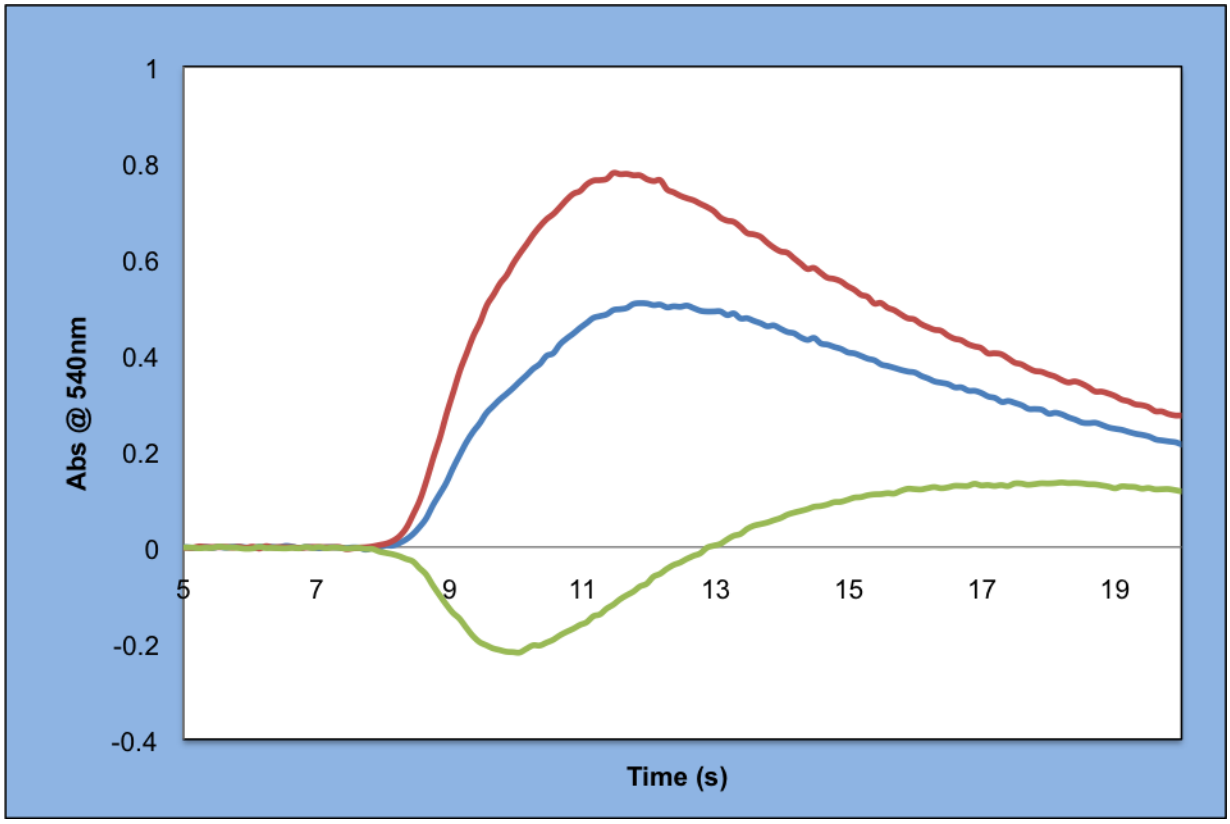

After confirming the successful extraction at 100 µM Ag with ZF, the method was optimized to determine the lowest limit of extraction based on the limit of detection of

the colorimetric chemistry, 0-6 µM (Figure 3.5). Within this range, a check standard of 4 µM Ag resulted in an absorbance of 1.2 abs units with 1.3% RSD on 5 replicates. The detection limit of this method based on the standard deviation of the blank was determined to be 0.6 µM.

Figure 3.5: Micro-scale liquid-liquid extraction of Ag with ZF

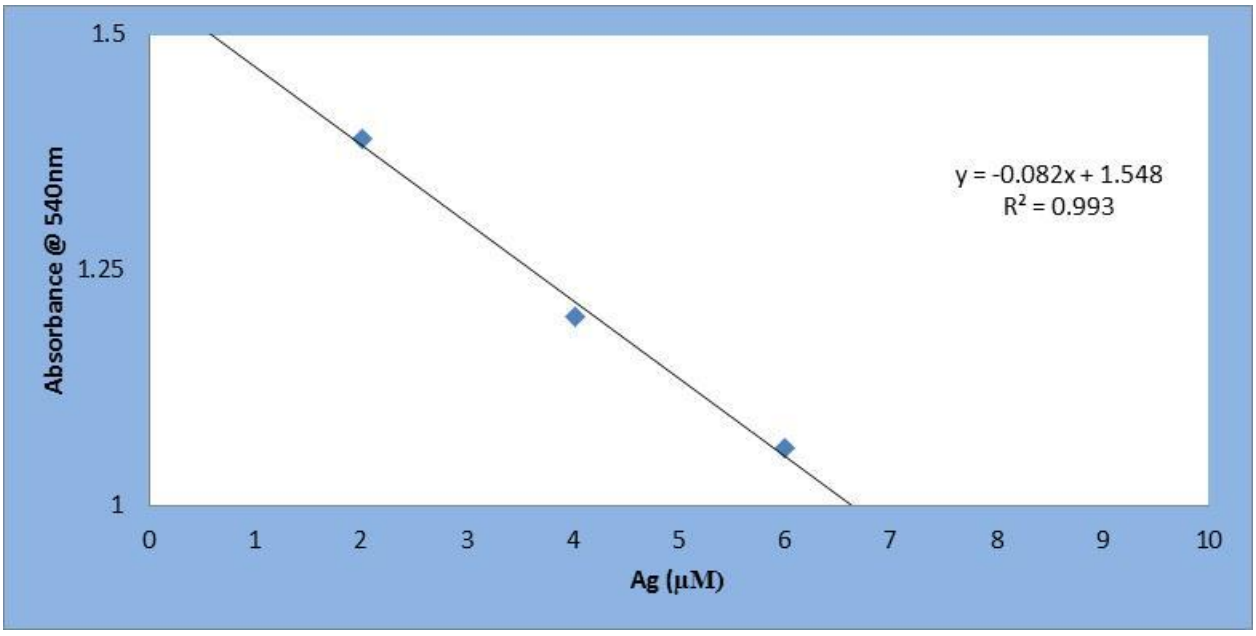

3.6 Conclusion

Based on the experimental data presented here, the ZF method for liquid-liquid extraction and colorimetric analysis of Ag is useful at the µM level. While not suitable for detecting Ag at open ocean concentrations (10^{-12} to 10^{-10} M) this technique could be implemented to measure wastewater effluents, or near shore water samples that contain concentrations approaching 10^{-7} to 10^{-5} M levels of Ag. The information collected from this extraction study with ZF, as proof of concept, suggests that micro-scale liquid-liquid extraction of metals can be a useful approach to preconcentrate

metals from the seawater matrix for subsequent analysis. The extraction and detection of dissolved Ag at 10^{-7}-10^{-5} M levels can be performed on the ZF analyzer in less than 30 minutes and greatly reduce the consumption of hazardous reagents making it ideal for shipboard detection or return of concentrates to the laboratory for more sensitive analytical techniques (e.g. inductively coupled plasma mass spectrometry; ICP-MS). Conventional extraction techniques typically involve a ~12 hour evaporation of the back extracted HNO_3 phase (Kinrade and Van Loon, 1974).

While this technique is suitable for µM Ag concentrations in order to measure relevant levels of trace metals in the open ocean the detection limit must be in the pM range. Due to these limits on detection but successful demonstration of metal extraction and preconcentration, the next step is to determine a detection chemistry that will allow for trace metal analysis with ZF as an analytical finish to the extraction technique. In Chapter 4, the development of a ZF technique suitable for 10^{-10} – 10^{-9} M Cu concentrations is presented where the adaptation and optimization of an existing chemiluminescence based FIA technique (Zamzow et al., 1998) is described.

Chapter 4. An Improved Method for Determining Dissolved Copper in Seawater

The purpose of this study was to determine an accurate and precise ZF method to determine dissolved copper (Cu) in seawater at the nanomolar (10^{-9} M) level. The goal of this chapter is to adapt and optimize the FIA-chemiluminesence method for a ZF platform. The current published method uses chemiluminescence (CL) to measure nanomolar levels of Cu in natural water samples (Coale et al., 1992, Sangi et al., 2003, Zamzow et al., 1998).

4.1 Introduction

4.1.1 Marine Geochemistry

In recent decades the recognized importance of trace metals as modulators of biogeochemical processes relevant to climate change, like carbon fixation, has led to renewed efforts to understand the marine biogeochemical cycles of trace metals (Henderson et al. 2007). Trace metals can serve as essential nutrients and potential toxins that act to control the species composition and biogeochemical rate processes of marine microbes. They impact the productivity of marine ecosystems and the production and consumption of climatologically active gases.

Copper is one such trace metal that is essential for some biological processes but that can be toxic to some marine microbes at environmentally relevant concentrations (Mann et al., 2002). Typical vertical dissolved (<0.2 µm based on filtration) Cu profiles in the open ocean marine environment display nutrient type depth profiles (Boyle et al. 1977; Bruland and Lohan, 2004; Moffett 1995; Moffett and Dupont 2007). Nutrient type

distributions are typical of bioactive metals where uptake occurs in the sunlit surface layer where photosynthetic microbes are active. The transport of sinking biomaterials from the surface layer followed by decomposition returns the metal to the dissolved phase in the ocean interior as seen in Figure 4.1.

Figure 4.1: Vertical profile of dissolved copper for VERTEX VII Sta. T-8 (55.5°N;147.5°W), collected 10 August 1987 (Martin et al., 1989).

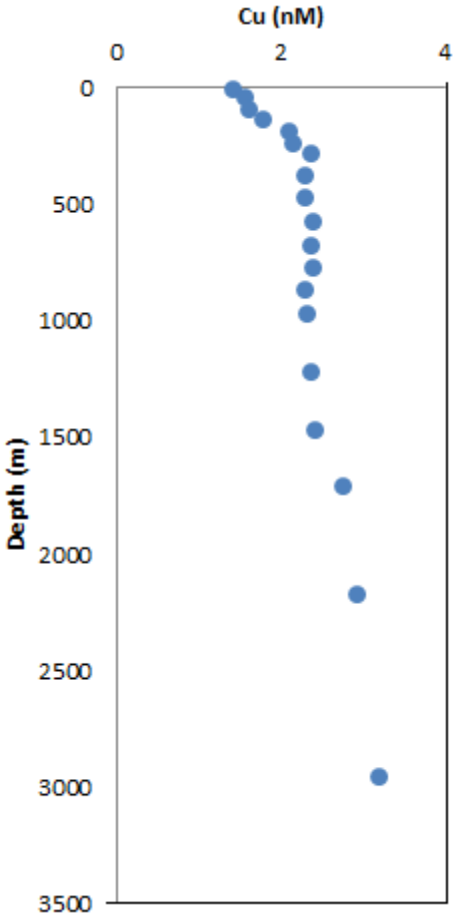

The continued increase of Cu at depth suggests that the sediment represents a significant source of dissolved Cu to the water column while advection-diffusion models correlating temperature and Cu concentration shows that Cu in bottom water not in

direct contact with the sediments is highly scavenged (Coale et al., 1992 and Boyle et al., 1977). Boyle et al. (1977) calculates a half-life of 1100 years for the removal or scavenging of Cu. The major sources of Cu to the upper ocean are from aeolian deposition of aerosols at the ocean surface and riverine input at the ocean margins (Bruland and Lohan, 2004).

Speciation, the chemical form that an element takes in solution, is an important factor that controls trace metal bioavailability and regulates its biogeochemical cycling in and ultimate removal from the ocean. Metals bind to organic or inorganic chelators abundant in natural waters. Uptake of Cu by marine organisms is heavily dependent on the speciation in the natural environment. Brand et al. (1986) determined that free ionic Cu^{2+} can be toxic at sub-nanomolar ($<10^{-9}$ M) levels to specific phytoplankton, including *oceanic* species of coccolithophores and the centric diatom *Thalassiosira oceanica*. However, organic Cu complexes dominate the dissolved Cu pool in seawater with more than 99.8% of Cu bound to strong ligands in the surface layer (Boyle et al., 1977). Without organic complexation of Cu^{2+}, free Cu ion concentrations would be at toxic levels for many phytoplankton in surface water. Strong copper-binding ligands are found in concentrations of 1-2 nM decreasing Cu availability by ~1000 fold (Bruland and Lohan, 2004). The exact provenance of these strong chelators is unknown but marine prokaryotic and eukaryotic plankton release an array of complexing ligands in response to elevated Cu concentration; however, at this point, only detoxifying chelators have been identified for metals other than Fe (Morel and Price, 2003). Due to the high

hydrophilic, organic complexation of Cu, a large percent of Cu in the surface layer is not depleted by biological activity.

Copper is an important co-factor in several physiologically essential metalloenzymes and proteins. Metal cofactors play a key role in the enzymatically catalyzed steps of the nitrogen cycle (Morel and Price, 2003). Copper is required by nitrous oxide reductase in the last step of denitrification breaking down N_2O to N_2 (Moffett et al., 2012). Copper is also a key metalloenzyme in ammonia monooxygenase that catalyzes the first step of ammonia oxidation. Despite the essential role it plays in microbial physiology Cu is normally thought to influence marine microbial community composition and productivity as a toxin by interfering with the uptake of other metals and inhibiting enzyme function due to the production of hydroxyl radicals or binding to –SH groups (Mann et al., 2002). More recently Cu has been demonstrated to play an important role in the strategies evolved by microorganisms to deal with chronic Fe-limited conditions in open ocean environments. For example a Cu-containing electron transfer protein called plastocyanin can be substituted for Fe-containing cytochrome c_6 to alleviate cellular demand for Fe (Peers and Price, 2006). In response to Fe-limitation some microbes can also upregulate a high affinity Fe transport system that depends in part on a multi-Cu containing oxidase and permease proteins (Maldonado et al., 1999). Observations suggest that open ocean microbes have significantly higher cellular demands for Cu and that their ability to obtain Cu from the environment might therefore impact the basin scale distribution of Cu and impact biogeochemical rate processes in Fe-limited ecosystems like C and N fixation (Annett et al., 2008). For this

reason research into distribution and chemical speciation of Cu is experiencing somewhat of a renaissance.

Figure 4.2: Conceptual drawing from Wells et al. (2005) demonstrating the role of Cu-oxidase in Fe uptake and the influx of Cu in Fe limited environments in *Pseudo-nitzschia*.

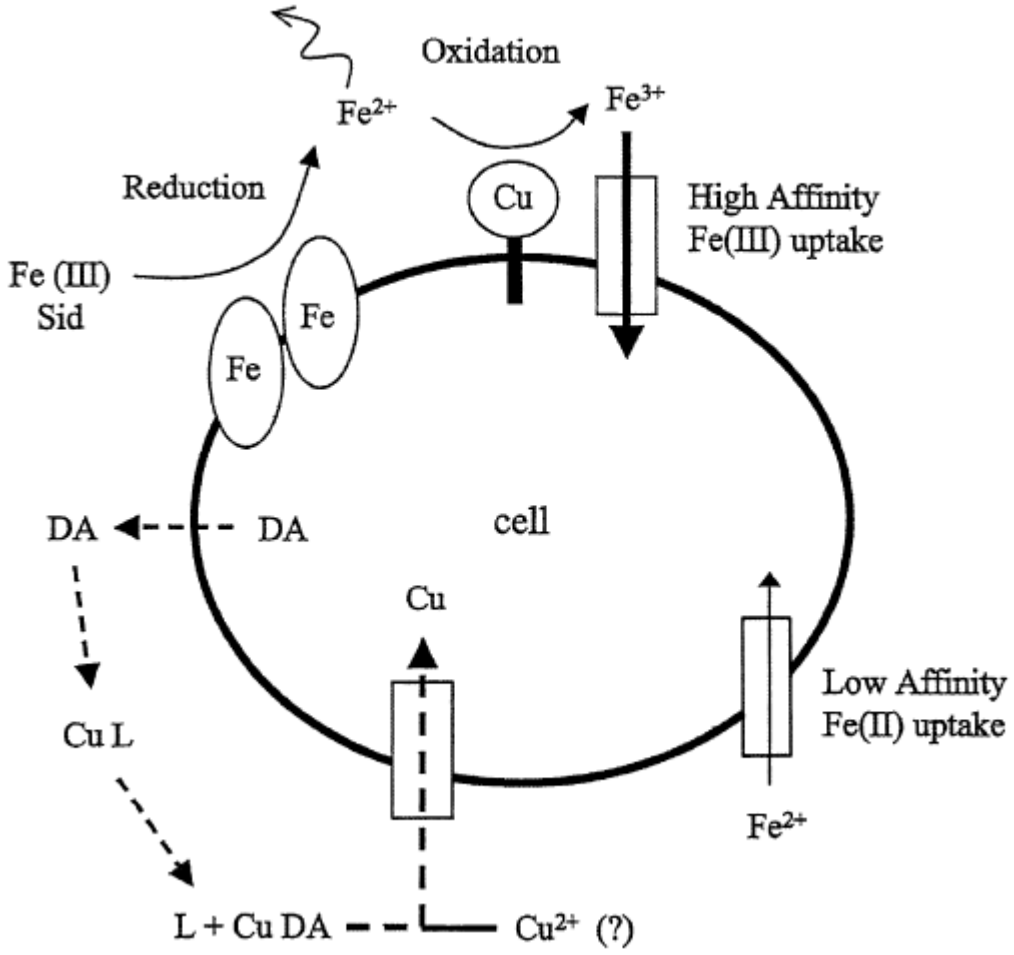

Wells et al. (2005), demonstrated the important relationship between Fe and Cu in Fe-limited environments. Wells et al. (2005), observed that open ocean pennate diatoms of the genus *Psuedo-nitzschia* produce domoic acid (DA) to alleviate stress in

Fe-limited environments. DA is a strong Cu chelator allowing increased Cu in the cell that can, in turn, enhance Fe uptake by the cell (Figure 4.2).

Phinney and Bruland (1997), looked at the effect of a dithiocarbamate based fungicide on metal uptake in phytoplankton due to complexing with the metal to form organic, neutrally charged lipophilic compounds. Lipophilic compounds were more readily absorbed through the cell membrane and available for phytoplankton uptake. The metals are transported across the cell membrane where they dissociate from the transport ligand and complex within the cell resulting in passive uptake of metals like Cu. This phenomenon has not been directly associated with natural uptake of Cu in phytoplankton but demonstrates the importance of available ligands for metal binding associated with uptake, assimilation and potentially toxicity.

4.1.2 Analytical Methods for Determining Copper in Seawater

Sample preparation for measuring copper in seawater range from techniques designed to remove the seawater matrix by extraction to detection directly in seawater. By removing the seawater matrix, interferences are removed allowing for Cu detection by flame atomic absorption (FAA) or graphite furnace atomic absorption (GFAA) spectrometry (Kinrade and Van Loon, 1974, Boyle et al., 1977, Moore and Burton, 1976, Bruland and Franks, 1979 among others) as well as other detection techniques. A detailed outline of a liquid-liquid extraction to remove the seawater matrix is described by Kinrade and Van Loon (1974) and was used in Chapter 3 for µM Ag analysis with ZF. Moore and Burton (1976) reported similar results in the Atlantic Ocean using solid phase extraction (SPE) chelating resin to isolate Cu from seawater. SPE limits the potential for

metal speciation determination compared with the commonly used competitive ligand exchange method discussed in detail in Section 3.3.

The other key component to method development for analytically accurate and meaningful data is detection. Detection techniques like GFAA, FAA and inductively coupled plasma mass spectrometry (ICP-MS) require the trace metal to be extracted from seawater to remove interferences and often require preconcentration in order to achieve low detection limits. This instrumentation is not ideal for shipboard analysis due to the complexity and size of the device. Zamzow et al. (1997) described an FIA method using chemiluminescence (CL) detection for measuring Cu directly in seawater. The CL technique is ideal for portability and ship-based analysis. By adapting this method to ZF, the goal was to achieve low detection limits while reducing sample and reagent volumes. After validating this method with acceptable reference standards, this detection method also allows for future ship-based liquid-liquid extraction and speciation determination.

Chemiluminescence is a chemical reaction where light is generated by an excited transition state prior to product formation. The electronic state of the intermediate fluoresces as it decays to the ground state of the product. In the reaction of 1,10-phenanthroline with H_2O_2, an excited intermediate state is formed generating a CL signal. The O_2^- radical is involved in generating the CL signal in this reaction. The proposed mechanism of this reaction forms several intermediates. The dioxetane intermediate thermally breaks down to form an excited carbonyl compound (Fedorova, 1979). The interaction of this excited state with an O_2^- radical forms the dicarboxylic

acid product. Cu is a known catalyst for this reaction by forming a Cu-1,10-phenanthroline complex (Yamada, 1984). The Cu concentration can be determined when the reactants are in excess over Cu in an alkaline solution. The excited products of the catalyzed reaction return to the ground state emitting photons collected by the photon counter. The limit of detection for this reaction is enhanced through the addition of an alkylammonium salt surfactant that forms micelles (Yamada, 1984). This creates a hydrophobic environment enhancing the solubility of the uncharged reactants and intermediates.

Figure 4.3: Proposed mechanism for CL generation of 1,10-phenanthroline and superoxide anion radical (Fedorova, 1979 and Sangi, 2003)

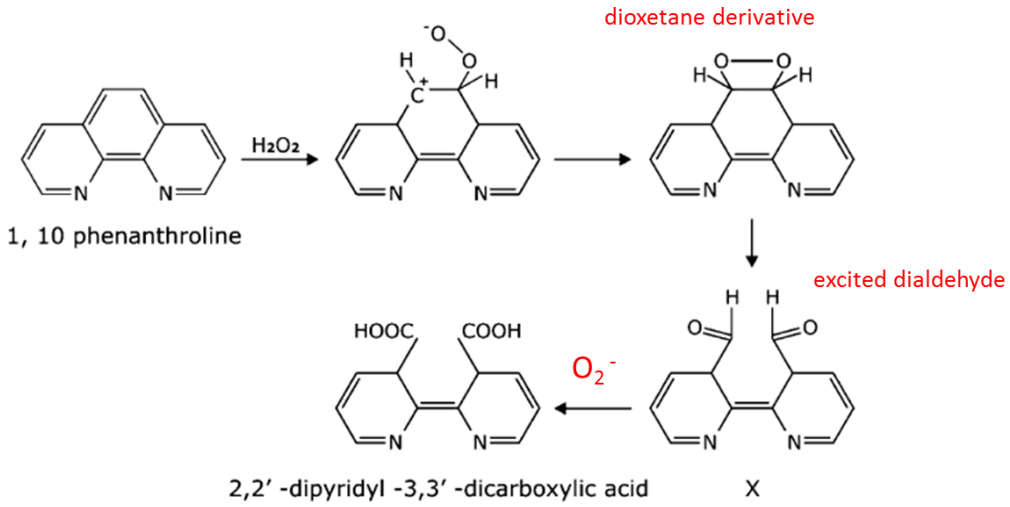

4.2 Methods

The platform for analysis was derived from the basic mini-FloPro apparatus discussed in Chapter 1 (Marshall et al., 2003). For low level Cu measurements, two pumps and two valves allowed the sample and reagent streams to merge at the face of the detector. The addition of a second pump was critical due to the nature of the CL reaction happening almost instantaneously. By merging the two streams as they

entered the flowcell the resulting signal is maximized which was lost if the reagent and sample were mixed in the holding coil. The manifold shown below has the potential to incorporate extraction coupled with detection; however, this research does not include the extraction method developed in previous chapters.

Figure 4.4: Copper CL ZF manifold

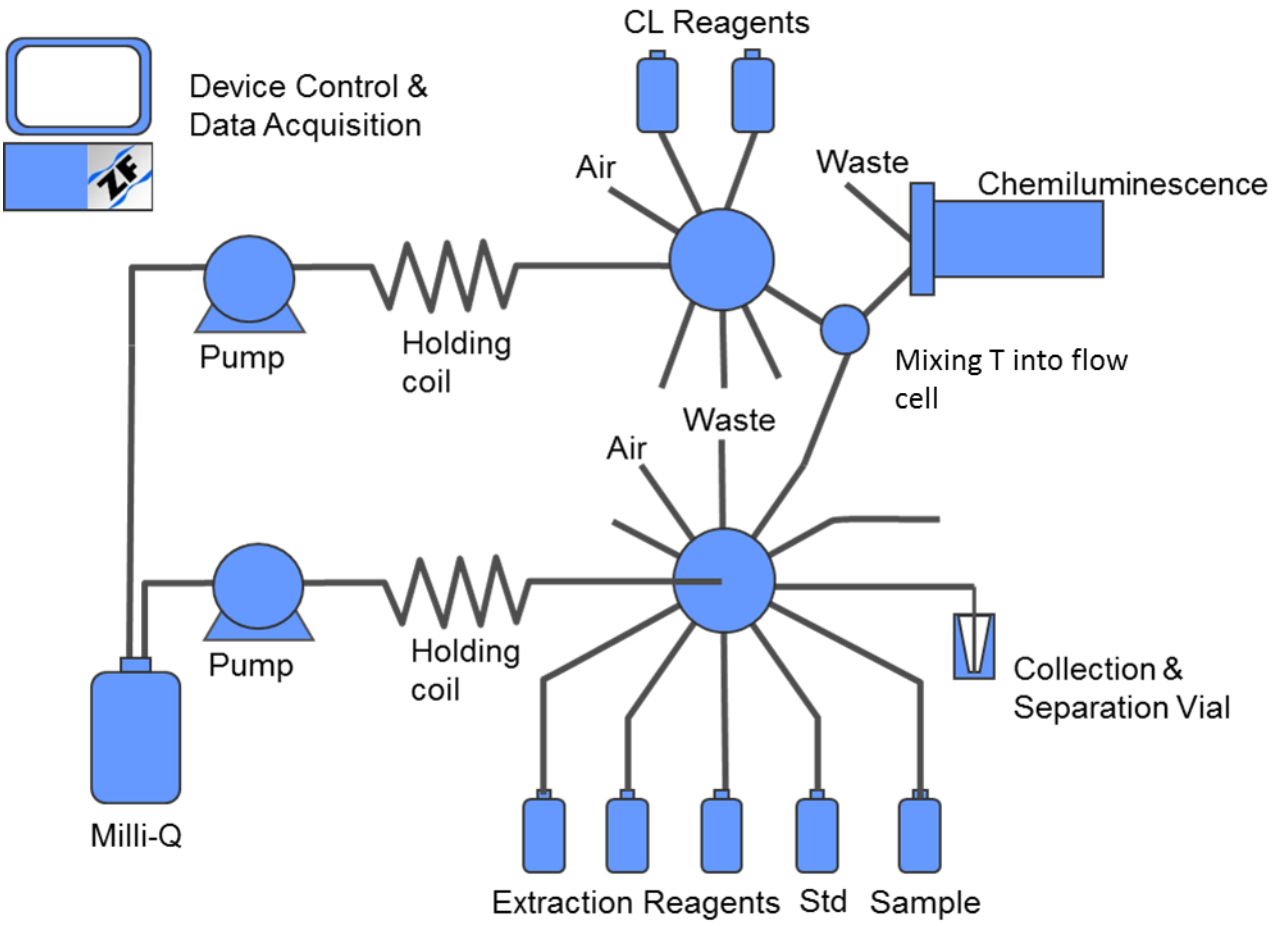

The CL reagent was prepared according to Zamzow et al. (1997). A stock solution of 1,10-phenanthroline (66-71-1, Alfa Aesar) was made by dissolving 65 mg into 3 mL of MQ and mixing for at least 1 hour stored at 4°C for 1 week. Tetraethylenepentamine

(TEPA) (112-57-2, Sigma) solution was prepared by diluting 7.5 µL of a concentrated stock from the manufacturer to 10 mL in MQ. The working CL reagent was prepared by dissolving 240 mg ethylhexadecyldimethyl ammonium bromide (CEDAB) (124-03-8, Alfa Aesar), 90 mg NaOH (1310-73-2, Integra), 3 µL TEPA stock and 138µL 1,10-phenanthroline stock in 30 mL MQ. This reagent was mixed on a shaker table for approximately 1 hour before use and prepared fresh daily. The carrier solution was MQ. A 10% H_2O_2 solution was used diluted from ultratrace grade 30% H_2O_2 (7722-84-1, Fluka) and prepared daily. A calibration stock solution was prepared daily through serial dilution of a concentrated AAS Cu standard (MSCU-10PPM, Inorganic Ventures) in 0.02 M HCl acid (double distilled from University of Victoria) in Bermuda seawater. All reagent and sample handling was conducted in laminar flow clean bench (AirClean) with HEPA filter under Class 100 conditions to minimize the potential for contamination. All bottles and volumetric-ware were cleaned according to stringent GEOTRACES trace element cleaning protocols found in Appendix D: LDPE Cleaning Procedure.

The procedure for Cu determination with the ZF system is as follows. Pump 2 is used to aspirate a bubble-bounded sample zone. A bubble bounded stack of CL reagent and H_2O_2 is aspirated into the holding coil via pump 1 and mixed. The zones are mixed in a 6 loop serpentine coil on the way into a "T" fitting where the reagent and sample zones merge ~2 cm from the flow cell and detector. The zone is bound by bubbles as it mixes into the flow cell. The signal from the photon counter is collected by the FloZF software at 0.5 sec intervals and the peak height and area are determined. A calibration curve generated from standards allows the unknown Cu concentration in the sample to

be determined. The flow cell is then flushed with carrier prior to the next sample. For a typical sequence code please see Appendix C: Copper CL Sequence.

4.3 Results

4.3.1 Flowrate

The optimal flowrate was adapted from the FIA method reported by Zamzow et al. (1998) where the premixed reagent stream flow was 2.85 times faster than the sample stream. The flowrates for ZF methods are typically slower than FIA methods as well as lower volumes used by ZF; therefore, the same flowrate ratio of sample to reagent was used to determine optimal flow for ZF. The initial tested range for sample flowrate, ranging from 5 to 15 µL/s, taking into account the volume of the flowcell and residence time for adequate signal. Using fast flowrates results in poor repeatability in peak profile due to compression of the air bubbles between the mixing sample/reagent zone and the carrier (MQ). The final flowrates were 12 and 34 µL/s for the sample and reagent stream resulting in a flowrate ratio of reagent to sample of 2.83.

4.3.2 Optimizing pH

Figure 4.5: Precipitate that formed in the flowcell due to high pH of the CL reaction. The flowcell insert (left) and quartz window (right) became blocked with precipitate.

The pH of the reaction is also critical in achieving a distinguishable signal for nM Cu concentrations. Coale *et al.* (1992), report that the chemilumenescence signal is maximized when the reaction pH is between 9.8 and 10.1. Initially, the pH of the reaction was too high causing a precipitate to form in and block the flowcell (Figure 4.5). The pH of the ZF method was changed based on the concentration of the NaOH used in the reagents. The pH of the reaction with the ratio of sample to reagent in this experiment was determined to be approximately pH 10 when mixing on the benchtop based on the optimal flowrates discussed in section 4.3.1. An online test was performed by placing a flow through pH meter at the merging point of the sample and reagent streams to determine the pH of the mixed zone as it entered the flowcell. The volume of the pH flowcell interrupted the CL signal so the pH meter was removed for analyses. This test data was lost due to a computer crash so the idea is presented here without data.

4.3.3 Flow cell Insert

Initial method development was conducted with a serpentine flow cell insert, Figure 4.7 (Terry *et al.*, 2008). Although a calibration was achieved at nM Cu concentrations the baseline value started below 200 counts and after the first run increased to over 5000 counts preventing future accurate measurements to be achieved at low nM levels. The high baseline is shown in Figure 4.6 in the Cu CL profile (green), where the Cu CL zone was stopped in the detector to monitor signal decay, and the baseline profile (aqua). Two tests were carried out to determine if the increase in baseline was due to

the sensitivity of the detector, carrier over, or due to the reagent chemistry: testing exposure to light and a coil type flowcell.

Paul Francis at Deakin University in Australia who had worked with the same flow cell and various inserts to achieve sensitive measurements saw similar results as shown in Figure 4.6 (Terry *et al.*, 2008). He too had noticed that the baseline was quite high with the serpentine insert but could not identify the cause. The first test to determine the source of high background was to expose the photon counter to light to determine if the detector was the cause of the baseline shift (Figure 4.6). Immediately after the light was removed from the detector, the baseline returned to less than ~200 counts leading to the conclusion that the chemistry or carry over was liable for the baseline shift.

Figure 4.6: Data showing high baseline and the test of light exposure to the photon counter with the serpentine flowcell. Shown is the Cu CL signal where the sample is stopped in the flowcell to see if the signal decays without flushing (green). The baseline is high after a Cu CL run (aqua) the signal due to introducing and removing light directly to the detector without a flowcell (blue).

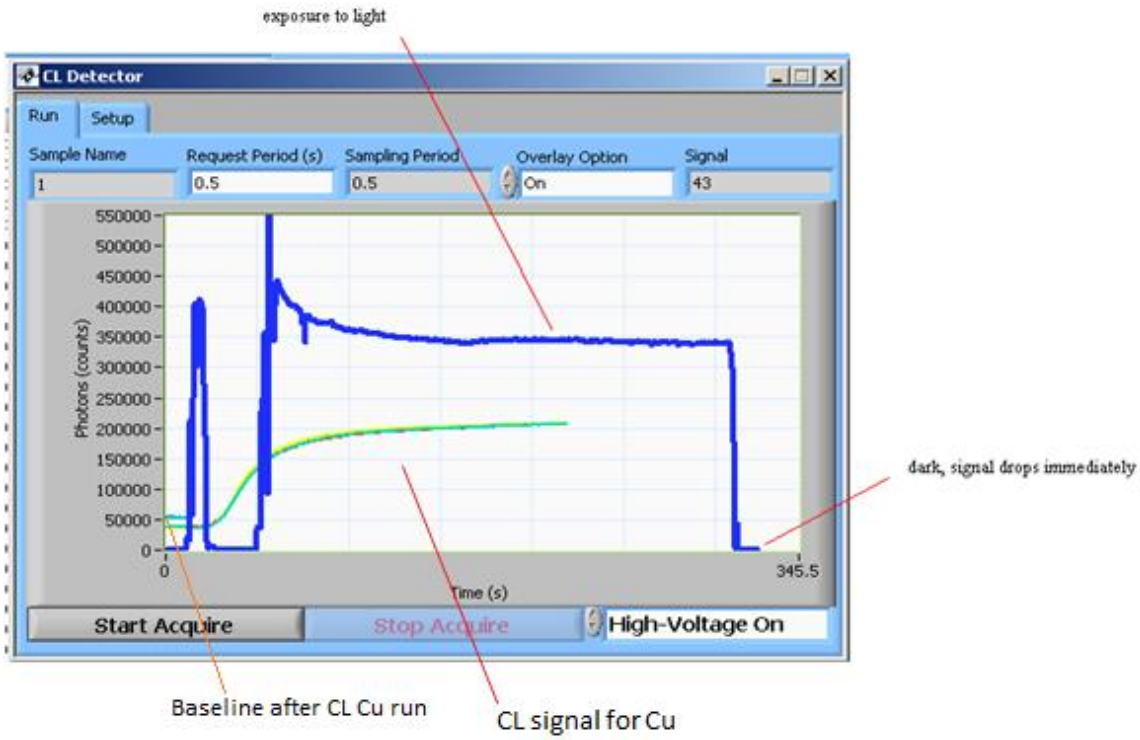

The only way to reduce the baseline during CL analysis was to wait over 10 minutes. No volume of flushing would reduce the baseline suggesting that there existed some amount of dead volume that prevented the flow cell from completely flushing out. The odd mixing pattern seen in Figure 4.7 supports this conclusion showing pockets of mixing and areas that potentially were not thoroughly flushed. Based on this data, the flow cell insert was switched from the serpentine geometry to the coil or spiral geometry.

Figure 4.7: Flow cell inserts: TOP - Mixing of acidic bromothymol blue (yellow) mixing with NaOH (clear) resulted in mixed zones (blue); serpentine (left) and coil (right); BOTTOM – empty flowcell insert; serpentine (left) and coil (right).

In previous studies at Global FIA with ATP, the coil insert was about 40% less sensitive than the serpentine. Initial tests with the coil for Cu CL chemistry proved that the serpentine was the cause of the high baseline. With the coil insert in place, the baseline returned to less than ~200 counts with less than 500 µL of flushing with carrier (Figure 4.8). It was also sensitive enough to distinguish between 0 nM and 1 nM Cu. The sensitivity of the CL reagents were found to decrease as the reagents aged so it is critical to have fresh reagents and to run check standards frequently to confirm that the reagent has not lost sensitivity during an experiment.

Figure 4.8: Peak profile overlay of ZF chemilumenescence method for 0 nM and 4 nM Cu with the coil flow cell

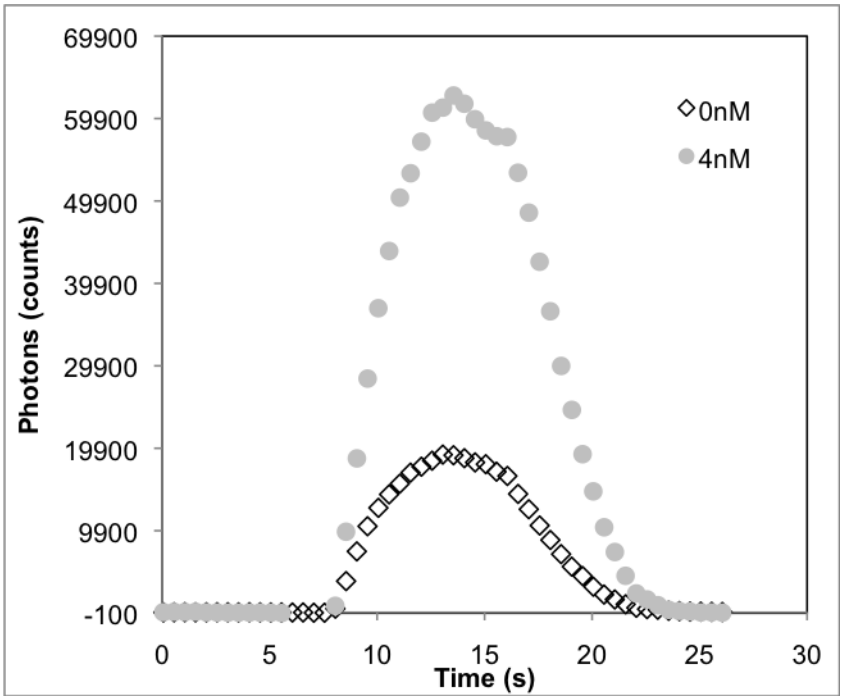

4.3.4 SAFe D2 Reference Determination

A calibration table was generated with the diluted Cu standards made up in acidified low Cu seawater, Figure 4.9, collected in Bermuda. The consensus in the field is that this area has little to no Cu and was validated for this method with a consensus standard. The precision of the calibration standards based on four replicates was less than 5% relative standard deviation. The method was validated for accuracy by determining the concentration of the SAFe (Sampling and Analysis of Iron) D2 consensus reference material (www.geotraces.org). The reference standard is a consensus value of several labs data based on various analysis methods; therefore, as techniques are improved the value of the standard can change (Table 4.1). The calculated value based

on the ZF method and calibration determined the reference material to be 1.77 ± 0.25 nM Cu. Lab A and B determined dissolved Cu using isotope dilution and Lab F and H utilized a UV oxidation step. These labs determined higher concentrations of Cu in the consensus standard. Based on the data in Table 4.1, there appears to be a necessary UV digestion or isotope dilution step in order to determine dissolved Cu in seawater by releasing all forms of Cu. UV oxidation is a step that can be implemented with the ZF platform in the future.

Figure 4.9: Calibration of nM Cu in seawater with ZF.

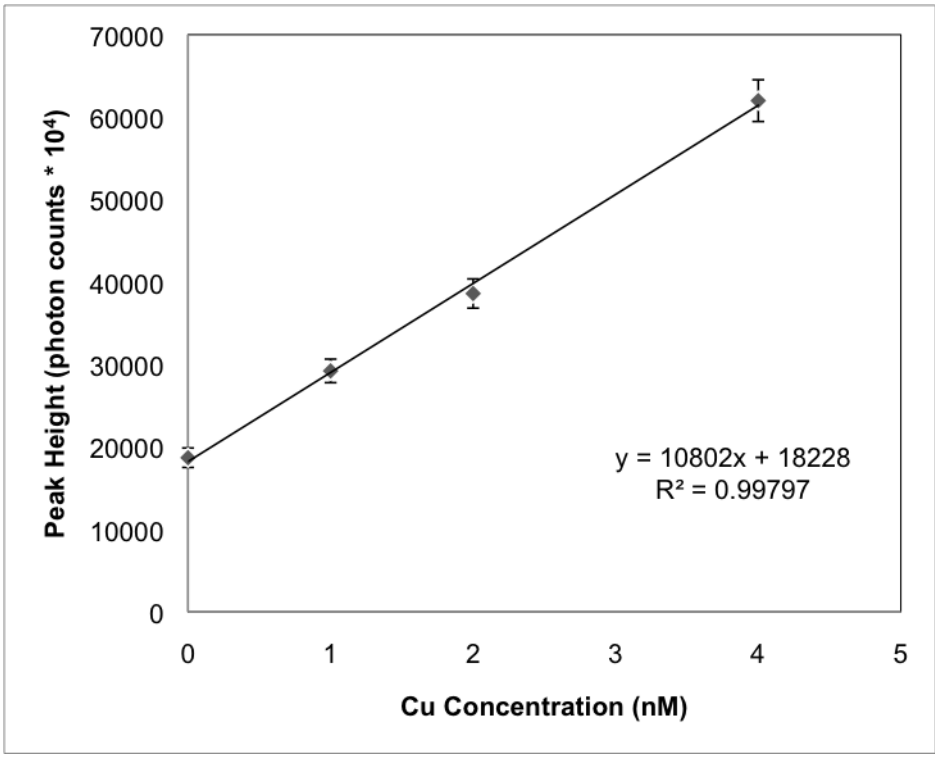

Table 4.1: Reference for Cu analysis – SAFe D2

Technique	*Average Cu (nM)*	*Standard Deviation*	*No. of analyses*
Zone Fluidics	1.77	0.25	n = 5
Certified Value	**2.02**	**0.17**	**n = 5**
Measurements from anonymous labs			
Lab A	2.33	0.09	
Lab B	2.49	0.10	
Lab C	1.92	0.06	
Lab D	1.95	0.13	
Lab E	2.15	0.09	
Lab F	2.26	0.35	
Lab G	2.28	0.03	
Lab H	2.10	0.13	
Lab I	1.84	0.06	
Lab J	2.01	0.14	
Lab K	1.76	0.25	

The method performance was determined by comparing literature data to the data collected by ZF. A set of samples was collected in February 2011 along the Line P transect in the subarctic northeast Pacific. These samples and a higher resolution depth profile reported by Martin et al. (1989) (50°N 145°W) are shown in Figure 4.10. The general nutrient-like distribution of Cu is evident in both profiles with analytically significant differences between the two most evident in surface waters (<100 m) and in waters >400 m. The mixed layer is the upper 70 m. The difference is surface concentrations is most likely due to seasonal variability in the water column as our samples were collected in February while Martin et al.'s (1989) data represent July conditions where biological processes have drawn down dissolved Cu concentrations in surface waters. The lower concentrations in the subsurface and to some degree in surface waters may reflect differences between the methods that allow a greater

proportion of total dissolved Cu to be detected by Martin et al. (1989) compared to the ZF-CL method reported here. The variation of Cu concentration within the mixed layer at each station is in agreement with Dave Seminuik's data, based on personal communication, suggesting that grab samples in the mixed layer vary with respect to Cu. The international GEOTRACES community, through its intercalibration efforts with a standard seawater reference material, recognizes now that in order for a total dissolved Cu measurement to be accurate an oxidative step (e.g. UV-digestion) must precede detection (Milne et al., 2010). Less than 100% recovery is typical when no aggressive oxidation step is used before commonly used preconcentration and detection methods (Milne et al., 2010). The method employed by Martin et al. (1989) is a solvent extraction from seawater stored at pH = 1.7 and then buffered to pH = 4 using the ligands ammonium I-pyrrolidinedithiocarbamate (APDC) and diethylammonium diethyldithiocarbamate (DDDC), a double extraction into chloroform, and back-extraction into nitric acid (Bruland et al. 1979). This method of preconcentration, even in the absence of UV-digestion, likely extracts more labile Cu from solution than our ZF-CL method leading to larger concentration differences at depth. Recent work in this part of the north Pacific documents significant anomalies in metal:macronutrient relationships consistent with the formation of more inert metal species at the onset of the oxygen minimum zone (OMZ, ~400-500 m) (Janssen et al., personal communication). These inert complexes, hypothesized to be metal sulfides, might accentuate the difference in the relative recoveries of the methods.

Figure 4.10: Copper concentration in the subarctic Pacific determined by (▪) Martin et al. (1989) and by (Δ) zone fluidics in 2011 at a station located at 50°N 145°W.

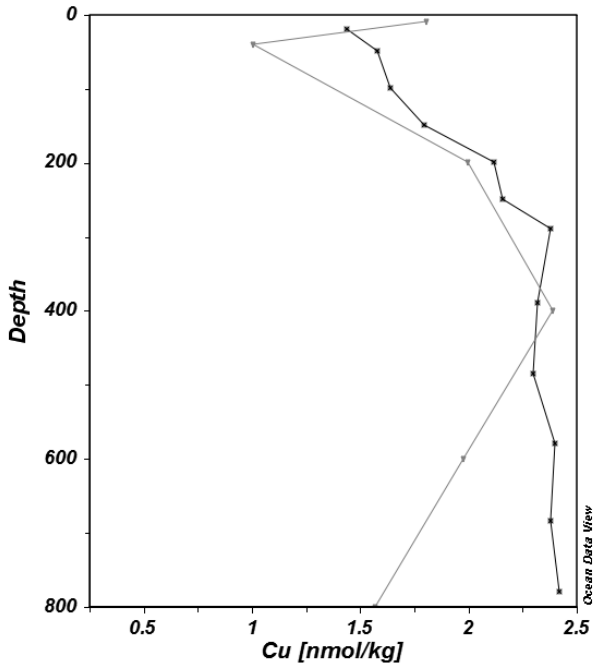

4.4 Conclusions

This method is suitable for determining open ocean concentrations of Cu in seawater due to its accuracy and precision of the certified reference material SAFe D2. Ongoing efforts by the GEOTRACES intercalibration community suggest that total dissolved (<0.2 µm based on filtration) Cu measurements require that samples be aggressively oxidized before analysis. In combination with UV-digestion the ZF platform and method is ideal for lab or ship based measurements of environmentally relevant concentrations of dissolved Cu in seawater.

Comparing the FIA and ZF methods, both techniques have similar method limits of detection, (Table 4.2); however, using ZF has advantages over the current FIA technique

with reagent use and absolute detection limits. The ease of use and transportability of the ZF mini-FloPro analyzer makes it a preferential option for real time Cu measurements onboard ship. With further method development, an extraction step can be added allowing for total Cu and speciation to be coupled with detection on this ZF platform.

Table 4.2: Trace copper measurement comparison between FIA and ZF

	FIA	*ZF*
Method Limit of Detection	0.3nM	0.3nM
Absolute Limit of Detection	1.9×10^{12} molecules	9.9×10^{9} molecules
Total Sample Volume per analysis	2-5mL	55µL
Total Reagent Volume per analysis	7-14mL	300µL
Total Volume	+20mL	<2mL
Time per analysis	~2min	~3min

In the following chapter, the ZF Cu method is applied to open ocean samples collected in the subarctic Pacific in 2011.

Chapter 5. Experimental – Labile Dissolved Cu concentrations and its relationship to algal macronutrients in the Fe-limited subarctic northeast Pacific

5.1 Introduction

Dissolved Fe concentrations are sufficiently low in open and some coastal ocean environments so as to be the proximate limiting nutrient for phytoplankton production (e.g. Martin et al. 1989; Hutchins et al. 2002; Kolber et al. 1994; Wells et al. 1994; Peers and Price, 2006). Chronic Fe limitation in the oceans on evolutionary timescales has shaped the physiology and elemental composition of marine microbes to access the limiting resource from their surroundings and to reduce intracellular demand for Fe (Katz et al. 2004; Saito et al. 2003; Annett et al., 2008). Copper plays a central role in these low Fe adaptive strategies through its substitution for Fe in important electron transport proteins (Cu-plastocyanin for Fe-cytochrome c_6) and presence in multi-Cu oxidases that are a component of a high affinity Fe uptake system that upregulated under Fe-limiting conditions (Peers and Price, 2006). Consistent with these strategies laboratory studies with oceanic phytoplankton indicate that they increase their cellular Cu quotas 2-3 fold under Fe-limitation and have higher Cu demand than coastal isolates (Annett et al., 2008). And using the relative remineralization of dissolved Cu and dissolved PO_4^{3-} in the main nutricline as a proxy for the Cu:P of algal biomass suggests that phytoplankton from Fe-limited waters have roughly 2 fold higher intracellular Cu than Fe-sufficient waters (Annett et al., 2008). Taken together, these lines of evidence support the idea that natural assemblages of phytoplankton in Fe-limited waters would

have a higher demand for Cu and might alter the biogeochemical cycling of Cu relative the major algal nutrients in these large, open ocean ecosystems.

Here we present measurements of labile Cu and the major algal nutrients (Si, N and P) along an onshore-offshore transect in the subarctic northeast Pacific. The transect spans highly productive, Fe-replete, coastal waters out to oligotrophic, Fe-limited, high nutrient-low chlorophyll waters offshore. The goal of the present study is to determine whether there is evidence for lower surface water dissolved Cu:PO_4^{3-} ratios in the HNLC region.

5.2 Study Site

The Line P program has operated in the subarctic northeast Pacific since April 1959, occupying a transect of stations and making hydrographic and biogeochemical observations (Freeland 2007). The transect is a natural laboratory that allows comparison and contrast between and Fe-sufficient coastal upwelling system with a classic HNLC regime offshore (Nishioka et al., 2001). Currently, there are 3 cruises annually to capture seasonal and inter-annual variability. Samples were collected from the CCGS John P. Tully in February 2011 along the Line P transect (48°N 125°W - 50°N 145°W), at stations P4, P12, P16, P20 and P26 (Ocean Station P) at various depths in the upper 800 m of the water column. Four 12L GO-Flo bottles (General Oceanics, Miami FL) were deployed on Kevlar line and tripped with Teflon messengers. Seawater was gravity filtered immediately after GO-Flo recovery through a 0.2 µm Acropak® filter attached with acid-cleaned, C-Flex (Cole Parmer) tubing to a Teflon stopcock. The samples were acidified to pH 1.7 with ultrapure (SeaStar Chemical) HCl (0.02 M) and

stored in low-density polyethylene (LDPE) bottles that had been cleaned according to stringent GEOTRACES trace element cleaning protocols (Appendix D: LDPE Cleaning Procedure).

Figure 5.1: Seawater samples were collected along the Line P transect located in the subarctic Pacific in February 2011

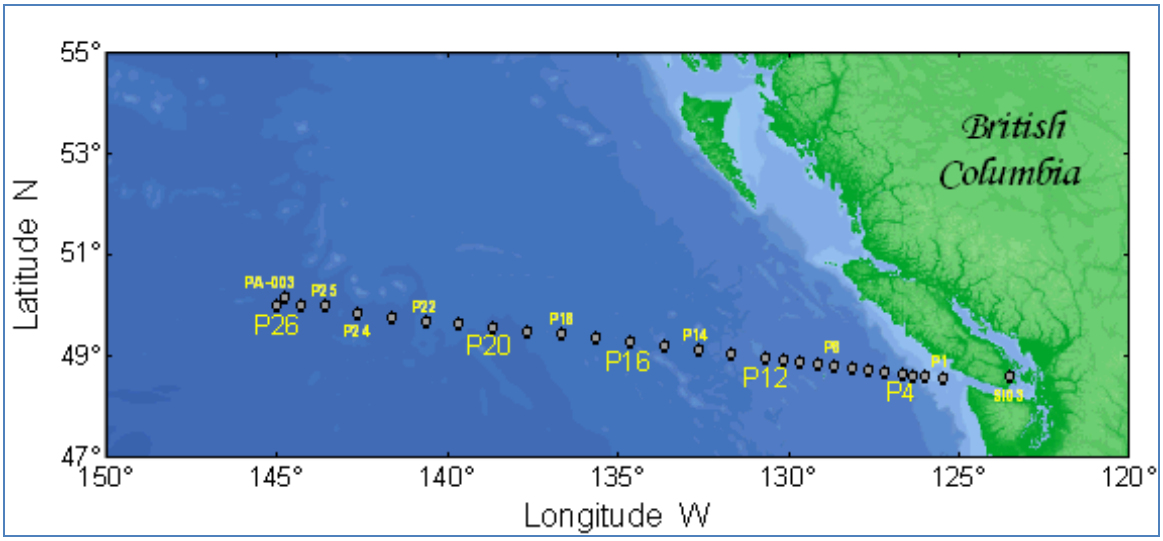

5.3 Method

The method used to determine Cu concentrations along Line P transect can be viewed in detail in section 4.2. Due to a limited supply of acidified Bermuda seawater as a blank/diluent, a standard addition curve was used for calibration by spiking the SAFe D2 reference material with AAS Cu standard (MSCU-10PPM, Inorganic Ventures). The calibration was back extrapolated to 0 nM Cu based. A calibration was run daily due to potential change in signal based on the strength of the reagents. Each sample was run in triplicate with a check standard between each station depth to ensure that the reagents/calibration was stable (Figure 5.2).

Figure 5.2: The bar graph shows SAFe D2 reference standard (1.77 ± 0.25 nM Cu, shown in line graph) used to determine reagent and calibration stability over the course of the day.

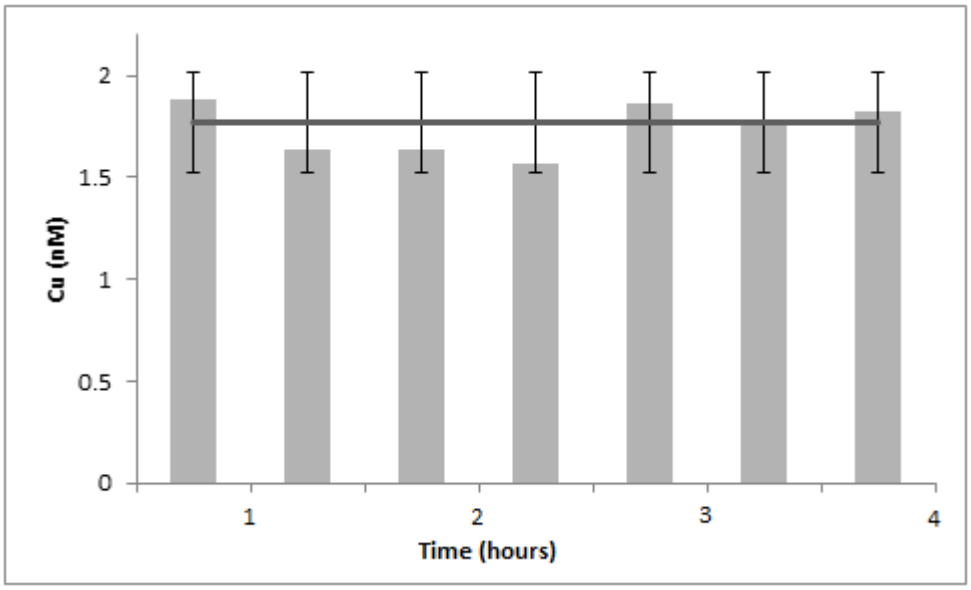

5.4 Results

5.3.1 Hydrography

A Temperature vs Salinity plot (Figure 5.3) for each station sampled along the Line P transect in February 2011 (winter) and August 2010 (station P26) (summer), indicates the presence of more saline, colder waters as one moves offshore. Fresher waters inshore reflect significant freshwater input from rivers, especially during Fall and Winter (Crawford et al. 2007). The predominant wind driven, cyclonic circulation in the Alaska Gyre brings colders waters to the surface offshore through upwelling while warmer waters are pushed toward shore explaining the onshore-offshore decrease in temperature (Crawford et al. 2007). Relative to longer term averages February 2011 was typified by inshore low salinity and T anomalies (Figure 5.4 & Figure 5.5).

Figure 5.3: Temperature vs Salinity plot for Line P transect from 2/2011 and 8/2010

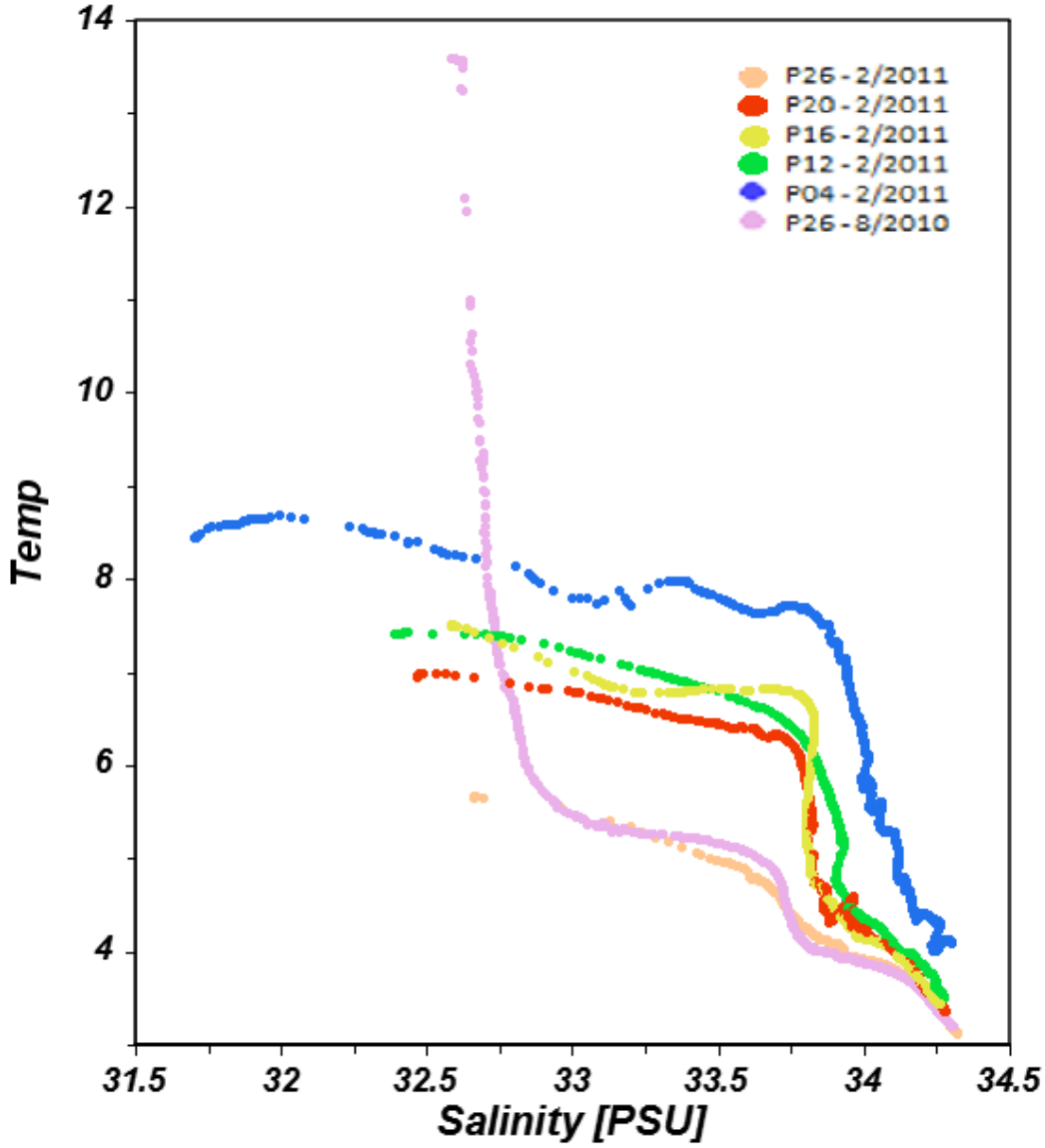

Figure 5.4: Salinity anomaly data along the Line P transect in 2/2011.

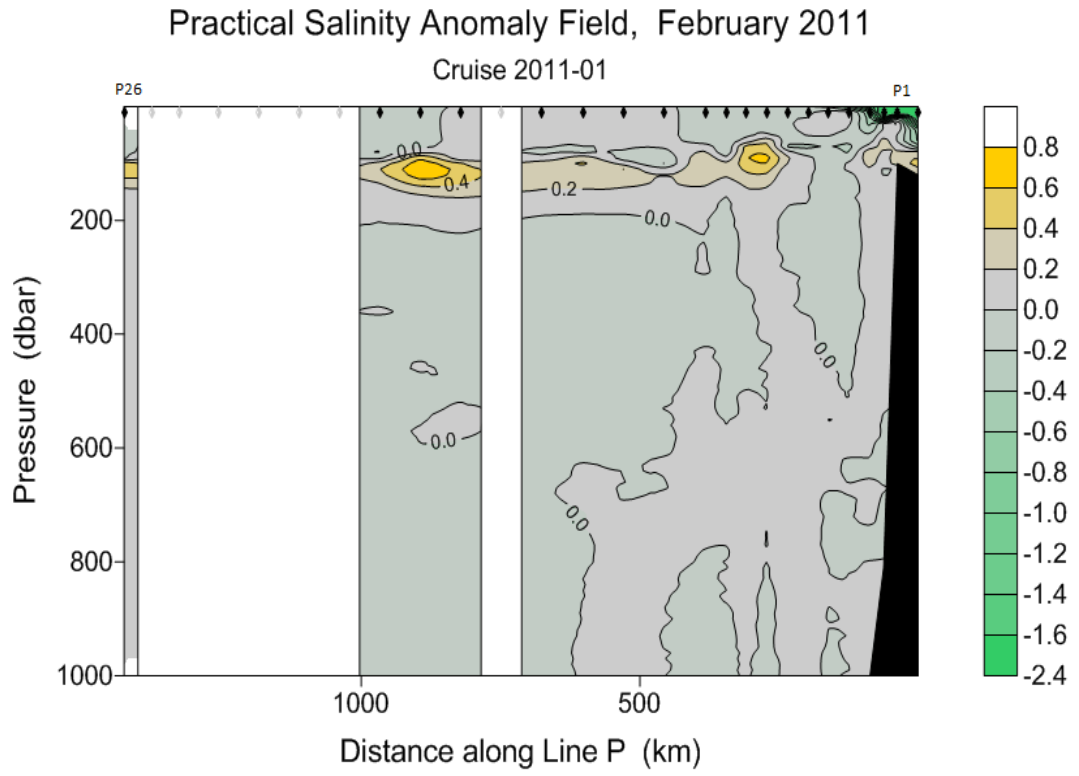

Figure 5.5: Temperature anomaly along the Line P transect 2/2011.

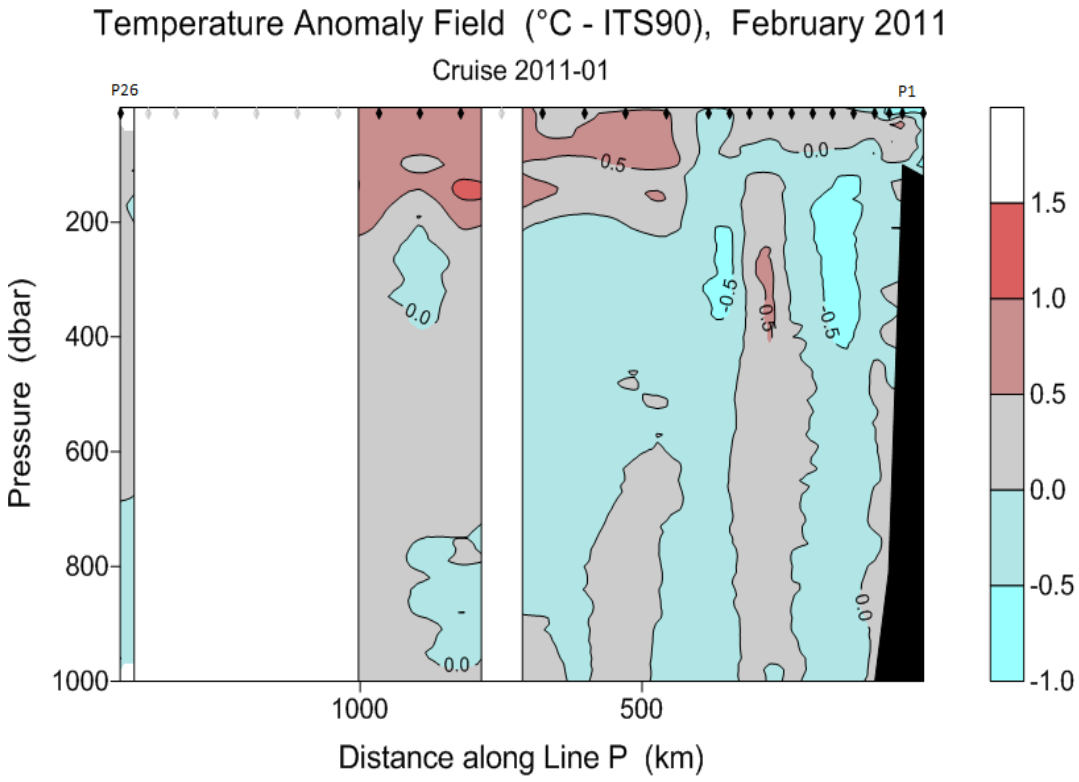

5.3.2. Dissolved Cu distributions

Figure 5.6: Line P Cu depth profiles determined by ZF CL technique with error bars (n = 3)

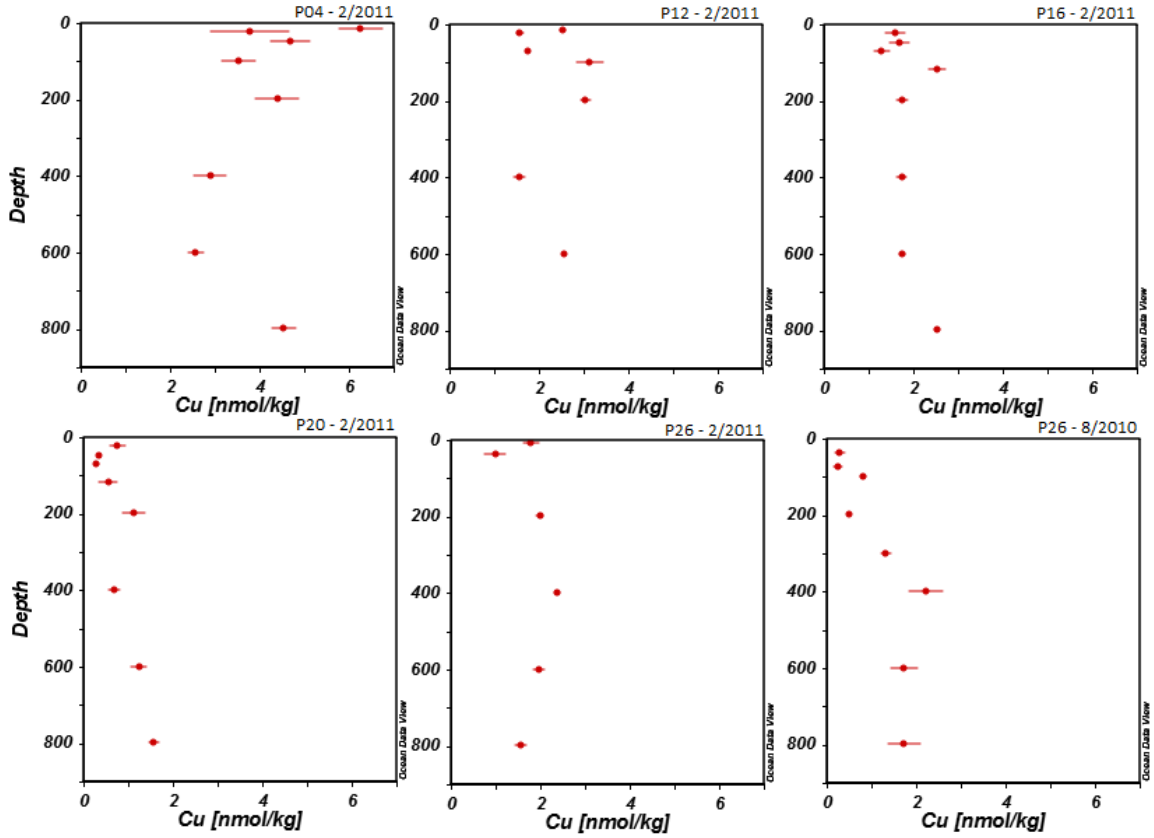

Dissolved (<0.2 µm) Cu concentrations along Line P fell in a range from 0.27±0.1 to 6.27±0.48 nM (Figure 5.6, Table 5.1). The minimum concentration was found offshore during August 2010 at P26 at a depth of 75 m while the highest Cu was measured inshore in February 2011 at P4 (depth 15 m). The general trend in the upper water column (< 70 m depth) was higher dissolved Cu concentrations inshore decreasing with distance offshore. During February 2011 P4 dissolved Cu concentrations were > 3 nM in the upper 50 m dropping to minimum concentrations at P20 of < 0.8 nM (Table 5.1). Dissolved Cu concentrations were highest in the higher T, lower S inshore waters which

likely reflects the impact of significant dissolved Cu inputs from the freshwater endmember (Figure 5.7).

Figure 5.7: Copper vs Salinity in the mixed layer (upper 70 meters) from Line P transect in February 2011 and from Martin et al. 1989.

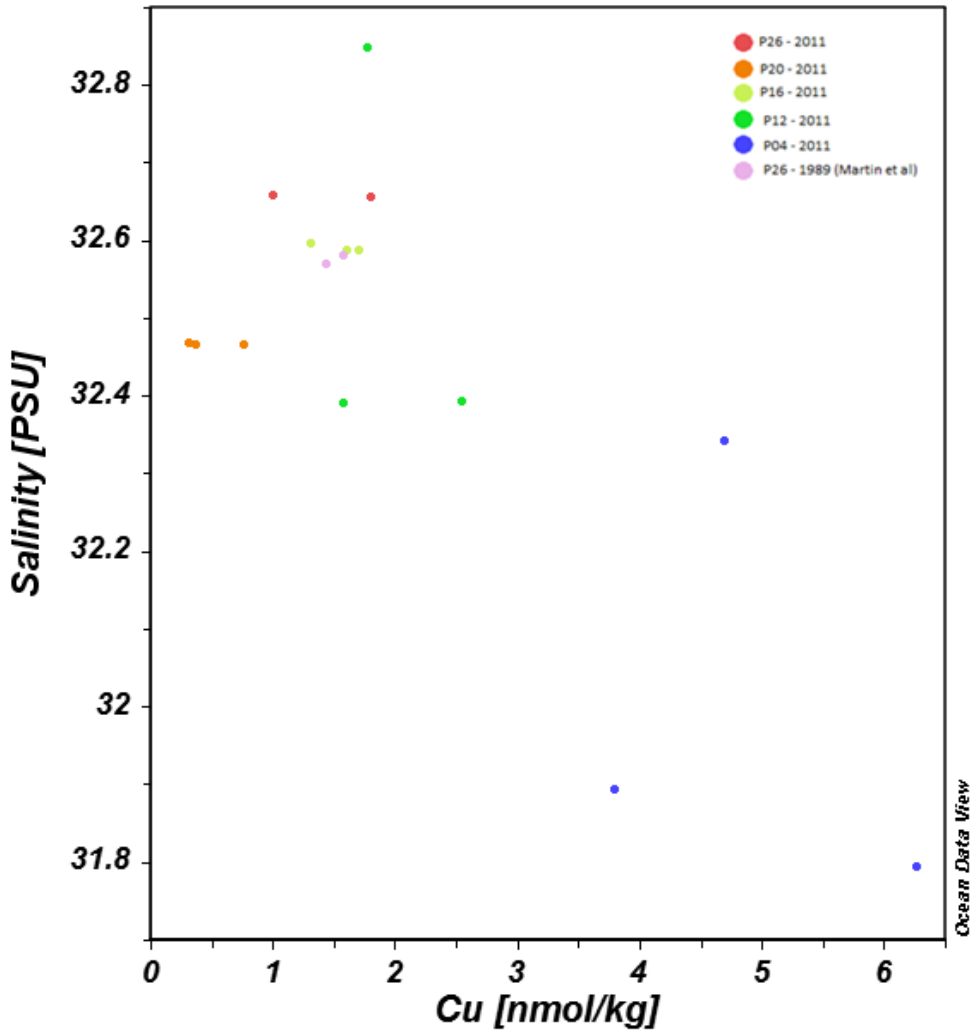

Table 5.1: Cu concentrations (nM) and standard deviation (nM) for the Line P transect collected in February 2011

Depth (m)	Temperature (°C)	Cu (nmol/l)		PO_4 (µmol/l)
Station P4; *48° 39' N, 126° 40' W - 2/2011*				
15	8.5612	6.27	±0.48	0.94
25	8.5611	3.80	±0.88	0.93

50	8.4681	4.70	±0.44	0.81
100	7.8371	3.55	±0.39	1.84
200	7.0215	4.41	±0.49	2.38
400	5.4152	2.91	±0.37	2.90
600	4.5630	2.59	±0.18	3.05
800	4.1170	4.56	±0.26	3.23

Station P12; *48° 58' N, 130° 40' W - 2/2011*

15	7.4140	2.55	±0.07	1.10
25	7.4042	1.58	±0.08	1.10
70	7.2941	1.78	±0.03	1.25
100	6.7643	3.15	±0.29	1.85
200	5.8508	3.06	±0.12	2.35
400	4.3934	1.58	±0.12	2.88
600	3.9099	2.59	±0.03	3.12

Station P16; *49° 16' N, 134° 40' W - 2/2011*

25	7.5113	1.61	±0.22	0.87
50	7.5121	1.70	±0.21	0.88
70	7.5121	1.31	±0.18	0.88
120	6.8047	2.55	±0.20	1.51
200	5.6022	1.76	±0.12	2.05
400	4.1963	1.75	±0.12	2.54
600	3.8655	1.76	±0.06	3.05
800	3.4320	2.55	±0.07	3.13

Station P20; *49° 34' N, 138° 40' W - 2/2011*

25	6.9541	0.77	±0.17	0.93
50	6.9539	0.37	±0.03	0.91
70	6.9601	0.31	±0.05	0.93
120	6.4983	0.57	±0.20	1.67
200	5.4932	1.14	±0.25	2.25
400	4.2343	0.70	±0.13	2.84
600	3.8418	1.25	±0.18	3.10
800	3.3312	1.59	±0.10	3.10

Station P26; *49° 60' N, 145° 00' W - 2/2011*

10	5.6376	1.81	±0.16	1.25
40	5.6431	1.01	±0.23	1.25
200	4.1726	2.00	±0.08	2.79
400	3.8554	2.39	±0.07	3.05
600	3.4523	1.98	±0.13	3.15
800	3.1389	1.57	±0.13	3.20

Station P26; 50° *00' N, 145° 00' W - 8/2010*				
40	8.3131	0.31	±0.12	1.11
75	6.6221	0.27	±0.10	1.25
100	5.5136	0.84	±0.06	1.46
200	4.1923	0.52	±0.01	2.56
300	3.9802	1.34	±0.11	2.84
400	3.8685	2.24	±0.37	3.06
600	3.5495	1.74	±0.30	2.98
800	3.1771	1.74	±0.36	3.14

5.3.3. Dissolved Cu:P ratios along Line P

Oceanic surface waters tend to contain extremely low concentrations of bioactive metals (Cd, Cu, Fe and Zn) as well as the major algal nutrients (Si, N and P). Generally speaking, marine phytoplankton have adapted to these onshore-offshore gradients with oceanic species requiring less metal or nutrient per cell compared to coastal species to maintain optimal growth (e.g. Brand et al. 1983). Dissolved Cu concentrations decrease dramatically distance offshore from coastal bays and estuaries (50 nM) to ~0.4-0.9 nM in surface waters of the oceanic gyres (Bruland 1980; Buck et al. 2007; Moffett et al. 1997). Despite the concentration of dissolved Cu being greatly diminished offshore, oceanic phytoplankton actually have a *higher* cellular demand for Cu than coastal species (Peers et al., 2005; Semeniuk et al. 2009). Higher biomass normalized Cu requirements are most likely the result of oceanic phytoplankton responding to Fe-limitation by replacing Fe containing electron transport proteins with Cu containing analogues (Peers and Price 2006) and the upregulation of a Cu dependent high affinity Fe transport system (Maldonado et al. 2006). Whether or not the relative onshore-offshore distribution of dissolved Cu in the chronically Fe-limited, high nutrient low

chlorophyll (HNLC) northeast Pacific is consistent with preferential uptake of Cu relative to PO_4^{3-} by oceanic phytoplankton is examined in detail below.

A useful concept to aid our efforts is the idea that, on average, marine plankton have relatively constant chemical composition within the constraints imposed by the availability of chemical elements in seawater that is normally attributed to Redfield (Redfield 1958). The elemental ratios of the major and trace elements are used by oceanographers to examine the interaction of biological and geochemical processes occurring in the oceans (Ho et al. 2003). Phosphorus normalized cellular content allows oceanographers to investigate how the cellular demand, of Cu here, varies within and among species independently of cell volume and will be used here. Most recent compilations of culture and field studies of the Cu content of marine phytoplankton and suspended particulate matter indicate that Cu:P falls in range between 0.18 – 0.52 (mmol/mol) (Ho et al. 2003 and references therein). A consensus value that incorporates field and laboratory values of 0.38 Cu:P (mmol/mol) will be adopted here to represent the Cu content of marine phytoplankton.

Nutrient input at near shore stations is mainly a result of terrestrial or atmospheric input. Moving off shore, nutrient concentration decreases; however, typical deep vertical mixing (100m) is expected in February in the north pacific station P26 resulting in nutrient input of PO_4 at the surface (Martin et al. 1989). Higher P concentrations are observed in the mixed layer as a result of reduced phytoplankton productivity from Fe-limitation due to minimal atmospheric Fe input. This results in offshore HNLC under Fe-limited conditions.

Dissolved Cu:P ratios along Line P in February 2011 (Figure 5.8) show elevated values at inshore stations with high coastal influence, such as terrestrial input or upwelling (P4 and P12) and decreasing ratios in the open ocean. The decrease in Cu:P ratio from P16 moving offshore correlates to the increase Cu uptake in primary productivity in Fe-limited waters. The biological consumption of Cu in open ocean species, as discussed above, is higher compared to their inshore counter parts decreasing the amount of available Cu (Peers et al. 2005, Semeniuk et al. 2009).

Figure 5.8: Redfield ratio of Cu:P (mol/mol) along Line P at various sampling times

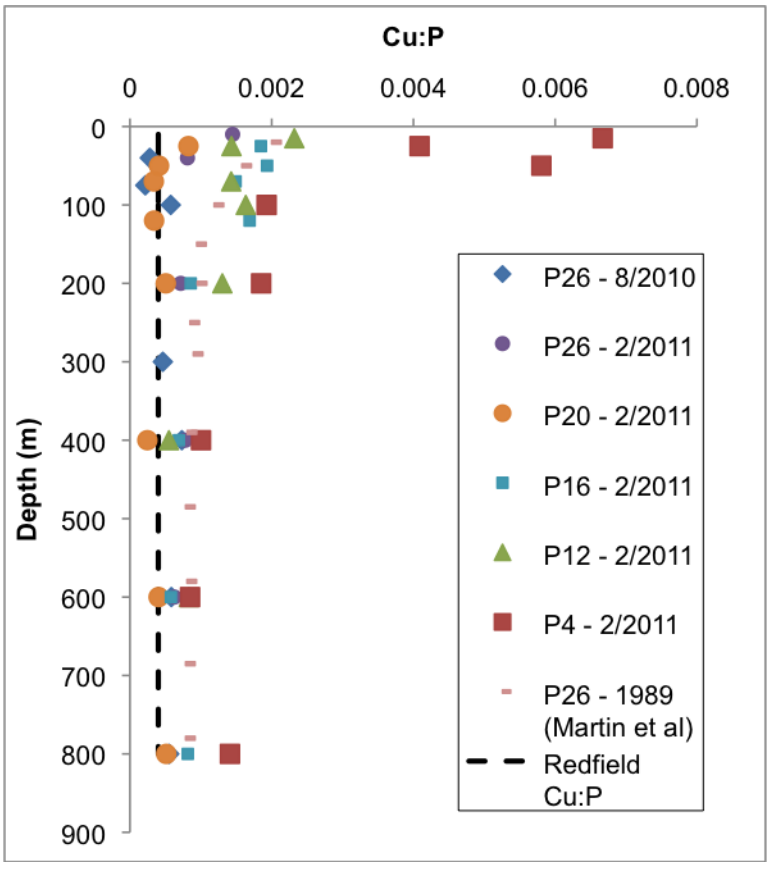

Several factors, including circulation and upwelling, contribute to nutrient availability and can also affect Cu:P ratios. In winter (P26 – 2/2011) deeper mixing due to cooler surface water at station P26 results in an increase in Cu at the surface relative to

nutrient availability. In the north pacific, the input of high nutrient coastal waters from water circulation from the Alaskan Gyre could also affect the uptake of Cu due to the influx of Fe and coastal phytoplankton (Whitney et al., 2005). These nutrient rich waters due to eddy re-circulation could account for the increase in Cu at station P26 in 2011 compared to P20 and P26 from 2010. In the summer (P26 – 8/2010) the surface depletion of Cu is related to the increase in nutrient demand (P) of phytoplankton in Fe limited waters.

The Redfield ratios observed in Figure 5.8 converge on the expected Redfield value at depths below the mixed layer (100m) where primary productivity is limited. Within the mixed layer, as described above, the cellular demand of Cu by marine phytoplankton increased in open ocean species compared to their onshore counterparts (Annett et al. 2008, Ho et al. 2003, Maldonado et al. 2006, and Semeniuk et al. 2009). The increase in phytoplankton uptake in Cu results in the open ocean decreasing the Cu:P ratio. Higher Cu:P ratios observed inshore support their findings in that there is less of a demand or uptake of Cu relative to the available nutrients onshore.

5.5 Conclusions

Several factors – upwelling, water circulation, biological uptake – can affect Cu concentrations discussed above. By monitoring seasonal variability of these conditions and Cu and P concentrations, a better understanding of fluctuations and changes in the ocean would aide in data interpretation. A plankton tow looking at the phytoplankton species present at station P26 in February 2011 would provide information on whether coastal water from the Alaskan Gyre was bringing in phytoplankton and nutrients

resulting in a slight increase in Cu:P compared to P20 (2/2011) and P26 (8/2010) (Whitney et al. 2005). Semenuik et al. (2009) determined that biogenic Cu uptake accounted for half the depletion of Cu in the mixed layer providing substantial evidence that phytoplankton play a key role in controlling the distribution of Cu in the ocean. Similar experiments to Semenuik et al. (2009) monitoring Cu uptake along line P would aide in understanding Cu availability and uptake providing information on sources and sinks of Cu. Understanding Cu concentration in relation to Cu speciation would provide information regarding the availability of Cu to phytoplankton and further understanding on modes of assimilation by phytoplankton. It is evident that there are gaps in understanding Cu distribution in the ocean. With additional analyses a greater understanding to the trends discussed here would provide a more conclusive understanding.

Chapter 6. The Future of Measuring Trace Metals in the Ocean

6.1 Introduction

"The marine biogeochemical cycles of micronutrients are known so poorly that their sensitivity to global change, and the impact of any resulting changes in elemental cycling on marine ecosystems and the ocean carbon cycle, cannot be predicted meaningfully (SCOR, 2006)."

Although the study of trace metals is over a half century old, the last decade has had a renaissance in understanding the ocean ecosystem with respect to trace elements and their isotopes (TEIs). TEIs measurement is important in understanding the role of the oceans in climate change, assessment of the anthropogenic contribution to TEIs, understanding of impact of changes in TEIs on marine organisms, and study of correlations between TEI distribution patterns and environmental phenomena. Important answers to the role of TEIs can be determined through furthering this research. Determining the role of micronutrients will lead to better understanding of uptake and regeneration of TEIs and how they affect larger cycles like carbon and nitrogen both locally (e.g. coastal eutrophication) and in the marine system as a whole (e.g. ocean acidification). Speciation plays a critical role in uptake and toxicity to biological organisms. As research is advanced, the chelation and release of ligands from biological and anthropogenic sources leads to better understanding of speciation and role of TEIs (Morel and Price, 2003). Understanding the complete cycling of metals will lead to the ability to monitor the transport and flux of toxins, introduced by human

activity, and how the oceans natural processes regulate and transport these contaminants.

TEIs also act as indirect tracers for past and present ocean processes (Henderson et al., 2002). The ocean chemistry of TEIs contribute to global ocean circulation models of mixing and ocean fluxes that are difficult to monitor directly. Tracer TEIs, such as ^{234}Th, allow the rates of processes to be determined for assessment of the carbon cycle and its evolving state (SCOR, 2006). As these proxies are understood, the future environmental changes and response to changes will allow new proxies to be established, one of the primary objectives of the GEOTRACES project.

6.2 Global Initiatives

There are numerous international oceanographic programs, NEPTUNE, GOOS, ORION, and GEOTRACES to name a few, that will rely on advances in *in situ,* chemical detection to better understand global change, climate and ocean cycling (past, present and future). The GEOTRACES program – an international study of the biogeochemical cycles of TEIs - is directly related to the research and technology presented in this document (Henderson et al., 2002; SCOR, 2006). One of the primary focuses of the GEOTRACES program is to monitor internal cycling of TEIs. The 3 general goals outlined in the GEOTRACES Science Plan are as follows (SCOR, 2006):

1. To determine global distributions of TEIs - concentration, speciation and physical form – in order to evaluate sources, sinks, and cycling and the physical, chemical and biological processes that regulate their distribution

2. To obtain sufficient understanding of TEIs cycling in order to predict the response and impact of these cycles regarding carbon cycling and global and climate changes
3. To understand the processes that control geochemical speciation.

These goals are organized into 3 themes – fluxes and processes, internal cycling, and proxies for past change. The GEOTRACES plan has emphasized that a major factor contributing to coordinating a global structural plan is the potential advances in sampling techniques and analytical technology. Programs such as this have recognized the need to utilize technological advances happening in the field of analytical chemistry and chemical oceanography creating a need for the research described in this paper. By utilizing advanced technology and methodology, current gaps in our understanding of marine biogeochemical processes can be closed.

6.3 Modus Operandi

The analytical burden faced by programs such as GEOTRACES has necessitated the development of interdisciplinary relationships among process, analytical and marine chemistry. This unique relationship among scientists will aim to aid in accomplishing the goals set out in the GEOTRACES Science Plan. The Collaborative on Oceanographic Chemical Analysis (COCA) conference in March 2013 points to the future direction and demand for approaches such as the automation of Cu measurements described in this research. The aim of this conference was to identify areas within the field of oceanography that can benefit from recent advances in analytical techniques and technology and provide a clear picture of the real needs of this scientific discipline.

From this, a long-term relationship between the field of chemical oceanography and advancing technology will begin to form the basis of autonomous oceanographic sampling and analytical techniques.

6.3.1 Instrumentation for shipboard and laboratory analysis

The ZF concept and hardware/software is discussed extensively in Chapter 1 and well suited for laboratory and shipboard analysis. The benefit to immediate, shipboard analysis of TEIs minimizes error due to aged or unstable samples. Shipboard analyses can also help to identify and troubleshoot sample contamination or compromised sample integrity during collection. The approach developed here, ZF, lends itself both to sample preparation/preservation for later analysis onshore and the quantification of TEIs at sea. In either circumstance, it is key to have an instrument that is modular, reagent and waste efficient, and easily maintained. The instrument must be able to perform under high and low frequency accelerations from the ship and the sea. It is advantageous to have a small platform or footprint as ship space is limited and in the case of TEIs the device must fit inside a laminar flow bench to ensure a particle free, clean work area. Power requirements for small devices must handle voltage fluctuations and spikes. Under power loss situations, the user must be able to pinpoint where the method stopped. These scenarios are easily dealt with by the FlowZF software which allows tracking of the executed method and instantaneous data storage. The FlowZF sequence library contains a sequence that the user can run under a power failure scenario to prepare for the next sample to be tested. A stand-alone device that has potential to be float or glider deployed is an end goal so minimal power

consumption is a desired goal. The foundation of a reliable analyzer is a robust and well documented assay.

6.3.2 Robust assays

This research begins the development of robust, ship or lab-based analysis of TEIs. For laboratory instrumentation the market is well developed and perhaps the greatest need is for methodology suited to marine chemistry. One well characterized and widely accepted assay is the iron method published by Obata et al. (1993). Many automated methods are adapted from bench based techniques. Automating a method is a multi-step process. Figure 6.1 depicts the steps of the research in this paper reaching the overall goal – automated speciation of trace metals in the ocean. Although the overall goal is yet to be accomplished, critical steps to reaching this goal have been attained. Within each step there are critical aspects that must be met and accepted by the community. This approach is used in each step to minimize and pinpoint errors and technique improvements along the way.

Figure 6.1: Steps of automating TEIs analysis with ZF; green – steps accomplished in this research, grey – steps still to be completed, orange – the overall goal

One advantage to studying new techniques with a ZF platform is the ease of adding or removing unit operations. The layout of the instrumentation is designed for development work as well as an end product. The tubing is easily disconnected from the valve, unit operations can be swapped for existing components and new test unit operations can easily be plumbed into the platform and removed as adaptations are produced. Because each unit operation stands alone off a valve port, the sequence modification of implementing a new or different unit operation is minimized enhancing the capability of testing new techniques and optimizing sample handling conditions. ZF implements a tree-like branching structure to a method whereas FIA is more of a linear sequence of events. There is no effect to downstream operations in ZF because each

step is isolated unlike FIA where timing, flowrates and changes to the system affects the entire method.

The flexibility of the ZF platforms allows a power user, an oceanographer or chemist, to develop techniques that are simple enough to run independent of the power user. One goal discussed at the COCA conference was the advantage to eliminating the need for the power user to constantly monitor the process or quantify the data and rather spend time qualifying the importance of the data.

6.4 Discussion of Cu research

The research outlined above initiates the process of developing a robust technique for micro-scale liquid-liquid extraction with ZF. The next step in this research is to couple the extraction of Cu at environmentally relevant concentrations with the CL method described in Chapter 4 utilizing the extraction data from Chapter 2 and Chapter 3. Based on Kinrade and Van Loon's (1974) research of extraction of multiple metals found in natural waters, the ideal choice of solvent, buffer, chelating agent ratio, pH and shake time to transition between extraction of Ag and Cu should be suitable for ZF. Danielson et al. (1978) also reports on the extraction efficiency under various conditions for Cu in the marine environment. It will be key to ensure that the product of a trace level (nM) Cu extraction with ZF is carried out at a viable pH in order to couple the CL method developed in Chapter 4. At this point, the ZF platform can be adapted to perform competitive ligand equilibration/liquid-liquid extraction as described by Moffett and Zika (1987) and Miller and Bruland (1994) to determine Cu speciation.

It is also critical to decrease detection limit of the CL method discussed in Chapter 4 as typical speciation requires pico-molar (pM) detection levels to achieve accurate metal speciation. By maximizing extraction efficiency in Chapter 2 the sample was preconcentrated up to 5 times with ZF. Using the extraction shaker cell (1.2.7) may allow for higher preconcentration due to the ability to increase the ratio of sample and organic phases. The goal of the ZF technique is to decrease the sample volume to micro-scale. The CL technique has a limit of 55µL needed to run a single detection. Based on the volume of the shaker (2mL), the maximum preconcentration assuming high extraction efficiency with ZF is ~20 times whereas the bench top technique achieves 100-1000 times preconcentration by using large volumes and evaporating to dryness. The bench top techniques are long and tedious unlike the proposed ZF method. With the reported method limit of detection for the ZF Cu CL method of 0.3 nM, this technique would allow 15 pM Cu to be determined assuming a preconcentration of 20 times. Sangi et al. (2004), report that by spiking the sample with 4 µM Fe^{3+}, the slope of the CL Cu peak for FIA is increased by 11.4 times increasing sensitivity. If this enhancement could be reproduced for ZF in addition to an extraction preconcentration of 20 times, the ZF CL Cu method limit of detection would allow for 1 pM of Cu to be determined. If this sensitivity could not be achieved by the ZF Cu CL method, the method can perform sample preparation for other forms of detection, like flame absorption spectrometry (FAAS).

Remaining challenges to furthering this method include generating consistent blanks and clean reagents to allow for low levels of detection. The data collected in

Chapter 5 required a standard additions curve with the SAFe D2 reference material in order to generate a calibration due to Cu contamination in the seawater blank. A synthetic seawater matrix may aid in repeatable calibration measurements as seen in Chapter 4.

In addition to total trace metal measurements, the idea of the ZF approach is to expand the extraction method to allow for metal speciation. This analyzer is suitable for ship-based measurements of trace metals allowing samples to be measured immediately after collection to enable superior speciation detection. In this scenario, the extraction product can be collected and analyzed later by more sensitive techniques like atomic absorption spectrometry. By determining metal speciation, the ability to better understand the biogeochemical cycles of trace metals will reveal new information regarding open ocean environments.

6.5 Future ZF Research for TEIs

ZF offers modularity and versatility to the oceanographic chemical analysis field. It lends itself to several methods of detection beyond CL, including electrochemistry, and upstream sample handling steps. These methods adapt well to a ZF platform due to low volume flowcells. In proprietary work at Global FIA (Fox Island, WA), an amperometric method has been developed using the ZF manifold for cyanide analysis. The drawback to electrochemistry is the step of conditioning the electrode not necessary for spectroscopy or CL; however, it is an obvious need to develop techniques for low level analysis that can be implemented in the field.

The broad spectrum of applications and easibility of ZF are being utilized by the pharmaceutical industry to implement powerful integration sampling strategies. The layout provides space and access to add sample handling process, like the addition of a UV digester for total Cu determinations as discussed in section 4.3.4. It will be critical for cross industry collaboration between oceanographers, analytical chemists and instrument developers to continually discuss needs and solutions. It is evident that the field of oceanography needs to establish baseline goals or needs to pass along. From information obtained at the COCA conference, it is evident that flexibility of the platform is key to determining these baseline needs.

With more discussion among analytical chemists and oceanographers needs, sample pre-treatment and preconcentration steps can optimize methods for spectroscopy or CL analytical finishes. The availability of powerful preconcentration membranes that can easily be coupled with ZF or designed to be implemented in a simple collection step could eliminate the use of organic solvents (Nghiem et al., 2006). Nghiem et al. discuss the capabilities of polymer inclusion membranes (PIMs) as metal ion transport and elimination of sample matrix. The flexibility in use of PIMs is ideal for oceanographic analysis. PIMs could be adapted to collection bottle or vial to enhance preconcentration or implemented online in a ZF or flow based platform depend on the extraction efficiency. These membranes pose an alternative to currently used liquid-liquid extraction or solid phase extraction techniques and have potential benefits to reducing water collection volume that needs to be returned to the lab.

6.6 Conclusion

The GEOTRACES mission statement is “to identify processes and quantify fluxes that control the distributions of key trace elements and isotopes in the ocean, and to establish the sensitivity of these distributions to changing environmental conditions” (SCOR, 2006). This goal is very broad yet key to understanding the ocean and its processes and role in climate change. With technology like ZF, the answers to these problems can be quantified. The modularity, robust software and ability to incorporate protection against power surges ensure the efficiency of ZF in the field or in the laboratory. By fulfilling specific needs ZF will continue to offer ship-based analysis beyond trace metal measurements. This requires investment in method development like the research described in this document. This research has taken the initial steps to reach the ultimate goal, a method for automated trace metal speciation (Figure 6.1), and should be continued to aid oceanographers in better understanding TEIs.

Bibliography

Anderson, J.M., Koshi, J.K. 1970. Silver (I)-Catalyzed Oxidative Decarboxylation of Acids by Peroxydisulfate. The Role of Silver (II). Journal of the American Chemical Society, 92(6): 1651-1659.

Annett, A., Lapi, S., Ruth, T., Maldonado, M. 2008. The Effects of Cu and Fe Availability on the Growth and Cu:C Ratios in Marine Diatoms. Limnology and Oceanography, 53(6): 2451-2461.

Berg, E.W. 1963. Physical and Chemical Methods of Separation, McGraw-Hill Book Company, New York.

Boyle, E.A., Sclater, F.R., Edmond, J.M. 1977. The Distribution of Dissolved Copper in the Pacific. Earth and Planetary Science Letters, 37:38-54.

Brand, L., Sunda, W., Guillard, R. 1983. Limitation of Marine Phytoplankton Reproductive Rates by Zinc, Manganese and Iron. Limnolology and Oceanography, 28: 1182-1198.

Brand, L, Sunda, W., Guillard, R., 1986. Reduction in Marine Phytoplankton Reproduction Rates by Copper and Cadmium. Journal of Experimental Marine Biology and Ecology, 96: 225-250.

Bruland, K., Franks, R.P., Knauer, G. A., Martin, J. H. 1979. Sampling and Analytical Methods for the Determination of Copper, Cadmium, Zinc and Nickel at the Nanogram per Liter Level in Seawater. Analytica Chimica Acta, 105: 233-245.

Bruland, K. 1980. Oceanographic Distributions of Cadmium, Zinc, Nickel, and Copper in the North Pacific. Earth and Planetary Science Letters, 47: 176-198.

Bruland, K.W., Lohan, M.C. 2004. Controls of Trace Metals in Seawater. Chapter 2 in The Oceans and Marine Geochemistry, 6: 23-47.

Buck, K. N., Ross, J.R.M, Flegal, A.R., Bruland, K.W. 2007. A Review of Total Dissolved Copper and Its Chemical Speciation in San Francisco Bay, California. Environmental Research, 105: 5-19.

Coale, K., Johnson, K., Stout, P., Sakamoto, C. 1992. Determination of Copper in Seawater Using a Flow-injection Method with Chemiluminescence Detection. Analytica Chimica Acta, 266: 345-351.

Cutter, G. Andersson, P., Codispoti, L., Croot, P., Francois, R. Lohan, M. 2007. Sampling and Sample-handling Protocols for GEOTRACES-related IPY Cruises. http://www.geotraces.org/documents/GEOTRACESIPYProtocols-Final_000.pdf

Danielson, L., Magnusson, B., Westerlund, S. 1978. An Improved Metal Extraction Procedure for the Determination of Trace metals in Sea Water by Atomic Absorption Spectrometry with Electrothermal Atomization. Analytica Chimica Acta, 98: 47-57.

Ensafi, A.A., Zarei, K. 1997. Flow Injection Determination of Silver with Spectrophotometric Determination. Fresenius Journal of Analytical Chemistry, 358: 475-479.

Freeland, H. 2007. A Short History of Ocean Station Papa and Line P. Progress in Oceanography. 75:120-125.

Fedorova, O.S., Berdnikov, V.M. 1979. Mechanism of Chemiluminecence in the Oxidation of 1,10-Phenanthroline by Hydrogen Peroxide in Aquoues Solution. Translated from Izvestiya Akeademii Nuak SSSR, 6: 1226-1230.

Handy, R.D., Owen, R., Valsami-Jones, E. 2008a. The Ecotoxicology of Nanoparticles and Nanomaterials: Current Status, Knowledge Gaps, Challenges, and Future Needs. Ecotoxicology, 17: 315-325.

Handy, R. D., Von Der Kammer, F., Lead, J.R., Hassellov, M., Owen, R., Crane, M. 2008b. The Ecotoxicology and Chemistry of Manufactured Nanoparticles. Ecotoxicology, 17: 287-314.

Henderson, G.M. 2002. New Oceanic Proxies for Paleoclimate. Earth and Planetary Science Letters, 203: 1-13.

Henderson, G.M., Anderson, R.F., Adkins, J., Andersson, P., Boyle, E.A., Cutter, G., de Baar, H.J., Eisenhauer, A., Frank, M., Francois, R., Orians, K., Gamo, T., German, C. Jenkins, W., Moffett, J., Jeandel, C., Jickells, T., Krishnaswami, S., Mackey, D., Masque, P., Measures, C., Moore, J., Oschlies, A., Pollard, R., Rutgers, V.D., Loeff, M., Schlitzer, R., Sharma, M., von Damm, K., Zhang, J. 2007. GEOTRACES – An International Study of the Marine Biogeochemical Cycles of Trace Metals and Their Isotopes. Chemie Der Erde-Geochemistry, 67: 85:131.

Ho, T., Quigg, A., Finkel, Z., Milligan, A., Wyman, K., Falkowski, P., Morel, F. 2003. The Elemental Composition of Some Marine Phytoplankton. Journal of Phycology, 39: 1145-1159.

Hutchins, D. A., Hare, C.E., Weaver, R.S., Zhang, Y., Firme, G.F., DiTullio, G.R., Alm, M.B., Riseman, S.F., Maucher, J.M., Geesey, M.E., Trick, C.G., Smith, G.J., Rue, E.L., Conn, J., Bruland, K.W. 2002. Phytoplankton Iron Limitation in the Humboldt Current and Peru Upwelling. Limnology and Oceanography, 47: 997-1011.

Johnson, K., Elrod, V., Fitzwater, S., Plant, J., Chavez, F., Tanner, S., Gordon, M., Westphal, D., Perry, K., Wu, J., Karl, D. 2003. Surface Ocean-Lower Atmosphere Intercations in the Northeast Pacific Ocean Gyre: Aerosols, Iron and the Ecosystem Response. Global Biogeochemical Cycles, 17(2): 1063.

Katz, M. E., Finkel, Z.V., Grzebyk, D., Knoll, A.H., Falkowski, P.G. 2004. Evolutionary Trajectories and Biogeochemical Impacts of Marine Eukaryotic Phytoplankton. Annual Review of Ecology Evolution and Systematics, 35: 523-556.

Kinrade, J.D., Van Loon, J.C. 1974. Solvent Extraction for use with Flame Atomic Absorption Spectromtry. Analytical Chemistry, 46(13): 1894-1898.

Klaine, S. J., Alvarez, P., Batley, G.E., Fernanades, T.F., Handy, R.D., Lyon, D.Y., Mahendra, S., McLaughlin, M.J., Lead, J.R. 2008. Nanomaterials in the Environment: Behavior, Fate, Bioavailability, and Effects. Environmental Toxicology and Chemistry, 27: 1825-1851.

Kolber, Z., Barber, R.T., Coale, K.H., Fitzwateri, S.E., Greene, R.M, Johnson, K.S., Lindley, S., Falkowski, P.G. 1994. Iron Limitation of Phytoplankton Photosynthesis in the Equatorial Pacific ocean. Nature, 371: 145-149.

Kramer, D., Cullen, J.T., Christian, J.R., Johnson, W.K., Pedersen, T.F. 2011. Silver in the Subarctic Northeast Pacific Ocean: Explaining the Basin Scale Distribution of Silver. Marine Chemistry, 123: 133-142.

Maldanodo, M.T., Price, N.M. 1999. Utilization of Iron Bound to Strong Organic Ligands by Phytoplankton Communities in the Subartic Pacific Ocean. Deep Sea Research II, 46: 2447-2473.

Maldonado, M. T., Allen, A.E., Chong, J.S., Lin, K., Leus, D., Karpenko, N., Harris, S.L. 2006. Copper-dependent Iron Transport in Coastal and Oceanic Diatoms. Limnolology and Oceanography, 51: 1729-1743.

Mann E. L., Ahlgren, N., Moffett J.W.and Chisholm, S.W. 2002. Copper Toxicity and Cyanobacteria Ecology in the Sargasso Sea. Limnology and Oceanography, 47(4), 976-988.

Marshall, G., Wolcott, D., and Olson, D. 2003. Zone Fluidics in Flow Analysis: Potentialities and Applications. Analytica Chimica Acta, 499: 29-40.

Martin, J. H., Knauer, G.A, Gordon, R.M. 1983. Silver Distributions and Fluxes in Northeast Pacific Waters. Nature, 305: 306-309.

Martin, J.H., Gordon, R.M., Fitzwater, S., Broenkow, W.W. 1989. VERTEX: Phytoplankton/Iron Studies in the Gulf of Alaska. Deep-Sea Research, 36(5): 649-680.

Michaelis, L., Eagle, H. 1930. Some Redox Indicators. The Journal of Biological Chemistry, 87: 713-727.

Miller, L., Bruland, K. 1994. Determination of Copper Speciation in Marine Waters by Competitive Ligand Equilibration/Liquid-liquid Extraction: An Evaluation Technique. Analytica Chimica Acta. 284: 573-586.

Miller, L.A., Bruland, K.W. 1995. Organic Speciation of Silver in Marine Waters. Environmental Science and Technology, 29: 2616-2621.

Milne, A., Landing, W., Bizimisb, M., Mortona, P. 2010. Determination of Mn, Fe, Co, Ni, Cu, Zn, Cd, and Pb in Seawater Using High Resolution Magnetic Sector Inductively Coupled Mass Spectrometry (HR-ICP-MS). Analytica Chimica Acta. 665: 200-207.

Moffett, J. W. 1995. Temporal and Spatial Variability of Copper Complexation by Strong Chelators in the Sargasso-Sea. Deep-Sea Research Part I-Oceanographic Research Papers, 42: 1273-1295.

Moffett, J.W., Zika, R.G. 1987. Solvent Extraction of Copper Acetylacetonate in Studies of Copper (II) Speciation in Seawater. Marine Chemistry, 21: 301-313.

Moffett, J. W., Brand, L.E., Croot, P.L., Barbeau, K.A.. 1997. Cu Speciation and Cyanobacterial Distribution in Harbors Subject to Anthropogenic Cu Inputs. Limnolology and Oceanography, 42: 789-799.

Moffett, J. W., Dupont, C. 2007. Cu Complexation by Organic Ligands in the Sub-Arctic NW Pacific and Bering Sea. Deep-Sea Research Part I-Oceanographic Research Papers, 54: 586-595.

Moffett, J.W., Tuit, C.B., and Ward, B.B. 2012. Chelator Induced Inhibition of Copper Metalloenzymes in Denitrifying Bacteria. Limnology and Oceanography, 57(1): 272-280.

Moore, R.M., Burton, J.D., 1976. Concentrations of Dissolved Copper in the Eastern Atlantic Ocean. Nature 264: 241-243.

Morel, F.M.M., Milligan, A.J., and Saito, M.A. 2003. Marine Bioinorganic Chemistry: The Role of Trace of Metals in the Oceanic Cycles of Major Nutrients. Treatise on Geochemistry, 6: 113-143.

Morel, F.M.M., Price, N.M. 2003. Biogeochemical Cycles Trace metals in the Oceans. Science, 300(5621): 944.

Morel, F. M. M. 2008. The Co-evolution of Phytoplankton and Trace Element Cycles in the Oceans. Geobiology, 6: 318-324.

Ndung'u, K., Thomas, M.A., Flegal, A.R. 2001. Silver in the Western Equatorial and South Atlantic Ocean. Deep-Sea Research Part II-Topical Studies in Oceanography 48: 2933-2945.

Nishioka, J., Takeda, S., Wong, C.S., Johnson, W.K. 2001. Size Fractionated Iron Concentrations in the Northeast Pacific Ocean: Distribution of Soluble and Small Colloidal Iron. Marine Chemistry, 74(2-3): 157-179.

Nghiem, L., Mornane, P., Potter, I., Perera, J. Cattrall, R., Kolev, S. 2006. Extraction and Transport of Metal Ions and Small Organic Compounds Using Polymer Inclusion Membranes (PIM). Journal of Membrane Science, 281: 7-41.

Obata, H., Karatani, H., Nakayama, E. 1993. Automated Determination of Iron in Seawater by Chelating Resin Concentration and Chemiluminescence Detection. Analytical Chemistry, 65: 1524-1528.

Peers, G., Quesnel, S.A., Price, N.M. 2005. Copper Requirements for Iron Acquisition and Growth of Coastal and Oceanic Diatoms. Limnology and Oceanography, 50: 1149-1158.

Peers, G., Price, N. 2006. Copper-containing Plastocyanin Used for Electron Transport by an Oceanic Diatom. Nature, 441(7091): 341-344.

Phinney, J. T., Bruland, K. W. (1997). Trace Metal Exchange in Solution by the Fungicides Ziram and Maneb (dithiocarbamates) and Subsequent Uptake of Lipophilic Organic Zinc, Copper, and Lead Complexes into Phytoplankton Cells. Environmental Toxicology and Chemistry, 16(10): 2046-2053.

Ranville, M.A., Flegal, A.R., 2005. Silver in the North Pacific. Geochemistry Geophysics Geosystems, 6: 13.

Ranville, M. A., Cutter, G.A., Buck, C.S., Landing, W.M., Cutter, L.S., Resing, J.A., Flegal, A.R. 2010. Aeolian Contamination of Se and Ag in the North Pacific from Asian Fossil Fuel Combustion. Environmental Science & Technology, 44(5): 1587-1593.

Ratte, H.T. 1999. Bioaccumulation of Silver Compounds: A Review. Envornmental Toxicology and Chemistry, 18(1): 89-108.

Redfield, A.C. 1958. Biological Control of Chemical Factors in the Environment. American Scientist, 46(3): 205-221.

Reinfelder, J., Chang, S. 1999. Speciation and Microalgal Bioavailability of Inorganic Silver. Environmental Science and Technology, 33(11): 1860-1863.

Rose, A., Webb, E., Wait, T., Moffet, J. 2008. Measurement and Implication of Nonphotochemically Generated Superoxide in the Equitorial Pacific Ocean. Environmental Science and Technology, 42(7): 2387-93.

Rue, E. L., and K. W. Bruland. 1995. Complexation of Iron(III) by Natural Organic Ligands in the Central North Pacific as Determined by a New Competitive Ligand Equilibration/Absorptive Cathodic Stripping Voltametric Method. Marine Chemistry, 50: 117-138.

Ruzicka, J., Hansen, E. 1978. Flow Injection Analysis: Part X Theory, Techniques and Trends. Analytica Chimica Acta, 99(1): 37-76.

Ruzicka, J., Marshall, G. 1990. Sequential Injection: A New Concept for Chemical Sensors, Process Analyzers and Laboratory Assays. Analytica Chimica Acta, 237: 329-343.

Saito, M. A., D. M. Sigman, and F. M. M. Morel. 2003. The Bioinorganic Chemistry of the Ancient Ocean: the Co-evolution of Cyanobacterial Metal Requirements and Biogeochemical Cycles at the Archean-Proterozoic boundary. Inorganica Chimica Acta, 356: 308-318.

Sangi, M.R., Jayatissa, D., Kim, J.P., Hunter, K.A. 2004. Determination of Liable Cu^{2+} in Fresh Waters by Chemiluminescence: Interference by Iron and Other Cations. Talanta, 62: 924-930.

Sarmiento, J., Gruber, N. 2006. Ocean Biogeochemical Dynamics. Princeton University Press, Princeton, USA.

Scientific Committee on Oceanographic Research (SCOR). 2006. Geotraces: An International Study of the Marine Biogeochemical Cycle of Trace Metals and Their Isotopes (Report No. 1). Baltimore, MD.

Semeniuk, D.M., Cullen, J.T., Johnson, D.M., Gagnon, K., Ruth, T.J., Maldonado, M.T. 2009. Plankton Copper Requirements and Uptake in the Subartic Northeast Pacific Ocean. Deep-Sea Research I, 56: 1130-1142.

Shijo, Y., Shimizu, T., Tsunoda, T. 1989. Determination of Silver in Seawater by Graphite Furnace Atomic Absorption Spectrometry after Solvent Extraction and Microscale Back-Extraction. Analytical Sciences, 5: 65-68.

Skeggs, L.T., Am. J. Clin. Pathol. 13 (1957) 451.

Smith, G.J., Flegal, A.R. 1993. Silver in San Francisco Bay Estuarine Waters. Estuaries, 16 (3A): 547-558.

Stewart, K.K., Beecher, G.R., Hare, P.E. 1976. Rapid Analysis of Discrete Samples: The use on Non-segmented Continuous Flow. Analytical Biochemistry, 70(1): 167-173.

Sunda, W.G. 1984. Measurement of Manganese, Zinc and Cadmium Complexation in Seawater Using Chelex Ion-Exchange Equilibria. Marine Chemistry, 14: 365-378.

Sunda, W.G. 1994. Trace Metal/Phytoplankton Interactions in the Sea. p. 213-247. *In* G. Bidoglio and W. Stumm [eds.], Chemistry of Aquatic Systems: Local and Global Perspectives. ECSC, EEC, EAEC.

Sunda, W.G., Huntsman, S.A. 1992 Feedback Interactions Between Zinc and Phytoplankton in Seawater. Limnology and Oceanography, 37: 25-40.

Sunda, W.G., Huntsman, S.A. 1995. Regulation of Copper Concentration in the Oceanic Nutricline by Phytoplankton Uptake and Regeneration. Limnology and Oceanography, 40(1): 132-137.

Terry, J.M., Adcock, J.L., Olson, D.C., Wolcott, D.K., Schwanger, C.L., Hill, L.A., Barnett, N.W., and Francis, P.S. 2008. Chemiluminescence Detector with a Serpentine Flow Cell. Analytical Chemistry, 80: 9817-9821.

Van Den Berg, C. 1984. Organic and Inorganic Speciation of Copper in the Irish Sea. Marine Chemistry, 14(3): 201-211.

Van Den Berg, C. M. G. 1995. Evidence for Organic Complexation of Iron in Seawater. Marine Chemistry, 50: 139-157.

Voelker, B., Sedlak, D., Zafiriou, O. 2000. Chemistry of Superoxide Radical in Seawater: Reactions with Organic Cu Complexes. Environmental Science and Technology, 34(6): 1036-1042.

Wang, L., Liang, A., Chen, H., Qian, B, Fu, J. 2008. Ultrasensitive Determination of Silver Ion based on Fluorecence Spectroscopy with Nanoparticles. Analytica Chimica Acta, 616: 170-176.

Wells, M. L., N. M. Price, and K. W. Bruland. 1994. Iron Limitation and the Cyanobacterium *Synechococcus* in Equatorial Pacific Waters. Limnology and Oceanography, 39: 1481-1486.

Wells, M.L., Bruland, K.W. 1998. An Improved Method for Rapid Determination of Bioactive Trace Metals in Seawater Using Solid Phase Extraction and High Resolution Inductively Coupled Plasma Mass Spectrometry. Marine Chemistry, 63: 145-153.

Wells, M.L., Trick, C.G., Cochlan, W.P., Hughes, M.P., Trainer, V.L. 2005. Domoic Acid: The Synergy of Iron, Copper and Toxicity of Diatoms. Limnology and Oceanography, 50(6): 1908-1917.

Whitney, F.A., Crawford, D.W., Yoshimura, T. 2005. The Uptake and Export of Silicon and Nitrogen in HNLC waters of the NE Pacific Ocean. Deep Sea Research II, 52: 1055-1067.

Yamada, Masaaki, Suzuki, Shigetaka. 1984. Micellular Enhanced Chemiluminescence of 1,10-Phenanthroline for the Determination of Ultratraces of Copper (II) by Flow Injection. Analytical Letters, 17: 251-263.

Zamzow, H., Coale, K., Johnson, K., Sakamoto, C. 1998. Determination of Copper Complexation in Seawater using Flow-Injection Analysis with Chemiluminscence Detection. Analytica Chimica Acta. 377: 133-144.

Appendix A
Metal (M) Speciation Equation

K = distribution coefficient of *M*A between aqueous and organic
K_1 = formation coefficient of *M*A
α = inorganic side reaction coefficient of *M*

See section 3.3 for more information.

Appendix B: Silver Extraction Sequence

Project: MScl 6/22/2012
Sequence:

	Device	Parameters	Function
Ag Extraction			
name sample	single channel data	Ag Standard	name sample
USB4000 get reference spectrum	USB4000	N/A	get reference spectrum
Mix Sample and Buffer			
Air Bubble			
Air Port	18 Port Valve	7	go to port
milliGAT aspirate	milliGAT	30,15,1	aspirate
Buffer Port	18 Port Valve	8	go to port
milliGAT aspirate	milliGAT	10,5,1	aspirate
Ag Std	18 Port Valve	10	go to port
milliGAT dispense	milliGAT	20,15,1	dispense
Air Bubble			
Air Port	18 Port Valve	7	go to port
milliGAT aspirate	milliGAT	600,55,1	aspirate
AG Std	18 Port Valve	10	go to port
milliGAT dispense	milliGAT	500,35,1	dispense
Waste Port	18 Port Valve	3	go to port
milliGAT dispense	milliGAT	150,50,1	dispense
Mix DDDC			
Air Bubble			
Air Port	18 Port Valve	7	go to port
milliGAT aspirate	milliGAT	30,15,1	aspirate
DDDC Port	18 Port Valve	9	go to port
milliGAT aspirate	milliGAT	10,5,1	aspirate
Std 3	18 Port Valve	10	go to port
milliGAT dispense	milliGAT	20,15,1	dispense
Air Bubble			
Air Port	18 Port Valve	7	go to port
milliGAT aspirate	milliGAT	600,55,1	aspirate
Std 3	18 Port Valve	10	go to port
milliGAT dispense	milliGAT	500,35,1	dispense
Waste Port	18 Port Valve	3	go to port
milliGAT dispense	milliGAT	150,50,1	dispense
Prime Mixed Sample			
Ag Std	18 Port Valve	10	go to port
milliGAT aspirate	milliGAT	200,35,1	aspirate
Waste Port	18 Port Valve	3	go to port
milliGAT dispense	milliGAT	350,50,1	dispense

1

Project: MScl 6/22/2012
Sequence:

	Device	Parameters	Function
Load Ag Chloroform Extrac			
Air Bubble			
Air Port	18 Port Valve	7	go to port
milliGAT aspirate	milliGAT	15,15,1	aspirate
Ag ZS		10	
Ag Std	18 Port Valve	8	go to port
milliGAT aspirate	milliGAT	10,5,1	aspirate
Chloroform Port	18 Port Valve	16	go to port
milliGAT aspirate	milliGAT	10,5,1	aspirate
Mix			
Air Port	18 Port Valve	7	go to port
milliGAT aspirate	milliGAT	100,25,1	aspirate
Waste Port	18 Port Valve	3	go to port
milliGAT dispense	milliGAT	100,25,1	dispense
Load Separation Cell			
Separator Bottom Port	18 Port Valve	5	go to port
milliGAT dispense	milliGAT	205,25,1	dispense
Air Bubble			
Air Port	18 Port Valve	7	go to port
milliGAT aspirate	milliGAT	60,15,1	aspirate
Separator Bottom Port	18 Port Valve	5	go to port
milliGAT dispense	milliGAT	60,25,1	dispense
IPA Wash			
Air Bubble			
Air Port	18 Port Valve	7	go to port
milliGAT aspirate	milliGAT	20,15,1	aspirate
IPA Port	18 Port Valve	13	go to port
milliGAT aspirate	milliGAT	50,35,1	aspirate
Air Bubble			
Air Port	18 Port Valve	7	go to port
milliGAT aspirate	milliGAT	250,15,1	aspirate
Flush Holding Coil			
Waste Port	18 Port Valve	3	go to port
milliGAT dispense	milliGAT	500,55,1	dispense
Air Bubble			
Air Port	18 Port Valve	7	go to port
milliGAT aspirate	milliGAT	20,15,1	aspirate
Flush Holding Coil			
Waste Port	18 Port Valve	3	go to port
milliGAT dispense	milliGAT	1500,55,1	dispense
Prime Sep Side			

Project: MScl 6/22/2012
Sequence:

	Device	Parameters	Function
Air Bubble			
Air Port	18 Port Valve	7	go to port
milliGAT aspirate	milliGAT	10,15,1	aspirate
Separator Side Port	18 Port Valve	4	go to port
Prime			
milliGAT aspirate	milliGAT	170,15,1	aspirate
Collection Vial	18 Port Valve	9	go to port
milliGAT dispense	milliGAT	250,50,1	dispense
Prime Sep Bottom			
Air Bubble			
Air Port	18 Port Valve	7	go to port
milliGAT aspirate	milliGAT	10,15,1	aspirate
Separator Bottom Port	18 Port Valve	5	go to port
Prime			
milliGAT aspirate	milliGAT	100,50,1	aspirate
Waste Port	18 Port Valve	3	go to port
milliGAT dispense	milliGAT	250,50,1	dispense
Load HNO3 Back Extract			
Air Bubble			
Air Port	18 Port Valve	7	go to port
milliGAT aspirate	milliGAT	15,15,1	aspirate
Back Ext ZS		10	
Separator Side Port	18 Port Valve	4	go to port
milliGAT aspirate	milliGAT	10,5,1	aspirate
HNO3 Port	18 Port Valve	17	go to port
milliGAT aspirate	milliGAT	10,5,1	aspirate
Mix			
Air Port	18 Port Valve	7	go to port
milliGAT aspirate	milliGAT	100,10,1	aspirate
Waste Port	18 Port Valve	3	go to port
milliGAT dispense	milliGAT	100,10,1	dispense
Load Separation Cell			
Separator Bottom Port	18 Port Valve	5	go to port
milliGAT dispense	milliGAT	205,35,1	dispense
Air Bubble			
Air Port	18 Port Valve	7	go to port
milliGAT aspirate	milliGAT	60,15,1	aspirate
Separator Bottom Port	18 Port Valve	5	go to port
milliGAT dispense	milliGAT	60,35,1	dispense
Prime Sep Side			
Air Bubble			

Project: MScl 6/22/2012
Sequence:

	Device	Parameters	Function
Air Port	18 Port Valve	7	go to port
milliGAT aspirate	milliGAT	10,15,1	aspirate
Separator Side Port	18 Port Valve	4	go to port
Prime			
milliGAT aspirate	milliGAT	90,15,1	aspirate
Waste Port	18 Port Valve	3	go to port
milliGAT dispense	milliGAT	250,50,1	dispense
Dilute HNO3			
Air Bubble			
Air Port	18 Port Valve	7	go to port
milliGAT aspirate	milliGAT	15,15,1	aspirate
Dilution Port	18 Port Valve	1	go to port
milliGAT dispense	milliGAT	43,10,1	dispense
Separator Side Port	18 Port Valve	4	go to port
milliGAT aspirate	milliGAT	8,5,1	aspirate
Dilution Port	18 Port Valve	1	go to port
milliGAT dispense	milliGAT	27,10,1	dispense
Air Bubble			
Air Port	18 Port Valve	7	go to port
milliGAT aspirate	milliGAT	15,15,1	aspirate
Dilution Port	18 Port Valve	1	go to port
milliGAT dispense	milliGAT	100,10,1	dispense
milliGAT aspirate	milliGAT	100,10,1	aspirate
Color Chem Ag			
Pre prime			
Air Bubble			
Air Port	18 Port Valve	7	go to port
milliGAT aspirate	milliGAT	20,15,1	aspirate
Chloroform Port	18 Port Valve	16	go to port
milliGAT aspirate	milliGAT	5,5,1	aspirate
Na2S2O8 Port	18 Port Valve	12	go to port
Prime			
milliGAT aspirate	milliGAT	5,5,1	aspirate
Waste Port	18 Port Valve	3	go to port
milliGAT dispense	milliGAT	350,50,1	dispense
name sample	single channel data	benchtop 1 to 1	name sample
Air Bubble			
Air Port	18 Port Valve	7	go to port
milliGAT aspirate	milliGAT	10,15,1	aspirate
Ag zone		2	

Project: MScI 6/22/2012
Sequence:

	Device	Parameters	Function
1 10 Phen GC Port	18 Port Valve	16	go to port
milliGAT aspirate	milliGAT	10,5,1	aspirate
Na2S2O8 Port	18 Port Valve	12	go to port
milliGAT aspirate	milliGAT	10,5,1	aspirate
Dilution Port	18 Port Valve	1	go to port
milliGAT aspirate	milliGAT	10,5,1	aspirate
Air Bubble			
Air Port	18 Port Valve	7	go to port
milliGAT aspirate	milliGAT	100,25,1	aspirate
Heater 2	18 Port Valve	1	go to port
milliGAT dispense	milliGAT	515,25,1	dispense
wait	system	180	wait
milliGAT aspirate	milliGAT	435,15,1	aspirate
detector port	18 Port Valve	15	go to port
milliGAT dispense	milliGAT	205,15,1	dispense
USB4000 start acquire	USB4000	0.5	start acquire
wait	system	30	wait
USB4000 stop acquire	USB4000	N/A	stop acquire
calc peak average	single channel data	N/A	calc peak average
save data to file	single channel data	N/A	save data to file
Flush USB4000			
USB4000 Port	18 Port Valve	15	go to port
milliGAT dispense	milliGAT	500,25,1	dispense
Flush Heater 2			
Heater 2	18 Port Valve	1	go to port
milliGAT dispense	milliGAT	500,25,1	dispense

Appendix C: Copper CL Sequence

Project: Copper Extraction.zf 6/22/2012
Sequence: Copper CL Measurement

Sequences/Steps	Device Name	Var Name	Input Parameters	Commands
Copper CL Measurement				
name sample	Data		P12 200M	name sample
CL meas				
Bubble 18				
Air Port 13	18 Port Valve		13	go to port
milliGAT Pump aspirate	milliGAT Pump		20,15,1	aspirate
Dilution Zone				
SW STD	18 Port Valve		3	go to port
milliGAT Pump aspirate	milliGAT Pump		55,15,1	aspirate
Air 2				
Air 10 Port	10 Port Valve		5	go to port
Pump Two aspirate	Pump Two		20,5,1	aspirate
Bubble 18				
Air Port 13	18 Port Valve		13	go to port
milliGAT Pump aspirate	milliGAT Pump		20,15,1	aspirate
Reagent Stack 2				
R1 10 Port	10 Port Valve		7	go to port
Pump Two aspirate	Pump Two		75,15,1	aspirate
R2 10 Port	10 Port Valve		2	go to port
Pump Two aspirate	Pump Two		75,15,1	aspirate
Mix				
Air 10 Port	10 Port Valve		5	go to port
Pump Two aspirate	Pump Two		500,10,1	aspirate
Waste Port	10 Port Valve		9	go to port
Pump Two dispense	Pump Two		520,10,1	dispense
Air 2				
Air 10 Port	10 Port Valve		5	go to port
Pump Two aspirate	Pump Two		20,5,1	aspirate
CL Detect 18				
set data window	Data		0,Inf	set data window
CL Port 12	18 Port Valve		14	go to port
CL Merge port	10 Port Valve		10	go to port
CL Detector start acquire	CL Detector		0.5	start acquire
milliGAT Pump dispense	milliGAT Pump		30,12,1	dispense
milliGAT Pump slew	milliGAT Pump		13	slew
Pump Two dispense	Pump Two		700,34,1	dispense
milliGAT Pump stop	milliGAT Pump		N/A	stop
CL Detector stop acquire	CL Detector		N/A	stop acquire
subtract baseline	Data		2	subtract baseline
activate table by number	Data		13	activate table by number
calc peak height	Data		N/A	calc peak height
calc value	Data	CalcPkH	N/A	calc value
add to table and meta	Data		'Calc Peak Height', CalcPkH	add to table and meta
calc peak area	Data		1	calc peak area

Project: Copper Extraction.zf 6/22/2012
Sequence: Copper CL Measurement

Sequences/Steps	Device Name	Var Name	Input Parameters	Commands
activate table by number	Data		16	activate table by number
calc value	Data	CalcArea	N/A	calc value
save data to file	Data		N/A	save data to file

Appendix D: LDPE Cleaning Procedure

All lab-ware were cleaned according to stringent GEOTRACES trace element cleaning protocols outlined below (Cutter et al., 2007). The cleaning took place in a laminar flow hood within a Class 100 lab space at the University of Victoria in 1L glass beakers. The cleaned lab-ware were double bagged for storage.

1. Rinse 4X in reverse osmosis (RO) water
2. Submerge in a detergent bath (FisherBrand Versa-Clean Concentrate) for 1 week at room temperature or 1 day at 60°C
3. Remove from detergent bath and rinse 4X with RO water
4. Rinse 3X with MQ water
5. Submerge in reagent grade 6 M HCl (Anachemia) for 1 month at room temperature or 1 week at 60°C
6. Remove from HCl bath and rinse 3X with MQ
7. Submerge in MQ overnight
8. Remove from MQ, rinse 3X with MQ and allow to dry

Special thanks to Christina Schallenburg (University of Victoria) and Elana Ramirez (University of Victoria) for cleaning lab-ware for this research.

Appendix E: Line P Cruise Data for February 2011

Depth (m)	Temperature (°C)	Salinity (PSU)	Dissolved O_2 (µmol/kg)	PO_4 (µmol/l)	Si (µmol/l)	Cu (nmol/l)	TN (µmol/l)
Station P4; *48° 39' N, 126° 40' W - 2/2011*							
15	8.5612	31.7933	295.2	0.94	15.4	6.27	8.8
25	8.5611	31.8940	294.0	0.93	14.9	3.80	8.8
50	8.4681	32.3429	288.1	0.81	7.8	4.70	6.4
100	7.8371	33.4801	171.0	1.84	28.4	3.55	25.4
200	7.0215	33.9477	91.1	2.38	48.3	4.41	34.7
400	5.4152	33.0546	39.2	2.90	75.3	2.91	42.1
600	4.5630	34.1599	17.3	3.05	96.9	2.59	43.5
800	4.1170	34.2940	9.7	3.23	113.3	4.56	45.7
Station P12; *48° 58' N, 130° 40' W - 2/2011*							
15	7.4140	32.3936	298.2	1.10	16.1	2.55	11.3
25	7.4042	32.3914	298.0	1.10	16.1	1.58	11.3
70	7.2941	32.8481	254.3	1.25	18.2	1.78	14.3
100	6.7643	33.5200	178.4	1.85	34.8	3.15	25.5
200	5.8508	33.8611	119.9	2.35	55.2	3.06	34.2
400	4.3934	33.9849	55.0	2.88	86.4	1.58	42.2
600	3.9099	34.1789	19.6	3.12	111.0	2.59	45.4
Station P16; *49° 16' N, 134° 40' W - 2/2011*							
25	7.5113	32.5862	296.6	0.87	10.9	1.61	8.2
50	7.5121	32.5867	296.4	0.88	10.9	1.70	8.2
70	7.5121	32.5967	295.8	0.88	11.0	1.31	8.3
120	6.8047	33.6005	222.6	1.51	28.2	2.55	21.2
200	5.6022	33.8038	168.7	2.05	49.7	1.76	29.9
400	4.1963	33.9548	64.3	2.54	86.6	1.75	41.3
600	3.8655	34.1458	27.6	3.05	109.6	1.76	44.8
800	3.4320	34.2750	18.6	3.13	126.9	2.55	45.5
Station P20; *49° 34' N, 138° 40' W - 2/2011*							
25	6.9541	32.4663	297.7	0.93	11.7	0.77	8.6
50	6.9539	32.4664	297.7	0.91	11.7	0.37	8.5
70	6.9601	32.4680	297.2	0.93	11.9	0.31	8.8
120	6.4983	33.3926	210.9	1.67	30.1	0.57	22.6
200	5.4932	33.8205	138.2	2.25	54.1	1.14	32.4
400	4.2343	33.9877	59.0	2.84	88.9	0.70	41.3
600	3.8418	34.1757	21.5	3.10	112.6	1.25	44.9
800	3.3312	34.2883	17.6	3.10	130.5	1.59	45.2

Station P26; *49° 60' N, 145° 00' W - 2/2011*							
10	5.6376	32.6562	304.3	1.25	19.4	1.81	14.0
40	5.6431	32.6588	303.6	1.25	19.5	1.01	14.1
200	4.1726	33.8235	82.5	2.79	75.6	2.00	40.5
400	3.8554	34.0646	34.8	3.05	103.9	2.39	44.1
600	3.4523	34.2303	20.4	3.15	124.7	1.98	45.7
800	3.1389	34.3142	19.0	3.20	136.4	1.57	45.8
Station P26; 50° *00' N, 145° 00' W - 8/2010*							
40	8.3131	32.7012	280.9	1.11	16.4	0.31	11.5
75	6.6221	32.7973	277.6	1.25	19.8	0.27	14.8
100	5.5136	32.9533	261.5	1.46	25.6	0.84	18.1
200	4.1923	33.7753	115.4	2.56	69.1	0.52	36.9
300	3.9802	33.8846	74.4	2.84	84.4	1.34	41.0
400	3.8685	34.0100	37.3	3.06	98.9	2.24	45.2
600	3.5495	34.2047	20.1	2.98	120.6	1.74	45.8
800	3.1771	34.3058	18.3	3.14	134.6	1.74	45.4

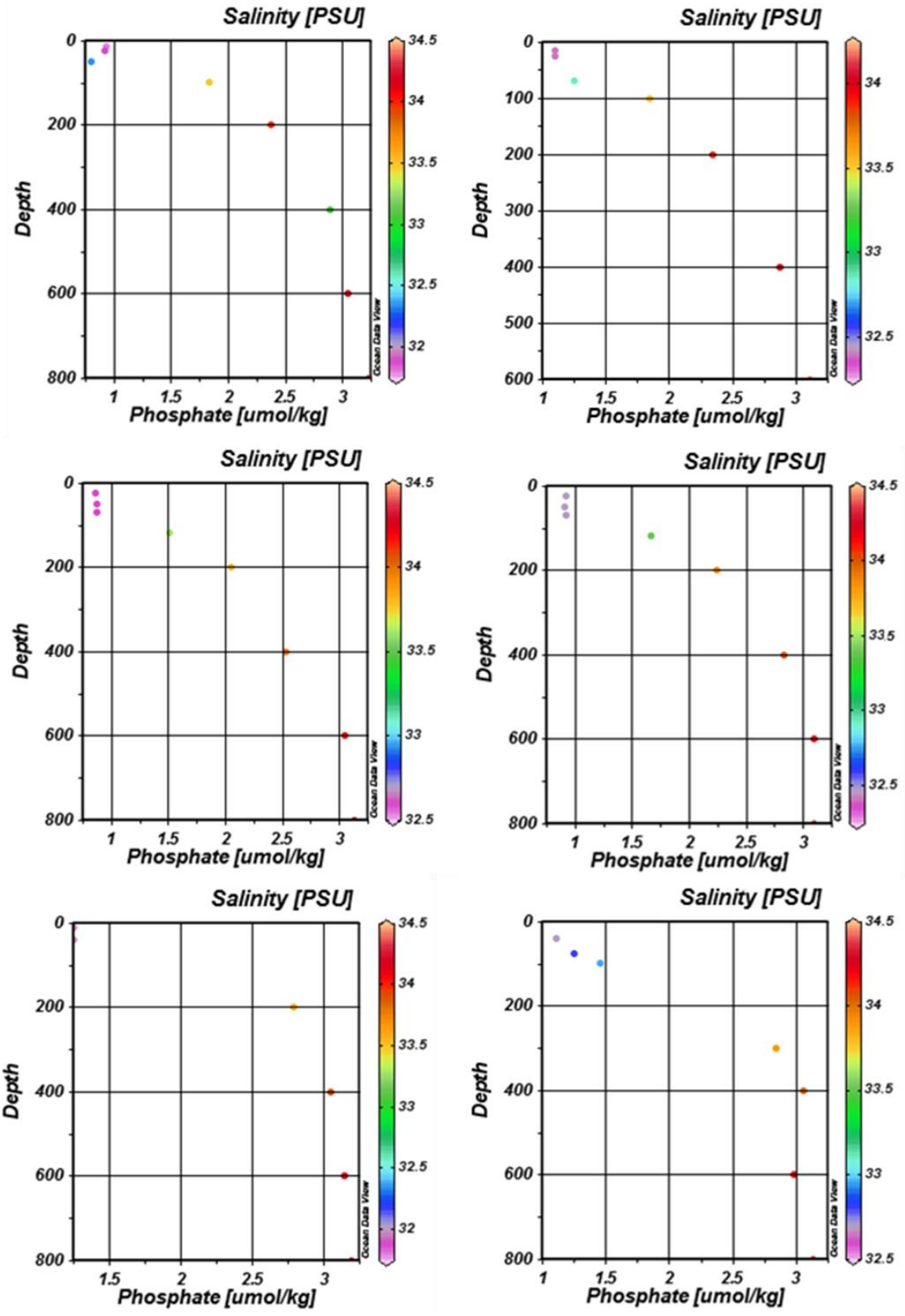
Salinity [PSU]
Depth
Phosphate [umol/kg]
Ocean Data View
Salinity [PSU]
Depth
Phosphate [umol/kg]
Ocean Data View
Salinity [PSU]
Depth
Phosphate [umol/kg]
Ocean Data View
Salinity [PSU]
Depth
Phosphate [umol/kg]
Ocean Data View
Salinity [PSU]
Depth
Phosphate [umol/kg]
Ocean Data View
Salinity [PSU]
Depth
Phosphate [umol/kg]
Ocean Data View

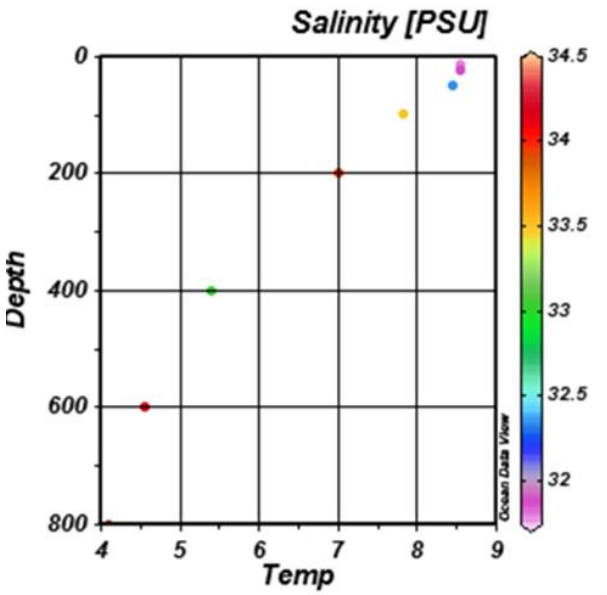
Salinity [PSU]
Depth
Temp
0
200
400
600
800
4
5
6
7
8
9
34.5
34
33.5
33
32.5
32
Ocean Data View

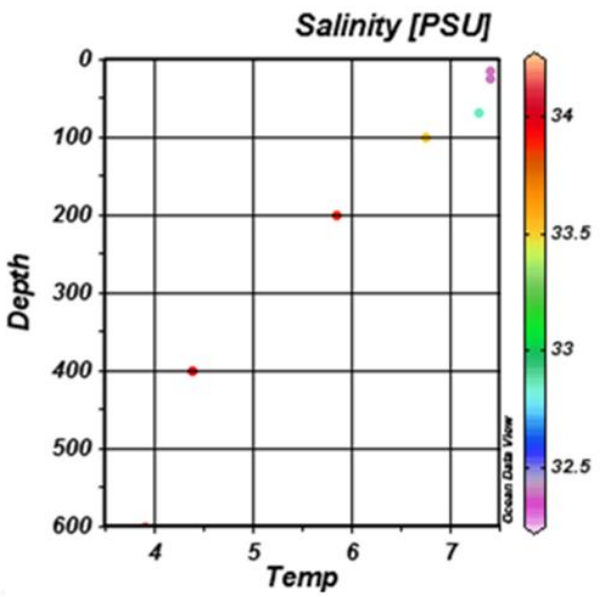
Salinity [PSU]
Depth
Temp
0
100
200
300
400
500
600
4
5
6
7
34
33.5
33
32.5
Ocean Data View

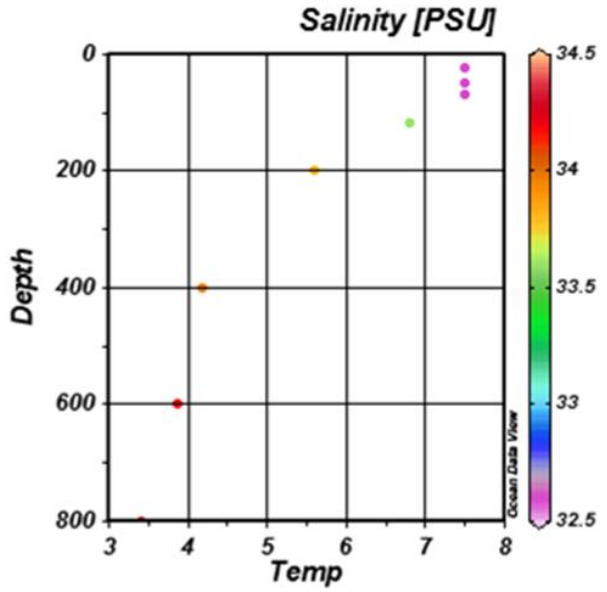
Salinity [PSU]
Depth
Temp
0
200
400
600
800
3
4
5
6
7
8
34.5
34
33.5
33
32.5
Ocean Data View

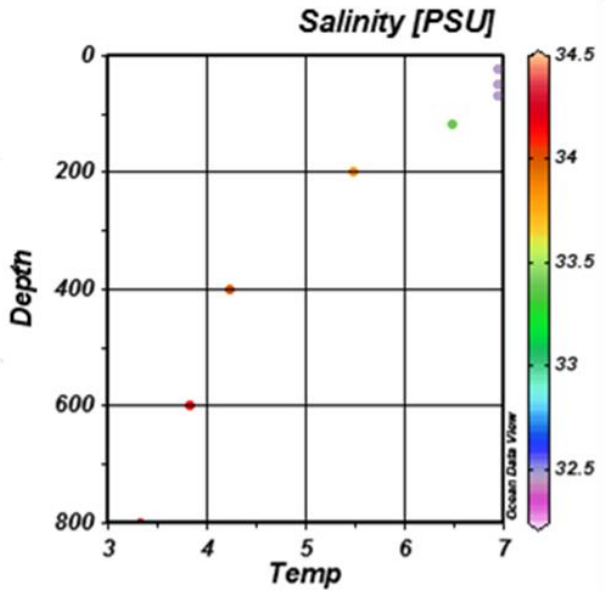
Salinity [PSU]
Depth
Temp
0
200
400
600
800
3
4
5
6
7
34.5
34
33.5
33
32.5
Ocean Data View

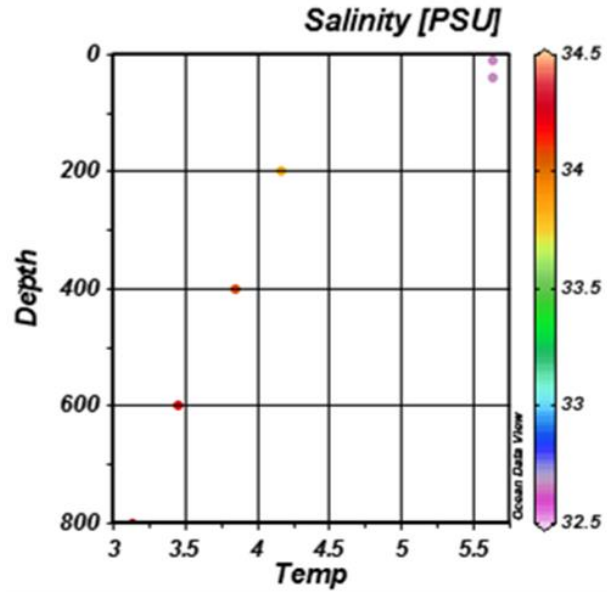
Salinity [PSU]
Depth
Temp
0
200
400
600
800
3
3.5
4
4.5
5
5.5
34.5
34
33.5
33
32.5
Ocean Data View

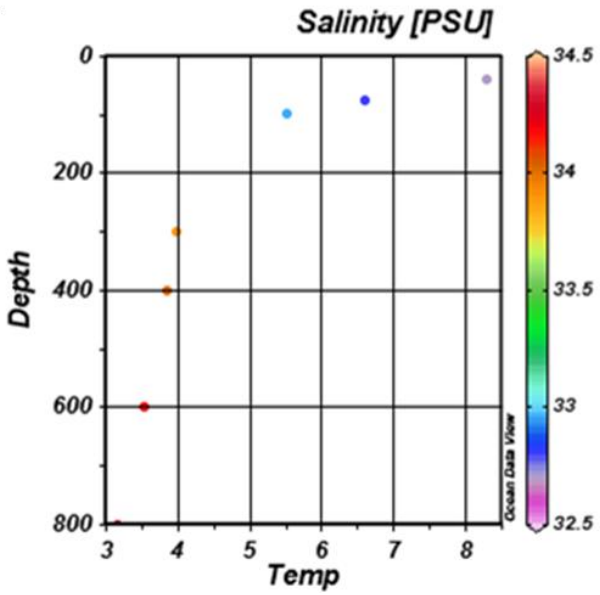
Salinity [PSU]
Depth
Temp
0
200
400
600
800
3
4
5
6
7
8
34.5
34
33.5
33
32.5
Ocean Data View

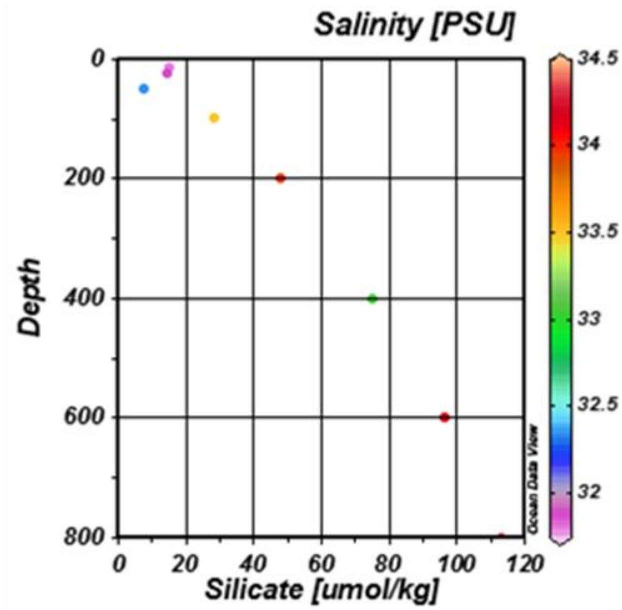
Salinity [PSU]
Depth
0
200
400
600
800
0 20 40 60 80 100 120
Silicate [umol/kg]
34.5
34
33.5
33
32.5
32
Ocean Data View

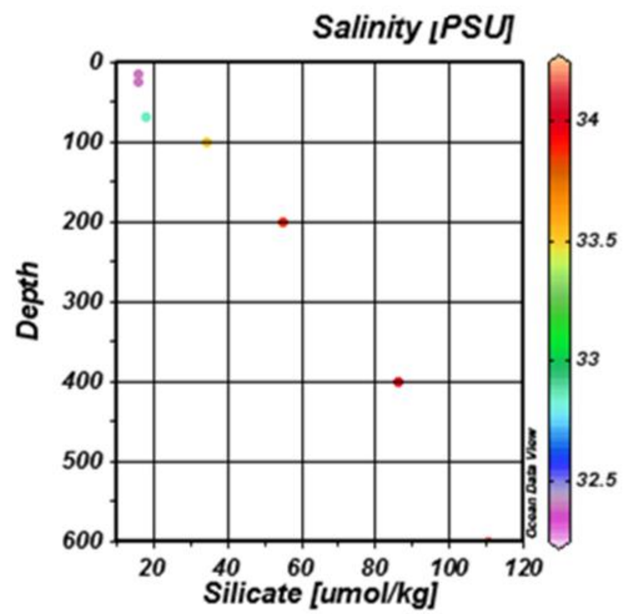
Salinity [PSU]
Depth
0
100
200
300
400
500
600
20 40 60 80 100 120
Silicate [umol/kg]
34
33.5
33
32.5
Ocean Data View

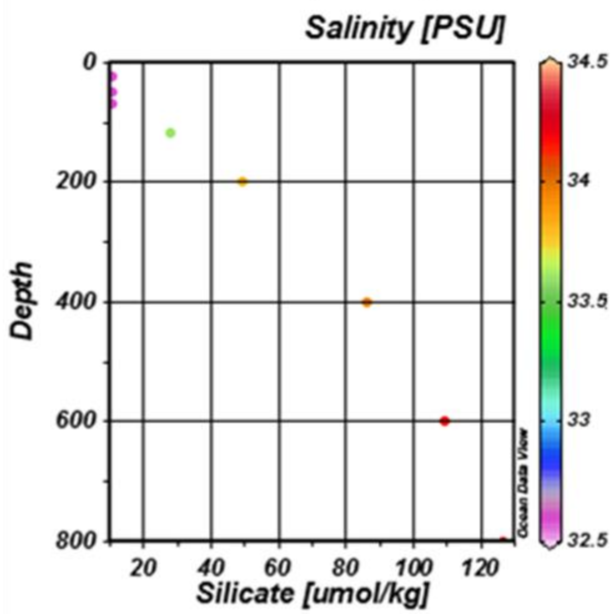
Salinity [PSU]
Depth
0
200
400
600
800
20 40 60 80 100 120
Silicate [umol/kg]
34.5
34
33.5
33
32.5
Ocean Data View

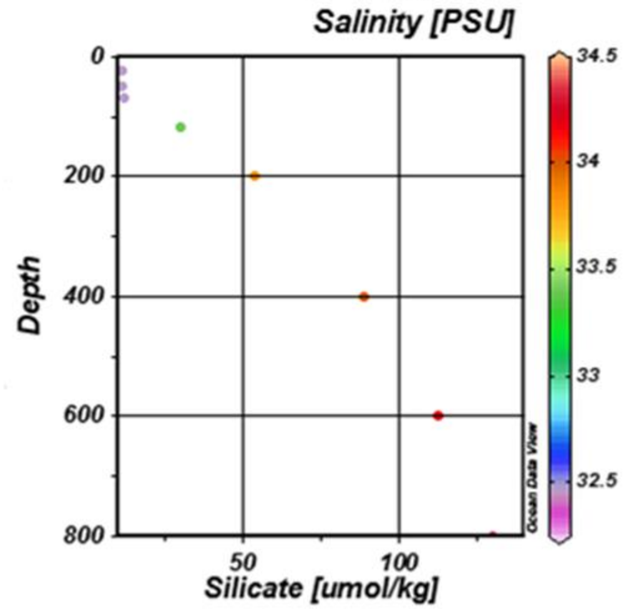
Salinity [PSU]
Depth
0
200
400
600
800
50 100
Silicate [umol/kg]
34.5
34
33.5
33
32.5
Ocean Data View

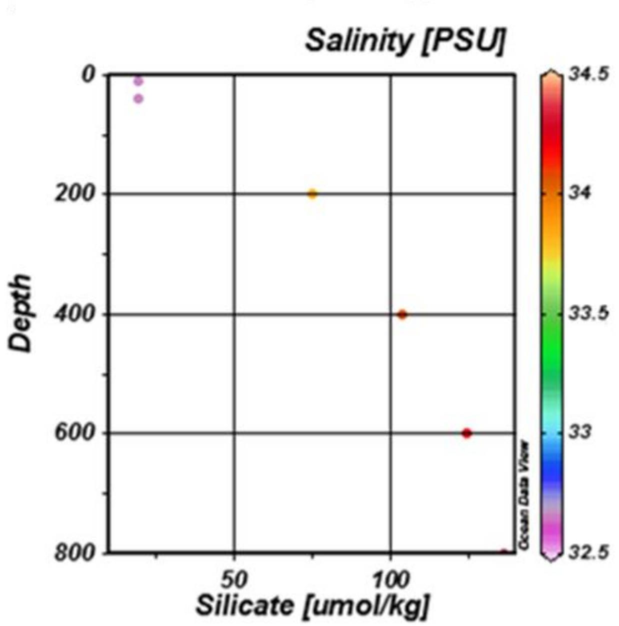
Salinity [PSU]
Depth
0
200
400
600
800
50 100
Silicate [umol/kg]
34.5
34
33.5
33
32.5
Ocean Data View

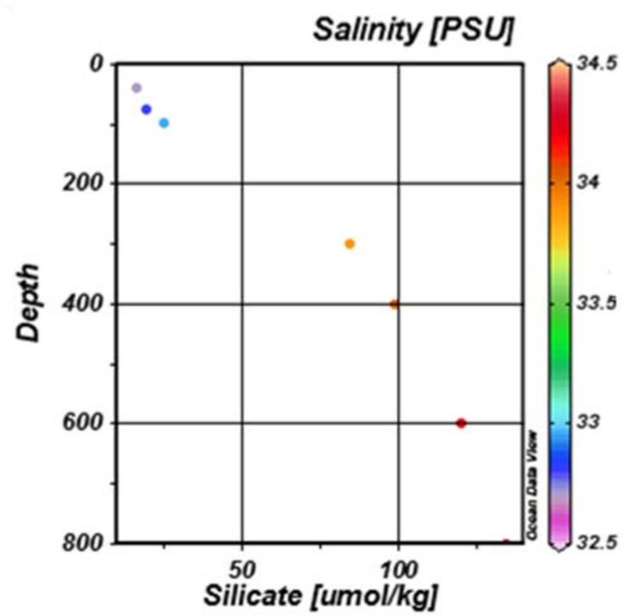
Salinity [PSU]
Depth
0
200
400
600
800
50 100
Silicate [umol/kg]
34.5
34
33.5
33
32.5
Ocean Data View

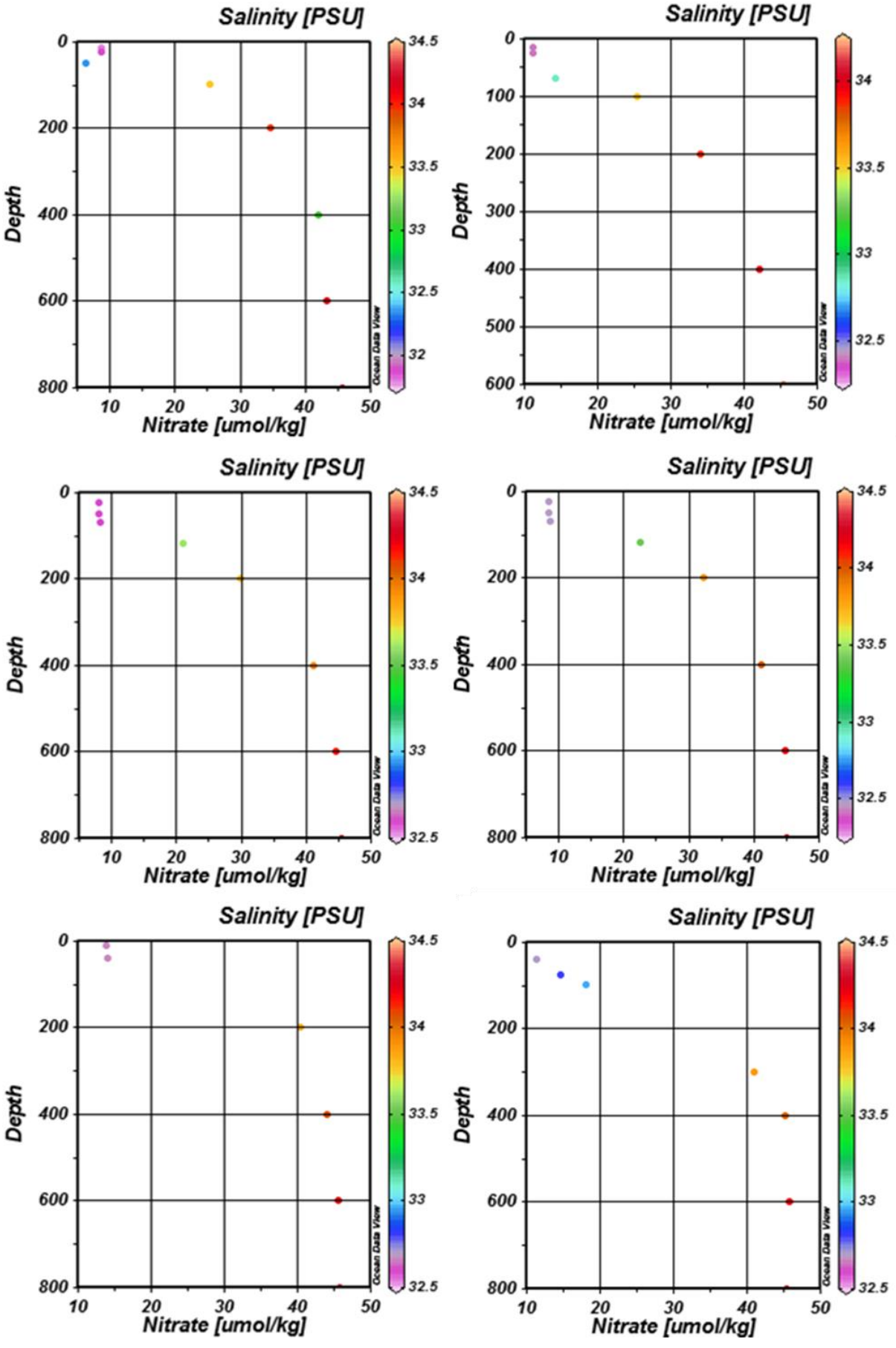
Salinity [PSU]
Depth
Nitrate [umol/kg]
Ocean Data View
Salinity [PSU]
Depth
Nitrate [umol/kg]
Ocean Data View
Salinity [PSU]
Depth
Nitrate [umol/kg]
Ocean Data View
Salinity [PSU]
Depth
Nitrate [umol/kg]
Ocean Data View
Salinity [PSU]
Depth
Nitrate [umol/kg]
Ocean Data View
Salinity [PSU]
Depth
Nitrate [umol/kg]
Ocean Data View